INFORMATION TO USERS

This manuscript has been reproduced from the microfilm master. UMI films the text directly from the original or copy submitted. Thus, some thesis and dissertation copies are in typewriter face, while others may be from any type of computer printer.

The quality of this reproduction is dependent upon the quality of the copy submitted. Broken or indistinct print, colored or poor quality illustrations and photographs, print bleedthrough, substandard margins, and improper alignment can adversely affect reproduction.

In the unlikely event that the author did not send UMI a complete manuscript and there are missing pages, these will be noted. Also, if unauthorized copyright material had to be removed, a note will indicate the deletion.

Oversize materials (e.g., maps, drawings, charts) are reproduced by sectioning the original, beginning at the upper left-hand corner and continuing from left to right in equal sections with small overlaps.

Photographs included in the original manuscript have been reproduced xerographically in this copy. Higher quality 6" x 9" black and white photographic prints are available for any photographs or illustrations appearing in this copy for an additional charge. Contact UMI directly to order.

ProQuest Information and Learning
300 North Zeeb Road, Ann Arbor, MI 48106-1346 USA
800-521-0600

A computational investigation of the effects of heterogeneity on the behavior of soil moisture in the unsaturated zone

By

M. Selim Uz Zaman

A dissertation submitted to the Graduate Faculty in Engineering in partial fulfillment of the requirements for the degree of Doctor of Philosophy, The City University of New York

2002

This manuscript has been read and accepted for the Graduate Faculty in Civil Engineering in satisfaction of the dissertation requirement for the degree of Doctor of Philosophy.

4/29/02
Date

Dr. Reza Khanbilvardi
Chair of Examining committee

4-29-2002
Date

Dean Mumtaz Kassir
Executive Officer

Dr. Lin A. Ferrand

Dr. Vasil Diyamandoglu

Dr. Georege Mylonakis

Dr. Michael A. Celia

Supervisory Committee

THE CITY UNIVERSITY OF NEW YORK

Abstract

A COMPUTATIONAL INVESTIGATION OF THE EFFECT OF HETEROGENEITY ON THE BEHAVIOR OF SOIL MOISTURE IN THE UNSATURATED ZONE

BY

M. Selim Uz Zaman

Adviser: Professor Reza Khanbilvardi

Proper prediction of water flow in the unsaturated zone is vital in the study of the migration of contaminants because water flow and contaminant transports are interdependent processes. Most hydraulic properties of soils vary significantly at different locations in the field. This heterogeneity of soil properties is often an important control on the migration and distribution of water. To completely characterize the movement of water in a heterogeneous soil at field-scale, we first need to identify local values of all relevant soil properties. But this approach is impractical because the data and computational requirements are unreasonable. An alternative to this approach is to estimate effective soil hydraulic parameters which, when used in a simulation, are able to capture the average effects of local soil heterogeneity. The ultimate objective of this research work is to investigate the feasibility of effective parameters to capture the effect of heterogeneity on the average flow of soil moisture through unsaturated heterogeneous soil.

Prediction of soil water movement in a given unsaturated soil requires knowledge of the pressure - moisture content relationship and pressure - relative permeability

relationship. Since the unsaturated flow model uses the combined pressure-moisture content-relative permeability model proposed by van Genutchten (VG), VG model parameters α and n becomes the most important parameters in this research.

For this research work, average behavior of water movement will be quantified by transient first and second spatial moments of moisture content distribution. A series of heterogeneous simulations reveal that there are mainly three types of impact of heterogeneity on the average movement of the moisture plume. The features of Type I impact of heterogeneity are reduced average velocity, reduced vertical spreading and increased transverse spreading. The features of Type II impact of heterogeneity are reduced average velocity, increased transverse spreading and increased vertical spreading. The features of Type III impact of heterogeneity are reduced average velocity, reduced transverse and vertical spreading. Based on Type curves developed in this research, it can be concluded that impact of heterogeneity cannot be captured in a homogeneous medium by a single set of parameters using the current unsaturated flow model.

Acknowledgements

First and foremost I wish to express my sincere thanks and appreciation to my advisor, Professor Lin A. Ferrand, for her constant guidance, encouragement, understanding, and valuable suggestions.

I can't go any further without mentioning my appreciation for Professor Reza Khanbilvardi, whose constant concern for my educational development and general well-being through the seven years I have known him. I would also like to thank Dean Mumtaz Kassir for his concern in my academic development.

I gratefully acknowledge a number of fruitful discussions with Professor Michael Celia who allowed me to use the unsaturated flow model that he developed and offered many invaluable suggestions that helped focus my thesis in the right direction.

I am indebted to Professor John Fillos, Chairman, Department of Civil Engineering for all the emotional & financial support he offered me during the course of this study. Without which this thesis would not have seen the light of the day.

My thanks are extended to Professor Vassil Diyamandoglu and Professor George Mylonakis for being the member of my thesis advisory committee. My special thanks to Project Manager, Krishnamurthy Ramalingam for not making my life more miserable during the last three years of the ordeal.

There is a history of long-suffering spouse behind every married graduated student. So I would like to express my gratitude to my wife Siddika Nurani for her love, encouragement, patience, and sacrifice during all those tough years. My newborn son Yusuf, provided me with strong motivation and renewed energy to quickly accomplish this task.

Table of Contents

Chapter 3: Computational flow model

Chapter 4: Homogeneous simulations

Chapter 6: Effective parameters

Chapter 7: Summary and conclusion

Chapter 8: Appendices

List of Tables

List of Figures

List of Notations

General

A_1, A_2, A_3, A_4 and A_5 = multiple regression coeffcients

BCh = pressure head of water at boundary

c = concentration of dissolved contaminant

d = formation thickness

g = acceleration due to gravity

h = water pressure head

H = pressure head in terms of reference fluid density

k_1, k_2 = fitting parameter for redistribution velocity model

k_3 = rate of change of vertical spreading of moisture plume with respect to change of vertical distances (Vertical spreading index)

k_4 = rate of change of transverse spreading of moisture plume with respect to change of vertical distances (Transverse spreading index)

k = instrinsic permeability of the medium

k_{pro} = pseudo-relative permeability to oil

k_{ri} = relative permeability of i_{th} fluid.

k_{roz} = laboratory measured relative permeability to oil at z

k_z = permeability at any vertical level z

K = saturated hydraulic conductivity

K_x,K_y,K_z = saturated hydraulic conductivity in x, y and z direction respectively

K_{eff} = effective saturated hydraulic conductivity

K_g = geometric mean of saturated hydraulic conductivity

m, n= fitting parameters for Van Genuchten model for moisture retention function.

n_{eff} = effective n

M_{ijk} = spatial moment of moisture content distribution (i,j,k=0,1,2)

N= number of fluids present in the pore space

N_l= total number of elements/blocks in the domain

p^i = pressure of i_{th} fluid

q^i = volumetric flux of i_{th} fluid

r^2 = square of the coefficient of correlation

R^i = volumetric measure of any source and sink terms of i_{th} fluid

S^i = saturation in terms of i_{th} fluid

S_s= specific storativity

$\bar{S}_o$ = average oil saturation

S_{oz} = oil saturation at any vertical location z

t = time

t_0= time when infiltration stops

t_{cmd} = time taken by the center of mass of the moisture plume to reach at the mid-depth of the soil column.

TSI =transverse spreading index

TSI_H= transverse spreading index in heterogeneous medium

TSI_B= transverse spreading index in homogeneous medium with background soil properties

$v(\tau)$ = velocity of center of mass of moisture plume during redistribution

v_{inf} = constant velocity of center of mass during infiltration

V_{avg} = time average velocity during redistribution

V_{Havg}= average velocity of the moisture plume in heterogeneous medium.

V_{Bavg}= average velocity of the moisture plume in a homogeneous medium with background soil properties

V_o= total volume of oil in a particular pore space volume

V_p= total pore space volume

VSI =vertical spreading index

VSI_H= vertical spreading index in heterogeneous medium

VSI_B= vertical spreading index in homogeneous medium with

background soil properties

x, y, z = location of a point in x,y and z-direction respectively

x_c, y_c, z_c = coordinate locations of center of mass of moisture plume

z_0 = location of center of mass when infiltration stops

$z_{c(red)}$ = location of the center of mass of the moisture plume during redistribution

Greek symbol

α = fitting parameter of Van Genuchten model

α_{eff} = effective α

β_B, β_L = properties of background soil and lenses respectively

δ = increment in pressure head

θ = moisture content

θ_r = residual moisture content

θ_s = moisture content when the pore space is fully saturated

λ = correlation length of soil properties

μ' = viscosity of ith fluid

ξ = vertical distance traveled by the center of mass of the moisture plume during redistribution

ρ' = density of i_{th} fluid in multiphase flow

ρ_0 = reference fluid density

$\sigma^2_{\log K}$ = variance of logarithm of saturated hydraulic conductivity

$\sigma_x^2, \sigma_y^2, \sigma_z^2$ = measure of spreading of moisture plume around its center in three coordinate directions

σ_0^2 = spreading of moisture plume when infiltration stops

σ_c^2 = spreading of moisture plume at any time t.

τ = time period during which redistribution occur

ϕ_z = porosity at any vertical level z.

ϕ = porosity of a porous medium

Φ_n, Φ_α = heterogeneity index with respect to n and α

Chapter 1: Introduction

1.1 Objective and motivation for the research

Land surface and groundwater table are linked by the unsaturated zone. In the unsaturated zone, the voids - that is, the spaces between grains of gravel, sand, silt, clay, and cracks within rocks - contain both air and water. Water is held by capillary forces or in other words, the soil water pressure potential is negative in this zone. During the past few decades, the motivation to understand and manage the unsaturated zone started from its recognition as a key factor in the improvement and protection of the quality of groundwater supplies (Nielsen, et al., 1986).

Proper prediction of water flow in the unsaturated zone is vital in the study of the migration of contaminants because water flow and contaminant transports are interdependent processes. Any error in computing the flow and distribution of water will propagate errors in defining the spatial and temporal distribution of the contaminant plume. In contrast to the saturated zone (where voids of soil are filled with only water), the movement of water and contaminant in the unsaturated zone is a highly nonlinear process. This process is controlled by the relationships between soil water pressure, water content, and relative permeability. These constitutive relationships are central when attempt is made to predict or simulate the movement of the water flow in the unsaturated zone. The nonlinear nature of these constitutive relationships complicates the analysis of unsaturated flow.

Most hydraulic properties of soil are variable in space. Last couple of decades, the effect of spatial variation of soil hydraulic properties on predictions of subsurface flow has received a great deal of attention among researchers (Dagan and Bresler, 1983, Yeh et al., 1985, Mantoglou and Gelhar, 1987, Polman et al., 1991, Russo, 1992, Wildenschild et al., 1999). Acknowledging the presence of spatial variability of hydraulic properties in natural field soils, the question arises how to handle or account for this heterogeneity in numerical flow and transport model. This heterogeneity in soil properties is often an important control on the migration and distribution of water. To completely characterize the movement of water in a heterogeneous soil at field-scale, we first need to identify local values of all relevant soil properties. But for most practical purposes the detailed water distribution in heterogeneous soil is not of interest. Rather, we are commonly interested in more overall measures and assessments of the water movement. Further more, this approach is impractical because the data and computational requirements are unreasonable. Thus, we are motivated to derive effective parameters that incorporate the average effect of heterogeneities and can be employed in an equivalent homogeneous model of any soil domain.

The first step in dealing with effective parameters is to clearly define the term effective parameters. We define effective parameters as equivalent parameters which when used in a numerical simulator, produce the same results, on average, as would be predicted by a detailed heterogeneous flow simulation. Effective parameters can be estimated using variety of methods. These include: (a) calibration of a model based on

simulation of a given field experiment; (b) stochastic analysis; (c) use of an algorithm for estimating effective parameters based on known information from small scale experiments regarding the physical distribution of different soils in the field (e.g. layering, lenses of one soil in another). The work reported in this thesis relates to third approach. The objective of this research work is to investigate the feasibility of replacing a medium containing heterogeneities with an equivalent homogeneous medium for unsaturated flow. More specifically, it concerns an attempt to determine under what conditions it is possible to estimate effective properties to capture the average behavior of soil water movement in unsaturated zone of heterogeneous soil.

1.2 Literature review

The literature review regarding effective parameters in heterogeneous soil is organized as follows. First, we review the works, the goal of which is to estimate effective soil hydraulic parameters in saturated flow. Second is a review of works, which address the problem of estimation of effective parameters in unsaturated flow. Third, we review some work that has been done at pore scale level to estimate effective parameter in unsaturated soil. Fourth, we review the works on effective parameter in multiphase flow. The common aim of all these research works is to study the effect of local spatial variability of soil hydraulic properties in subsurface flow and to find the answer of the fundamental question how to incorporate this effect into large-scale description of subsurface flow.

In steady state saturated flow, geometric mean or harmonic mean of hydraulic conductivity can be used as effective parameter depending on the flow dimension. For one-dimensional flow the effective conductivity is equal to harmonic mean. For two-dimensional flow, geometric mean of the hydraulic conductivity best approximated the effective parameter. For three-dimensional flow, effective hydraulic conductivity must be higher than geometric mean. For low variances effective hydraulic conductivity (K_{eff}) can be expressed in terms of geometric mean hydraulic conductivity, K_g, (Gutjahr, 1978, Dagan, 1979,) as follows:

One dimension

$$K_{eff} = K_g\left[1-\left(\frac{\sigma^2_{\log K}}{2}\right)\right] \qquad (1.1)$$

where, $\sigma^2_{\log K}$ = variance of logarithm of hydraulic conductivity.

Two dimensions

$$K_{eff} = K_g \qquad (1.2)$$

Three dimensions

$$K_{eff} = K_g[1+(\sigma^2_{\log K}/6)] \qquad (1.3)$$

For unsteady flow, Dagan (1982b) found that effective hydraulic conductivity depends on statistics of the hydraulic conductivity distribution in space and also on time. The effective hydraulic conductivity decreases from the arithmetic mean at the early stage to the effective value given above by Dagan (1979).

Definition of effective parameters is more difficult in unsaturated zone because unsaturated flow is non-linear. In the saturated zone, the most common assumption is

that local physical flow models are valid on a large scale and the parameters of these models are smoothed functions of the local, and highly variable soil properties. In other words, aquifer properties are the mean of the local soil properties and it varies smoothly over space. This assumption allows estimation of the model parameters from a data set since these parameters are smooth functions of space unlike the local, and highly variable, soil properties. Mantoglou and Gelhar (1987) pointed out that the assumption used in saturated flow is inappropriate in the case of unsaturated flow to estimate model parameter. Instead, they developed large-scale model of transient unsaturated flow in heterogeneous soil. In deriving the general methodology for large-scale model, soil properties are treated as random variable. Probabilistic approach is used to incorporate the complex spatial variability of the actual soil properties through a practical framework requiring only a limited amount of information. The general form of the large-scale transient unsaturated flow model is derived by averaging the local governing flow equation over the ensemble of soil property realizations introducing two key assumptions. First, mean value of local soil properties do not vary significantly (are stationary) over several correlation lengths and time. This is an important feature because if it occurs, it implies some kind of repetition of the process. Thus there is a prospect that statistical interpretation can be based on analysis of a single realization. Second, it is reasonable to expect that statistical analysis of single realizations will be approximations of ensemble statistics (ergodic hypothesis) only if the overall length of sample is larger than the integral scale by at least an order of magnitude. Critics of stochastic model argue that these restricting assumptions are unreasonable especially for unsaturated flow concerning stationary assumptions.

Basically, the large-scale model has the same form as the classic small-scale equation of unsaturated flow (Richards equation). Parameters used in this modified form of equation are referred as effective parameter and are also random in nature. And these effective parameters can be evaluated in terms of the statistical properties (mean, covariances, correlation length) of the local soil properties. With these random effective parameters, the modified flow equation becomes random or stochastic partial differential equation. This stochastic equation is then solved to produce probabilistic results.

Mantoglou and Gelhar (1987) concluded that effective parameters of large-scale model depend upon the statistics of local variability of soil properties (i.e. variances, correlation lengths). They also found that the unsaturated flow system is highly nonlinear in the parameters, and the variability of the local soil properties has important large-scale effects such as hysteresis and anisotropy. This large-scale hysteresis effect is due to local spatial variability rather than to hysteresis of the local properties.

Some work has been done about the effect of heterogeneity at the pore-scale level on the pressure–saturation relationship by Ferrand and Celia (1992). The results of their work demonstrate that an effective moisture retention curve cannot be obtained by a simple averaging procedure. Effective curve in heterogeneous medium depends on the structure of the material and type of heterogeneity. They concluded in their paper that the underlying nonlinear nature of the moisture retention curve might have significant influence on the large-scale effective curve. Rahman (1994) evaluated the use of weighted average of hydraulic parameters as effective parameter. He concluded that this

simple averaging procedure might lead to significant errors in prediction of the position of the wetting front during infiltration.

Some work has been done on effective parameters in multiphase flow in a porous medium (Butts et el., 1996; Braun, 1998; Ataie-Ashtiani et al, 2001). Ataie-Ashtiani et al. developed a method to estimate effective parameters (pressure, saturation and relative permeability relationships) based on the concept of representative elementary volume (REV) for a periodic heterogeneous medium. Average permeability and constitutive relationships for the representative block were calculated numerically. They found that the upscaled relative permeability curves were directional dependent and anisotropy in relative permeability was a function of saturation. These relationships are referred as effective relationship or upscale relationships. Next, three different homogeneous simulations were run to capture the average effect of heterogeneity. First simulation ignored the presence of lenses i.e. effective parameters were considered to be same as background soil parameters. Second simulation considered only the effect of saturated permeability of lenses and ignored its two-phase flow characteristics. Third simulation included both saturated permeability and two-phase flow effects. The closest results to the detailed heterogeneous model were obtained with fully homogeneous model using effective parameters, which incorporated the effect of both saturated permeability and two-phase flow properties. However, the lateral spreading of DNAPL (Dense non-aqueous phase liquid) plume is underestimated and the vertical extent is overestimated when fine-grained lenses are embedded in coarse-grained soil.

In the literature of petroleum reservoir modeling, essentially horizontal flow in horizontal stratum of sedimentary rock is dealt with via a vertically averaging function called pseudo-functions. Two types of pseudofunctions have been widely used in reservoir studies: (a) vertical equilibrium pseudofunctions and (b) dynamic pseudofunctions.

The vertical equilibrium concept assumes that potential for each phase is constant vertically in every gridblock in the reservoir model. Vertical equilibrium pseudo-functions can be derived from vertical distribution of saturation and relative permeability by applying the following equations.

$$\bar{S}_0 = \frac{\int_0^d \phi_z S_{oz} dz}{\int_0^h \phi_z dz} = \frac{V_0}{V_p} \qquad (1.4)$$

$$k_{pro} = \frac{\int_0^d k_z k_{roz} dz}{\int_0^h k_z dz} \qquad (1.5)$$

Where ϕ_z = porosity at any vertical level z, $\bar{S}_0$ = vertically averaged oil saturation, S_{oz} = oil saturation at any vertical level z, d = formation thickness, V_0 = total volume of oil, V_p = total pore space volume, k_{pro} = pseudo-relative permeability to oil, k_z = permeability at any depth z, k_{roz} = laboratory measured relative permeability to oil at depth z.

2D cross sectional model is run with detailed vertical discretization for incorporating the effect of heterogeneity. Rock curves or laboratory measured pressure-saturation-relative permeability relationships for each type of rock are used in cross

sectional model. Cross sectional model results is used to approximate the pseudo capillary pressure and pseudo-relative permeability functions for a specific site using equation (1.4) and (1.5). Then these pseudo-functions can be used in 2D areal models of the entire field. This approach allows less expensive 2D models to be substituted for 3D models (Mattax and Dalton, 1990).

It is often not appropriate to assume vertical equilibrium in actual field situations. An alternative is to use dynamic pseudofunctions or introduce the third dimension in the simulator. Dynamic pseudofunctions are calculated from the cross sectional model results. At each run, the average water saturation and pseudo-relative permeabilities to oil and water are determined for each block of each column of the cross-sectional model. In contrast to vertical equilibrium pseudofunctions, dynamic pseudofunctions vary with location and with the oil depletion rate.

1.3 Outline of the thesis

This work is organized in seven chapters including the introductory chapter. Objective and motivation of the work has been described in the introductory chapter. As indicated in the previous sections, reliable application of computer models to field-scale flow depends on our ability to determine effective hydraulic properties describing the unsaturated flow. An outline of the remainder of the thesis follows.

In Chapter 2 the equations governing fluid flow in unsaturated porous media are presented. These equations are derived as a special case of general multiphase systems. The simplifying assumptions that result in the standard Richards equation are discussed, as are the properties of nonlinear unsaturated flow. Constitutive relationships proposed by Van Genuchten (1980), which are used in the computational model are described.

A brief description of the SPH3D3 flow model, which is used as a tool for numerical experiments for this research, is presented in Chapter 3. One additional routine is added to the original computer code to estimate the spatial moments (average behavior) of the transient moisture plume. Spatial moment calculations are based on the equation originally developed by Aris et al. (1956) for solute transport. The physical interpretation of zeroth, first and second spatial moments of moisture content distribution are given in this chapter. Comparisons of models for time rate of change of first spatial moment (velocity) of moisture plume are discussed. The best fitted model for redistribution velocity is selected. Also, we describe how spreading (second spatial moment) varies with vertical displacement (first spatial moment) of a moisture plume. The last section of this chapter describes how this selected redistribution velocity model and relationship between first and second spatial moment might be useful to estimate effective parameters.

The objective of Chapter 4 is to investigate the effect of constitutive relationships on average flow behavior of a moisture plume. Parameters describing the constitutive relationships are varied one at a time in a series of homogeneous simulations to develop

relationships between flow properties (average velocity, extent of spreading in transverse and vertical directions) of the moisture plume and the input parameters. Physical interpretations of theses relationships are discussed. Simulation results are used to develop Type Curves, which may be useful in estimating effective parameters for a heterogeneous medium.

In Chapter 5 we describe numerical experiments on the effects of heterogeneity in constitutive relationships on flow properties. Soil properties (other than unsaturated constitutive relationships) and initial & boundary conditions are chosen to be same as homogeneous simulations presented in Chapter 4. Both layered and random block heterogeneity of the soil medium with different degrees of contrast, different ratios of correlation length and different volumetric proportions of lenses are evaluated.

The effects of heterogeneity on the average flow properties are categorized into three types in Chapter 6. Then we evaluate the feasibility of effective parameters for each type of impact of heterogeneity. Chapter 6 also discusses what best can be done to capture the average effect of heterogeneity if no feasible effective parameters is found for a heterogeneous medium.

Finally, Chapter 7 concludes the thesis after summarizing the work presented in this thesis. Pertinent observations are put into perspective through a discussion of suggestions for future research.

Chapter 2: Unsaturated flow

2.1 Unsaturated flow equation

Flow in the unsaturated is more complex than flow in the saturated zone, because the variables (such as hydraulic conductivity) that govern the response of the system to environmental forcing are highly dependent on soil-water saturation. The governing equations of unsaturated flow can be derived from the basic mass conservation equation with the help of some constitutive relationships. Mass balance equations of fluids in a multiphase porous medium can be written as

$$\frac{\partial(\rho^i \phi S^i)}{\partial t} + \nabla.(\rho^i q^i) = R^i \qquad (i = 1, \ldots\ldots, N) \qquad (2.1)$$

where N = number of fluids present in the pore space; ρ^i = density of the fluid i; ϕ = porosity of the medium; S^i = percentage of pore space occupied by the fluid i; q^i = volumetric flux of fluid; R^i = volumetric measure of any source and sink terms of fluid.

If we assume that only two fluids, air (or soil gas) and water, exist in a naturally occurring unsaturated soil system, then the multiphase flow equation can be reduced to:

$$\frac{\partial(\rho^w \phi S^w)}{\partial t} + \nabla.(\rho^w q^w) = R^w \qquad (2.2)$$

$$\frac{\partial\left(\rho^a \phi S^a\right)}{\partial t} + \nabla\left(\rho^a q^a\right) = R^a \qquad (2.3)$$

where the superscripts w and a correspond to water and air respectively.

Solution of (2.2) and (2.3) for fluid velocities, pressure heads and saturation distributions within the flow domain and their time variations requires the addition of Darcy's equation and four constitutive relationships. The multiphase version of Darcy's equation can be stated as

$$q^i = -k_{ri}\frac{k}{\mu^i}\left(\nabla p^i + \rho^i g \nabla z\right) \qquad i = a, w \qquad (2.4)$$

Where k_{ri} = relative permeability of fluid i; k = intrinsic permeability of the medium; μ^i = Viscosity of the fluid i; $k\rho^i g/\mu^i = K_s$ = saturated conductivity; p^i = pressure in the fluid i; z = height from a reference datum, assumed positive downward. Additional constitutive equations must relate capillary pressure, fluid saturation and relative permeability.

Flow in the unsaturated zone is a special case of simultaneous flow of two immiscible fluids, because the gas phase can be assumed to be infinitely mobile relative to the water phase. Gas pressure is approximately constant usually taken as atmospheric pressure. This assumption implies that in the air-water system, the movement of air has insignificant effect on water movement through unsaturated zone. So we can eliminate

equation (2.3) from the system. If we also assume no mass transfer between phases ($R^w = 0$) and incorporate (2.4) then (2.2) becomes

$$\rho\phi\frac{\partial S}{\partial t}+S\frac{\partial(\rho\phi)}{\partial t}-\nabla.k_r(S)\frac{k\rho}{\mu}(\nabla p+\rho g\nabla z)=0 \qquad (2.5)$$

where the first term has been expanded and subscript w has been dropped.

To further simplify the equation, one can state that changes in fluid density and porosity are proportional to changes in pressure head. Numerous hydrologists have investigated this simplification and have found that it is not an unreasonable assumption (e.g. Freeze and Chery, 1979). The constant of proportionality is the specific storativity, S_s. After introducing the S_s and making some rearrangement, the final form of unsaturated flow equation becomes

$$\left[\frac{\partial\theta}{\partial t}+S_s\frac{\theta}{\varphi}\frac{\partial h}{\partial t}\right]-\nabla K(\theta)(\nabla h+\nabla z)=0 \qquad (2.6)$$

where $\theta = \phi S$ = moisture content; $K(\theta) = k_r(\theta)\, k\rho g/\mu$ = unsaturated hydraulic conductivity; $h = p/\rho g$ = pressure head; S_s = specific storativity. To solve these equations, constitutive relations between θ and h and between K and h (or K and θ) must be provided. The functional relationships $\theta(h)$ and $K(\theta)$ are strongly material dependent. Thus characteristics of the soil are reflected in these two relationships. These are the essential ingredients for predicting water flow in unsaturated soils. These functions are usually highly nonlinear, which means that the governing equation (2.6) is also highly

nonlinear. It is clear that heterogeneity in these functions adds more complexity to this problem. Note that in saturated flow, S =1 (i.e. $\phi = \theta$) and hydraulic conductivity is independent of moisture content. Therefore, equation (2.6) also describes saturated flow.

2.2 Functional forms of the constitutive relationships

Direct methods to determine the unsaturated hydraulic conductivity functions are time consuming and expensive. An attractive alternative to direct measurement is the theoretical calculation of the hydraulic conductivity from moisture retention characteristic curves. Moisture retention curves for a particular soil can be determined by either of two approaches. The first approach is to actually measure the soil moisture retention curve directly in the laboratory. Incremental equilibrium methods allow the soil to come to equilibrium at some moisture content θ, and then water pressure is measured. Next θ is changed and time is allowed for equilibrium to reestablish and capillary pressure is measured again. The process is repeated until a sufficient number of $h - \theta$ points have been measured to define the entire curve. The second approach (indirect method) is to make use of regression equations to predict the moisture content at specified values soil-water potential using properties such as particle-size distribution, percentage of organic matter, and bulk density. Much work has already been invested in the development of this technique (Ghosh, 1980, Gupta and Larson, 1979; Rawls et al., 1983). For example, Gupta and Larson (1979) used multiple linear regression equation of the form

$$\theta = A_1(\%\,\text{sand}) + A_2(\%\,\text{silt}) + A_3(\%\,\text{clay})$$
$$A_4(\%\,\text{organic matter}) + A_5(\text{bulk density, g/cm}^3) \qquad (2.7)$$

to predict the soil water content, where A_1, A_2, A_3, A_4 and A_5 are regression coefficients. A table of these regression coefficients are developed for 12 given soil-water potentials. The majority of the research has been concentrated on the water contents between –4 kPa and -1500 kPa capillary pressures. Intermediate values could be linearly interpolated between the calculated points. Mishra et al.(1989) estimated the retention characteristic from particle size distribution of 250 soils and evaluated the parameter uncertainty. Despite relatively promising results, these methods are rather empirical and still require quite a significant amount of secondary information about the investigated soil.

Once a series of the retention points are measured, they are commonly approximated by empirical models for use in numerical simulation models. While a variety of empirical functions describing the pressure ~ moisture relationship have been discussed in the literature, empirical functions proposed by Brooks and Corey (1964) and Van Genuchten (1980) are the most popular among unsaturated flow modelers. As compared to the Brooks and Corey function, the Van Genuchten function has the favorable property that its derivative is continuous and moves asymptotically toward zero at residual and full saturation. For the work reported here, we use Van Genuchten model in which the moisture retention function is given by

$$\theta = \theta_r + \frac{\theta_s - \theta_r}{\left[1 + |\alpha h|^n\right]^F} \qquad (2.8)$$

where θ_r and θ_s are residual and field-saturated volumetric water contents, respectively, and α and n are empirical parameters. While these empirical parameters arise from curve

fitting to experimental data, in the literature their relations to physical soil properties have been discussed. Larger values of n correspond to very uniform soils, which drain or imbibe over a relatively small range of capillary pressures. Alternatively it can be said that parameter n is a measure of the steepness of the moisture retention curves. (Rajaram et al., 1997). The inverse of the parameter α is analogous to the air entry pressure of the soil, i.e., small values of α are characteristic of soil profiles with large capillary fringe areas. In general, we can say that finer soil has lower α. And higher n represents soil with uniform pore size distribution; lower n indicates more variability in pore sizes. The values of α in Van Genuchten relationships for soils are roughly in a range of 0.004 to 0.15 cm^{-1} (Carsel and Parrish, 1988). It was found from the literature, the usual range of n is between 1 and 10. (Warrick, 1991). Table 2.1 shows some soil parameters reported in the literature. VG parameter values are compiled in Table 2.2 according to soil textural groups by Carsel and Parish (1988). Figure 2.1 illustrates the effect of α and n on the $\theta(h)$ curves. Using the simplifying assumption that m =1-1/n, (2.8) can be combined with the model of Mualem (1976) to yield an expression for unsaturated conductivity.

$$K(h) = K_s \frac{\left[1 - |\alpha h|^{n-1}\left\{1 + |\alpha h|^{n}\right\}^{-(n-1)/n}\right]^2}{\left[1 + |\alpha h|^{n}\right]^{(n-1)/2n}} \qquad (2.9)$$

These combined water-retention-hydraulic conductivity models have been widely used for numerical modeling of soil water movement. Figure 2.2 shows the effects of α and n on relative permeability functions. Relative permeability is the ratio between unsaturated hydraulic conductivity and saturated hydraulic conductivity.

Prediction of soil water movement in a given unsaturated soil requires knowledge of these constitutive relationships. Since we use the combined water-retention-hydraulic conductivity model proposed by Van Genuchten in our studies and do not vary the saturated hydraulic conductivity, VG parameters n and α can be said to fully characterize our soils.

In the real world, soil is rarely homogeneous and this makes prediction even more difficult. We will investigate the effect of spatial variability of these two parameters on soil water flow. We attempt to learn whether a single set of these parameters (n_{eff}, α_{eff}) used in a homogeneous model can replace the natural heterogeneity of these two parameters and capture the average movement of moisture.

Table 2.1 Van Genuchten and other soil parameters reported in the literature.

	depths	α, cm^{-1}	n	θ_s	θ_r	K_s cm/s
Yolo light Clay (Warrick, 1985)		0.015	2.0	0.495	0.124	$1.23x10^{-5}$
Glendale Clay loam (Hills, 1989)		0.0104	1.39	0.469	0.106	$1.52x10^{-4}$
Berino Loamy sand (Bouloutas, 1989)		0.028	2.239	0.3658	0.0286	$6.26x10^{-3}$
Field Site in Las Nutrias, NM (Mohanty et al. 1997)	0-40 cm	0.004/ 0.015	1.44/ 1.55	0.484/ 0.475	0.08/0.12	$4.08x10^{-3}$/ $9.5x10^{-4}$
	40-100 cm	.01/.021	1.25/ 1.38	0.464/ 0.459	0.045/ 0.05	$3.5x10^{-3}$/ $6.8x10^{-4}$
	100-700 cm	.063/ .083	2.12/ 2.12	0.43/ 0.43	.07/.09	$2.73x10^{-3}$/ $2.73x10^{-3}$
Cape Cod Site soil Gravel to coarse sand, (Stevens, 1994)		0.08	3.47	0.34	0.06	K_z=0.099 K_x=0.123
Las Cruses field site soil (Wierenga, 1994)	0-15 cm	.042	1.90	0.3483	0.09	$6.23x10^{-3}$
	540-600 cm	.046	1.43	0.3060	0.077	$2.61x10^{-3}$
Beit Netofa Clay (Vogel, 2001)		0.0017	1.17	0.45		
Coarse Sand (Schroth et al. 1996)		0.151	7.35	0.35	0.034	

Table 2.2 Average values of VG soil hydraulic parameters for 12 major soil textural groups according to Carsel and Parrish (1988).

Texture	α, cm^{-1}	n	θ_s	θ_r	K_s, cm/day
Sand	0.145	2.68	0.430	0.045	712.80
Loamy sand	0.124	2.28	0.410	0.057	350.20
Sandy loam	0.075	1.89	0.410	0.065	106.10
Loam	0.036	1.56	0.430	0.078	24.960
Silt	0.016	1.37	0.460	0.034	6.00
Silt loam	0.020	1.41	0.450	0.067	10.80
Sandy clay loam	0.059	1.48	0.390	0.100	31.44
Clay loam	0.019	1.31	0.410	0.095	6.24
Silty clay loam	0.010	1.23	0.430	0.089	1.68
Sandy clay	0.027	1.23	0.380	0.100	2.88
Silty clay	0.005	1.09	0.360	0.070	0.48
Clay	0.008	1.09	0.380	0.068	4.80

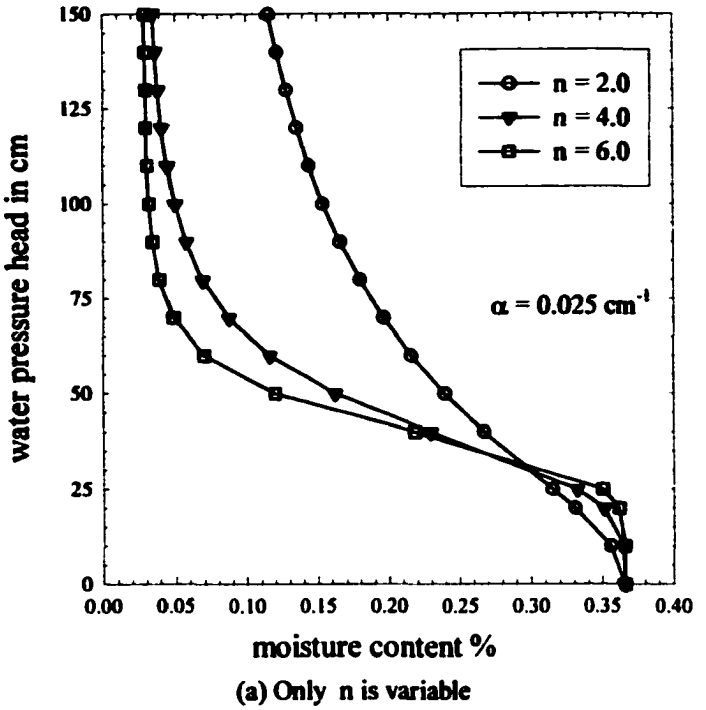

(a) Only n is variable

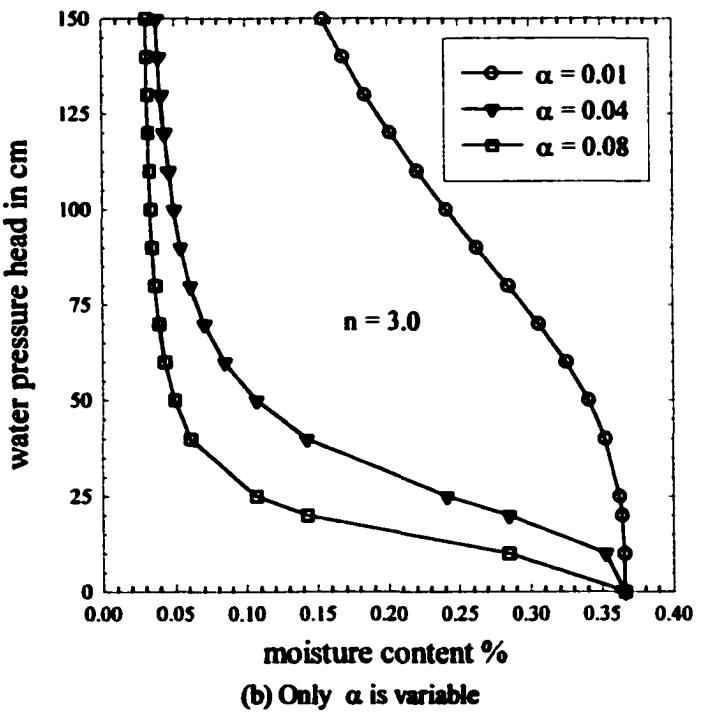

(b) Only α is variable

Figure 2.1 Effect of variability of Van Genuchten parameters on the moisture retention curve.

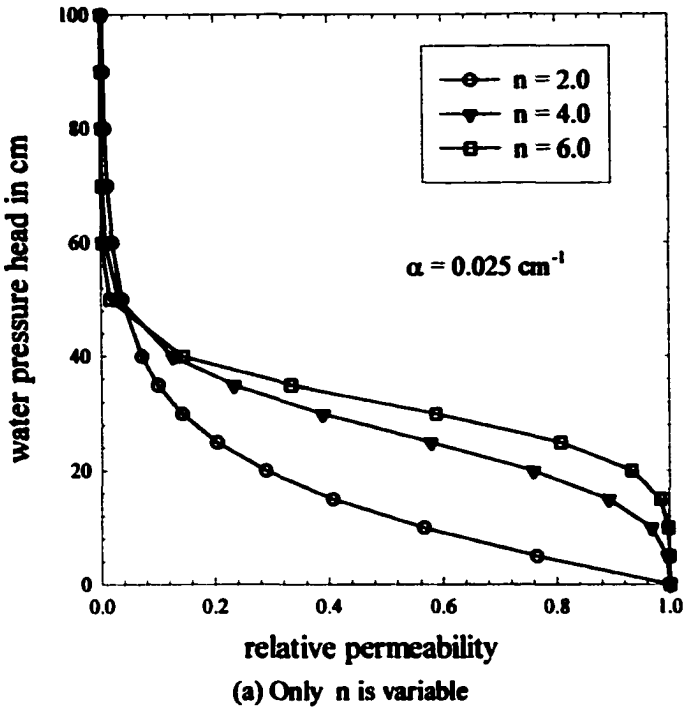

(a) Only n is variable

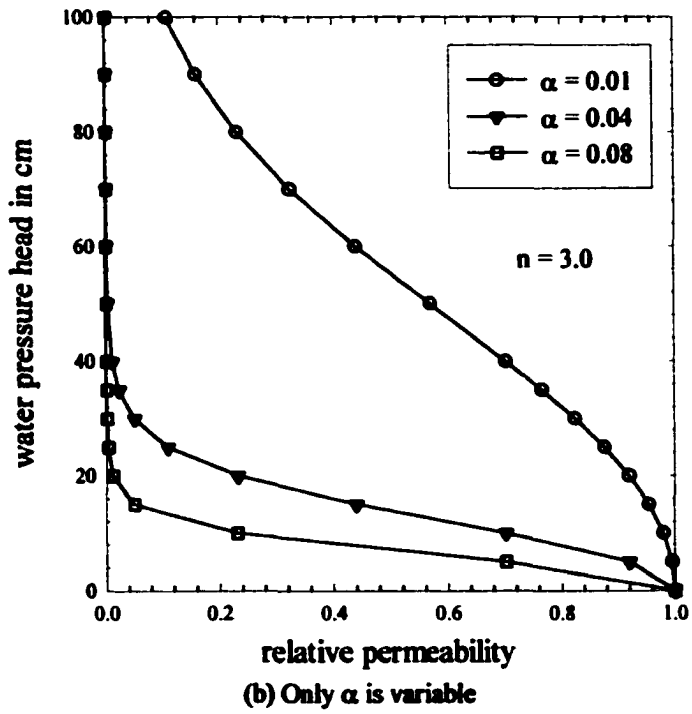

(b) Only α is variable

Figure 2.2 Effect of variability of Van Genuchten parameters on the relative permeability curve.

Chapter 3: The computational flow model

3.1 Subsurface flow models

Subsurface flow models simulate the movement of one or more fluids in porous or fractured rock system. The goal of subsurface modeling is to predict the value of an unknown variable such as water pressure head or the moisture content distribution in a porous medium in time and space. In developing a subsurface flow model, the first step is to develop a conceptual model consisting of a description of the physical process, which governs the behavior of the system. The next step is to transform the conceptual model into mathematical expressions, which are usually a set of partial differential equations.

In order to solve these equations, boundary conditions and, for transient simulations, initial conditions are necessary. Boundary conditions for flow simulation may be any of three types: (1) specified head (Dirchlet or first type), (2) specified flux (Neumann or second type) and (3) head dependent flux (Cauchy, mixed or third type). Boundary conditions are specified on the periphery of the modeled domain, either at the boundary or at locations within the system where system responses are fixed. Finally, solutions of flow equations can be derived by either analytically or numerically depending on geometries of the domain and on boundary condition. The most common numerical formulations for approximating the partial differential equations of flow include: (a) finite difference method and (b) finite element method.

Two major advantages of Finite element methods over Finite difference methods are as follows:

(1) Non-rectangular complex geometry of domain can be modeled.

(2) Large change of dependent variable over a small distance can be captured more accurately (i.e. less numerical dispersion).

3.1.1 SPH3D3

In this thesis, the computational model used is SPH3D3, which was developed by Michael A Celia, of the Department of Civil and Environmental Engineering at Princeton University. This model solves the three-dimensional flow and solute transport equations. Both saturated and unsaturated flow can be simulated by this model. The numerical solution is based on finite element methods. The flow equation that can be solved by model SPH3D3, can be written as follows:

$$\frac{\rho}{\rho_0}\left[\frac{\partial\theta}{\partial t}+S_s\frac{\theta}{\phi}\frac{\partial H}{\partial t}\right]+\frac{\theta}{\rho_0}\frac{\partial\rho}{\partial c}\frac{\partial c}{\partial t}-\nabla\cdot K\cdot\left(\nabla H+\frac{\rho}{\rho_0}\nabla z\right)=\frac{R^w}{\rho} \qquad (3.1)$$

where ρ_0 = reference fluid density (M/L3)

H = pressure head (L) $\equiv p/(\rho_0 g)$

c = concentration of dissolved contaminant (M/L^3)

Since there is no solute involved in the numerical experiment that will be performed for this study, moisture density is not a function of solute concentrations. Therefore, reference fluid density (ρ_o) becomes equal to constant moisture density (ρ). Upon

substituting $\rho_o = \rho$ and $R^w = 0$ (no sink or sources), Equation (3.1) can be transformed into equation (2.6).

3.1.2 Numerical solution method

Equation (2.6) with the Van Genuchten expressions for the constitutive relationships (2.8) and (2.9) are solved numerically using lumped finite element in space and a fully implicit (backward Euler) time stepping algorithm. Finite element approximations tend to "distribute" the approximation for the time derivative to several nodal points in space (Celia et al., 1990). Lumping eliminates this spatial distribution, thereby evaluating the time derivative term at one node only.

If unsaturated conditions are present, then an iterative solution procedure is used to solve the resulting nonlinear equations. Let integer u denote discrete time level, and v denotes iteration level. The discrete approximation to pressure head at node i and time level u is denoted by h_{iu}, while the approximation at node i, time level u+1, and iteration level v is $h_{iu+1,v}$. Assume that the solution has been determined for all time steps up to and including u. That is, if h_u denote pressure head at time $t = t_u$ then these values are known at all discrete spatial locations in the domain. To solve for the solutions h_{u+1} at the next time level t_{u+1}, the first step is to determine the velocity field at time t_u. This is accomplished by via Darcy's equation (equation (2.4) when i = w), using pressure head solution at time level u. Now for iterative process, at given time step u+1, h_{v+1} are determined using known information at iteration level v. In the next iteration h_{v+2} will be

estimated. Iteration continues until the increment in pressure head $\delta^m = h^{n+1,m+1} - h^{n+1,m}$ is reduced sufficiently small, and the governing equation is solved with acceptable degree of accuracy.

3.1.3 Features of the code

All approximating equations are developed using element-by-element integration procedures in the standard finite element paradigm (Celia, 1992). Basis functions for pressure head are tri-linear, and all finite elements are eight node (possibly nonrectangular) cubes. The grid geometries are restricted to rectangular in the horizontal (x, y) plane, while the vertical (z) direction can have non-uniform node spacing. Boundary conditions can be time-varying, and it is possible to specify three different types of initial condition, (1) initial pressure head constant at all nodes (2) any arbitrary initial conditions, (3) for hydrostatic initial conditions at all nodes.

3.2 Input parameters

The primary unknowns in this set of numerical equations are the pressure heads h_{iu}, ($i = 1,\ldots N_l$; $u = 0, \ldots t_{max}$) where N_l = number of elements. Functional dependencies that must be specified as part of the input to the problem are: $\theta = \theta(h)$, and $K = K(h)$. Because the code uses the VG model, these functions are fully specified by specifying n, α, θ_r, θ_s and K_s. If the system is saturated, the difficult nonlinear dependencies between θ and h and between k_r and θ disappear ($\theta = \phi$ and $k_r = 1$ in this case).

3.3 Spatial moment analysis

The ultimate goal of this investigation is to determine whether it is feasible to estimate the effective moisture retention and relative permeability functions for a heterogeneous soil. The first step toward achieving this goal is to define average soil water flow in soils. One way to define average quantitative descriptions of soil water flow is by spatial moment analysis. The next step is to comprehend the sensitivity of the first and second spatial moment of the moisture plume to α and n. First spatial moment of the moisture plume, normalized by mass of water, is equal to the location of center of mass of the plume. The second spatial moment about the center of mass is a measure of the spreading or dispersion of moisture plume.

3.3.1 Moisture distribution calculation

In any finite difference/finite element flow simulation, pressure heads or moisture contents are calculated at discrete points in space: these points are termed the nodes of the mesh. Models are frequently described as either block centered or mesh-centered depending on the way in which hydraulic parameters are specified in relation to the nodes. Under a block-centered scheme, the domain of simulation may be visualized as divided into cells or blocks surrounding each node; these cells are separated by grid lines or interfaces between adjacent nodes, as in Figure 3.1(a). Hydraulic properties are normally specified for each cell, and are considered uniform within the cell.

Under the mesh-centered scheme, the nodal points are located at the intersections of the grid lines, as in Figure 3.1(b). The dashed lines in Figure 3.1(b), located half way between adjacent nodes, serve to differentiate different regions for which hydraulic properties are specified in the mesh-centered scheme. Soil properties such as moisture retention function or hydraulic conductivity in a given direction are specified over an interval aligned in that direction and extending the full distance between adjacent nodes. A resultant hydraulic conductivity is calculated for the interval between adjacent nodes, in each coordinate direction, prior to initiation of the actual numerical solution procedure (Bennett et al., 1995).

The computer program used in this research work is uses a mesh-centered domain. Since we are primarily interested in moisture plume development, we would like to have moisture content instead of pressure head at each node. The transformation of pressure head distribution to moisture distribution can be done simply by using constitutive relationship ($\theta \sim h$ relationship) in homogeneous simulation where soil properties are same all over the domain. But in case of heterogeneous simulation, there will be discontinuity in moisture content (two different moisture content at each node) at those nodes lie on the boundary between two different soil regions. To offset this problem, a small change has been made to modify the code to calculate the moisture content at the center of the grid block. This is done by estimating moisture content at each of 8-nodes of the rectangular block and then averaging the moisture content. We assume that this moisture content is average for the block or cell and location of this moisture content is right at the center of the block.

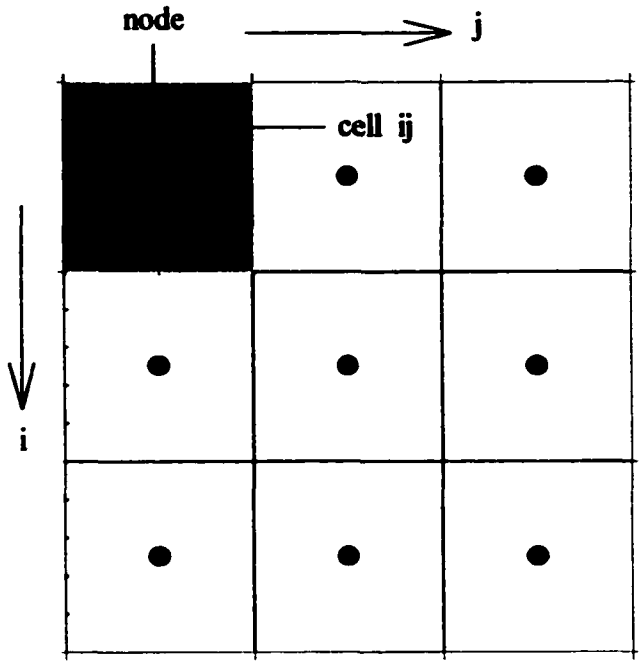

(a) Block-centered

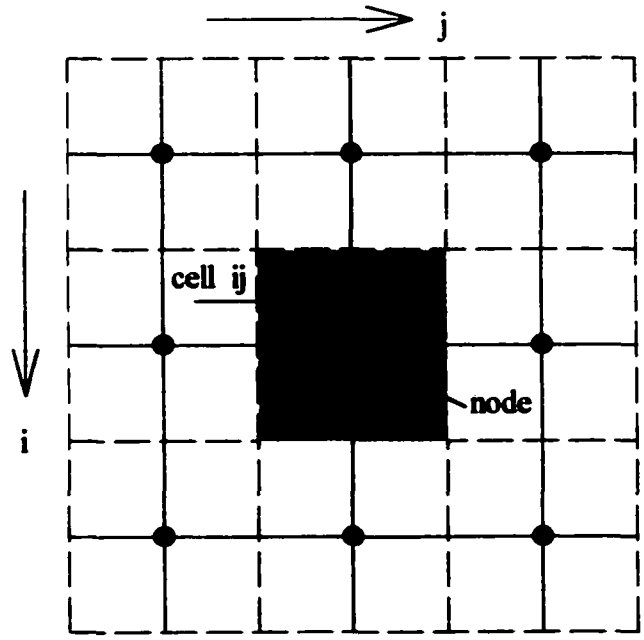

(b) Mesh-centered

Figure 3.1 Illustration of block-centered and mesh-centered finite element (rectangular) grids.

3.3.2 Spatial moments calculation

Routines to calculate first and second spatial moments of incoming water have been added to the main code (see Appendix). Three dimensional spatial moment calculations are based on the following equation (after Aris, 1956)

$$M_{ijk}(t) = \int_{-\infty}^{\infty}\int_{-\infty}^{\infty}\int_{-\infty}^{\infty}\rho\theta(x,y,z,t)\, x^i\, y^j\, z^k\, dx\, dy\, dz \qquad (3.2)$$

In this study, we focus on the zeroth, first and second moments. Therefore, the value of i, j, k could be 0, 1 or 2 depending on the spatial moment being evaluated. These moments provide measures of the mass, location, and spread of the moisture plume. The first moment about the origin, normalized by mass of new water, defines the coordinate location of the center of mass (x_c, y_c, z_c):

$$x_c = M_{100}/M_{000} \qquad (3.3a)$$

$$y_c = M_{010}/M_{000} \qquad (3.3b)$$

$$z_c = M_{001}/M_{000} \qquad (3.3c)$$

The second moment about the center of mass defines a spatial covariance tensor. The principal components of the tensor can be calculated as (after Freyberg, 1986):

$$\sigma_x^2 = M_{200}/M_{000} - x_c^2 \qquad (3.4a)$$

$$\sigma_y^2 = M_{020}/M_{000} - y_c^2 \qquad (3.4b)$$

$$\sigma_z^2 = M_{002}/M_{000} - z_c^2$$

$$\sigma_z^2 = M_{002}/M_{000} - z_c^2 \qquad (3.4c)$$

The physical interpretation of these tensor components is the spreading of the moisture plume around its center. So if we know first and second spatial moment of moisture distribution at each time step, we can get an overall picture of how the moisture plume changes its position and shape with time.

The three dimensional integral (3.2) can be evaluated numerically by a set of algebraic equations. As a first step in the procedure, we need to estimate the total mass of water that has been introduced during infiltration, i.e., the zeroth spatial moment. For the zeroth spatial moment the values of i, j, and k of equation (3.2) become zero. Since it is assumed that the moisture content within each element is constant and if the density of water is taken to be unity throughout the domain, total mass of incoming water can be estimated as:

$$M_{000} = \sum_{i=1}^{N_i} \theta_i \Delta x_i \, \Delta y_i \Delta z_i \qquad (3.5)$$

where θ_i = moisture content in element i minus initial moisture content in element i; Δx_i = grid spacing for i_{th} element in x direction; Δy_i = grid spacing for i_{th} element in y direction; Δz_i = grid spacing for i_{th} element in z direction.

The second step is to evaluate the integral equation (3.2) for first spatial moment along the coordinate axes. The first spatial moment in x, y, and z-direction can be estimated by the following equations respectively:

$$M_{100} = \sum_{i=1}^{N_i} \theta_i \Delta y_i \Delta z_i \left(\frac{x_{i+1/2}^2 - x_{i-1/2}^2}{2}\right) \qquad (3.6a)$$

$$M_{010} = \sum_{m=1}^{N_i} \theta_i \Delta z_i \Delta x_i \left(\frac{y_{i+1/2}^2 - y_{i-1/2}^2}{2}\right) \qquad (3.6b)$$

$$M_{001} = \sum_{i=1}^{N_i} \theta_i \Delta x_i \Delta y_i \left(\frac{z_{i+1/2}^2 - z_{i-1/2}^2}{2}\right) \qquad (3.6c)$$

where, $x_{i+1/2}$, $x_{i-1/2}$ = x-coordinate of right and left boundary of the i_{th} element respectively; $y_{i+1/2}$, $y_{i-1/2}$ = y-coordinate of front and back boundary of the i_{th} element respectively; $z_{i+1/2}$, $z_{i-1/2}$ = z-coordinate of bottom and top boundary of the i_{th} element respectively.

The final step is to evaluate the integral equation (3.2) for second spatial moment along the coordinate axes. The second spatial moment in x, y, and z-direction can be estimated by the following equations respectively:

$$M_{200} = \sum_{i=1}^{N_1} \theta_i \Delta x_i \Delta y_i \Delta z_i \left(\frac{x_{i+1/2} + x_{i-1/2}}{2} \right)^2 \quad (3.7a)$$

$$M_{020} = \sum_{i=1}^{N_1} \theta_i \Delta x_i \Delta y_i \Delta z_i \left(\frac{y_{i+1/2} + y_{i-1/2}}{2} \right)^2 \quad (3.7b)$$

$$M_{002} = \sum_{i=1}^{N_1} \theta_i \Delta x_i \Delta y_i \Delta z_i \left(\frac{z_{i+1/2} + z_{i-1/2}}{2} \right)^2 \quad (3.7c)$$

3.4 Analysis of the first spatial moment.

The computational method to estimate spatial moments described above may be used to investigate the influence of VG parameters on the mean flow movement of the moisture plume. An example of transient first spatial moment evolution is shown in Figure 3.2. The first part of the plot represents moisture plume displacement during infiltration and the other part of the plot represents moisture plume displacement during redistribution. The slope of this curve represents the velocity of the center of mass of the moisture plume. As we can see from the Figure 3.2, velocity during infiltration is constant. In other words, the first spatial moment varies linearly with time during infiltration. But during redistribution, the relationship between first spatial moment and time is not linear. Three model equations: a simple power law, a modified power law and exponential model were tested for usefulness in quantifying the transient velocity of the plume during redistribution.

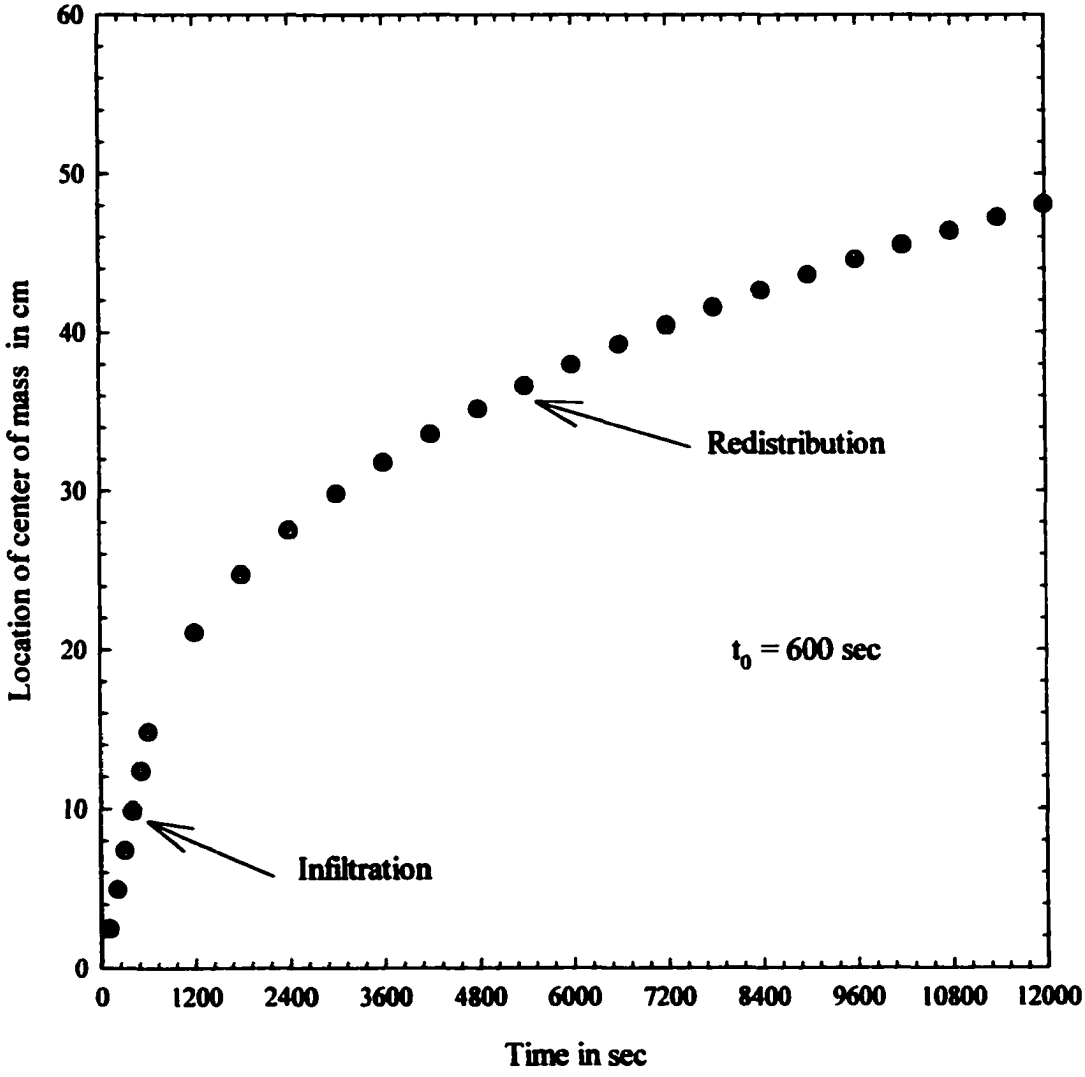

Figure 3.2 Evolution of transient first spatial moment of moisture distribution in 1D soil colum when constant flux is applied on the top boundary for 600 sec (n = 4.25 and α = 0.045)

3.4.1 Simple power law

The location of the center of mass of the moisture plume during redistribution ($z_{c(red)}$) can be represented by a simple power law relationship

$$z_{c(red)}(\tau) = z_0 + \left(\frac{k_1}{1-k_2}\right)\tau^{(1-k_2)} \qquad (t > t_0) \qquad (3.8)$$

where $z_0 = z_c$ at $t = t_0$, t_0 = time when redistribution starts; $\tau = t - t_0$, and k_1 and k_2 are fitting parameters.

$$\text{Or, } \xi(\tau) = \left(\frac{k_1}{1-k_2}\right)\tau^{(1-k_2)} \qquad (3.9)$$

where $\xi = z_{c(red)} - z_0$. Equation (3.9) can be differentiated to get the transient redistribution velocity

$$v(\tau) = \frac{d\xi}{d\tau} = k_1\tau^{-k_2} \qquad (3.10)$$

While this model provides a good description of simulation data for most values of τ, v becomes unrealistically large at small times. In fact, rather than approaching the constant infiltration velocity v_{inf}, $v(\tau)$ approaches infinity as τ approaches zero. This fact motivated the investigation of two other empirical models.

3.4.2 Modified power law model

An alternative power-law based model for the location of the center of plume mass during redistribution can written as

$$\xi(\tau) = (v_{inf})\tau - \left(\frac{k_1}{1+k_2}\right)\tau^{(1+k_2)} \qquad (3.11)$$

Equation (3.11) can be differentiated to give an alternate expression for redistribution velocity

$$v(\tau) = v_{inf} - k_1\tau^{k_2} \qquad (3.12)$$

while this model also provides a good fit to simulation data over most values of τ, and eliminates major discrepancies for small τ, it fares poorly at large τ. In fact, equation (3.12) predicts that v (τ) will become negative as $\tau \rightarrow \infty$. This clearly non-physical behavior proves to be greater disadvantage in modeling simulation data than the small τ discrepancy inherent in (3.12).

3.4.3 Exponential growth to a maximum

A third empirical model is suggested by the observation that the location of the center of mass of the plume seems to asymptotically approach a maximum value of z_c as its velocity approaches zero. This behavior can be expressed as

$$\xi = \frac{k_1}{k_2}(1 - e^{-k_2\tau}) \qquad (3.13)$$

which may be differentiated to find velocity

$$v(\tau) = k_1 e^{k_2\tau} \qquad (3.14)$$

Unfortunately application of this model to sample simulation data provides unsatisfactory results. If we apply the initial condition ($v(\tau = 0) = v_{inf}$) to (3.14), we find that k_1 should be equal to the infiltration velocity; fits to sample data consistently result in larger values

of k_1. Even more problematic is the fact that fit values of $\frac{k_1}{k_2}$ have been found to be highly sensitive to the maximum simulation time.

3.4.4 Selection of redistribution velocity model

From the comparative analysis of the above three models, it appears that the simple power law model is the best model for the transient first spatial moment during redistribution. Therefore, equation (3.10) is selected as the model for redistribution velocity of the center of mass of moisture plume despite its limitation at early stage of simulation. Next, we see how it affects our research objective because of disregarding this limitation of redistribution velocity model.

As we mentioned in section 3.4.1, at $\tau = 0$

$$v(\tau) = v_{inf} \tag{3.15}$$

Substituting the expression for $v(\tau)$ in (3.15)

$$k_1(\tau)^{-k_2} = v_{inf} \tag{3.16}$$

Rearranging the variables, τ becomes

$$\tau = \left(\frac{k_1}{v_{inf}}\right)^{\frac{1}{k_2}} \tag{3.17}$$

Therefore, model predicted redistribution velocity approaches to infiltration velocity not at $\tau = 0$ but some later time when $\tau = \left(\frac{k_1}{v_{inf}}\right)^{\frac{1}{k_2}}$. In other words, the model is not valid

when $0 \le \tau \le \left(\frac{k_1}{v_{inf}}\right)^{\frac{1}{k_2}}$. It has been observed from simulation data analysis that the value of term $\left(\frac{k_1}{v_{inf}}\right)^{\frac{1}{k_2}}$ is very small in comparison to total length of simulation time. It has also been observed that the difference between the simulation data and fitted model is diminishing as τ becomes larger. An example is shown in Figure 3.3. Since we will use this redistribution velocity model for comparison purposes (between velocity through homogeneous and heterogeneous medium), this type of model discrepancy is less likely to affect our overall research goal.

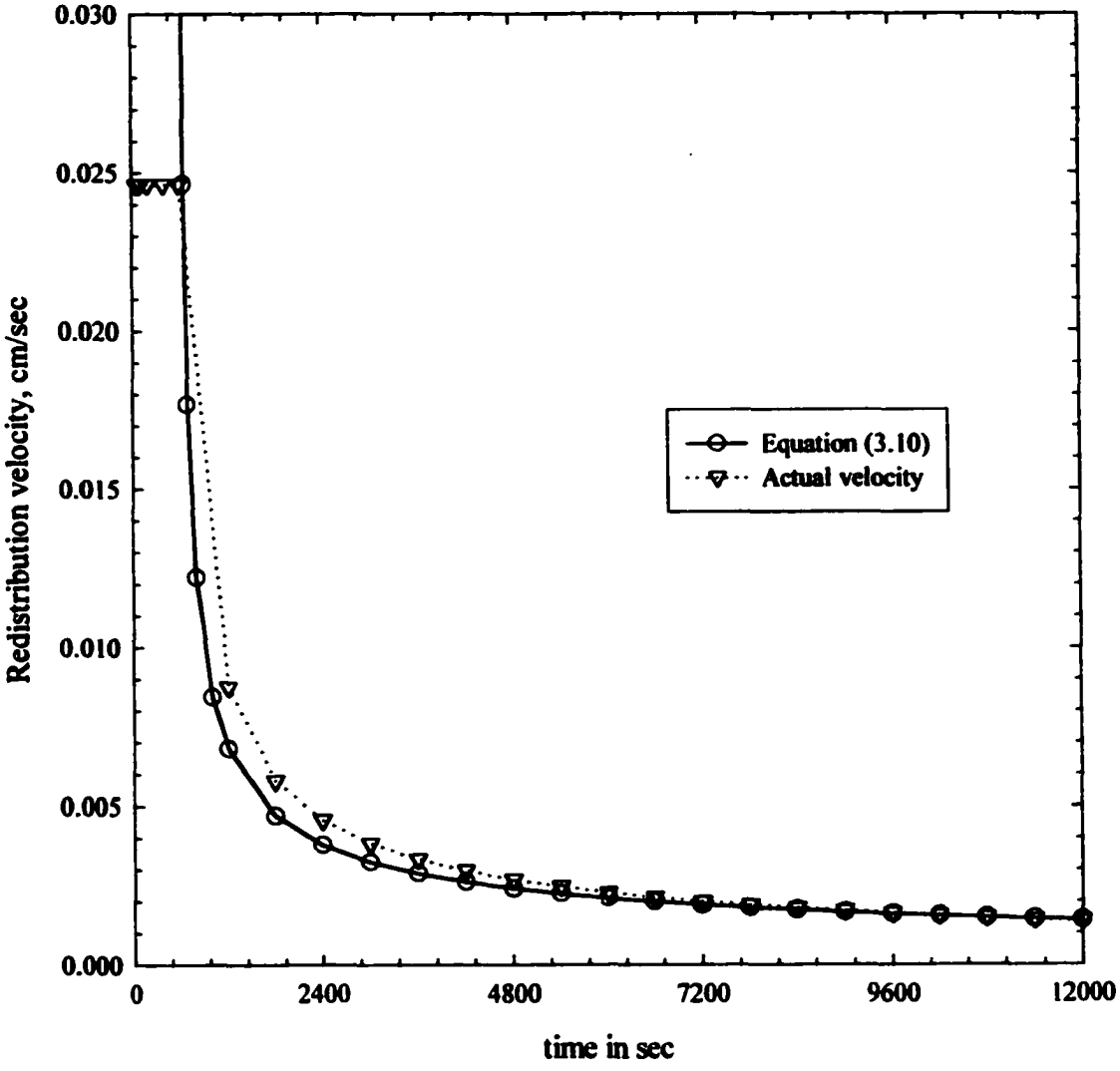

Figure 3.3 Transient redistribution velocity: comparison between actual velocity (based on flow simulation results) and modeled velocity (using power law equation).

3.5 Analysis of second spatial moment

There is a strong linear trend to the second spatial moment and vertical distance traveled by the center of mass of the moisture plume (correlation coefficient, r = 0.97). This is shown in Figure 3.4. Therefore, we will use the linear model for the transient second spatial moment. Slope of the change in second spatial moment with respect to the vertical travel distance of the center of mass can be defined as vertical spreading in, which is described by the following equation:

$$\sigma_c^2 - \sigma_0^2 = k_3(z_c - z_0) \qquad (5.18)$$

where σ_c^2 is the second spatial moment when the location of center of mass is at z_c. σ_0^2, z_0 are the second spatial moment and vertical location of center of mass respectively at $\tau = 0$. The constant of proportionality will be called the vertical spreading index (VSI).

3.6 Methodology

The effective hydraulic parameters of a heterogeneous soil can be derived by conceptualizing the heterogeneous medium as an equivalent homogeneous medium. Under the same boundary condition and infiltration rate, homogeneous simulation using effective parameters should predict the same location of the center of mass of the moisture plume and the same spreading around the center of the moisture plume as are observed in the heterogeneous soil. In other words, the velocity and the extent of the moisture plume in heterogeneous soil should be predicted by a homogeneous simulation using effective parameters. Our attempt to estimate effective parameters will be to

minimize the difference in velocity and spreading of the moisture plume for heterogeneous and equivalent homogeneous medium with the aid of relationship between flow properties and VG parameters. To achieve this goal, first a series of transient spatial moments for a range of VG parameters for homogeneous soils was calculated. Chapter 4 is committed to develop a relationship between flow properties and VG parameters.

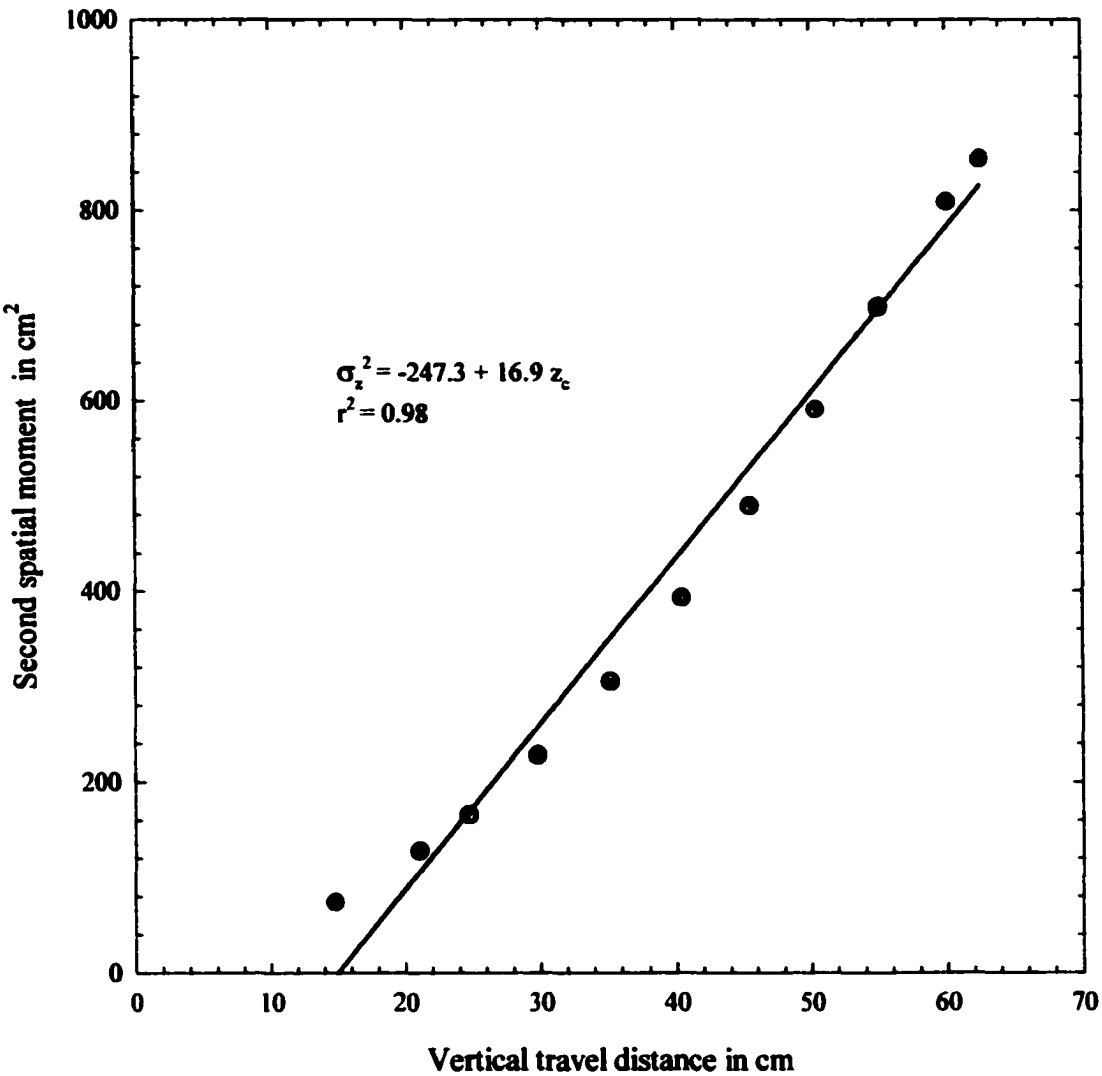

Figure 3.4 Change in second spatial moment of moisture distribution with vertical travel disatnce in 1D soil column when constant flux is applied on the top boundary for 600 sec (n = 4.25 and α = 0.045)

Chapter 4: Homogeneous simulations

4.1 One dimensional flow simulations

In the work described below a series of computational experiments is performed to observe how VG parameters affect the mean behavior of the soil water movement in one-dimensional simulations. It is also important to identify any interactions between boundary and VG parameters. Since it is important to identify whether boundary condition has any effect on the spatial moment calculations, different types of boundary conditions have been explored.

The soil properties other than VG parameters used for this study are taken from a Berino loamy sand soil (Boultous, 1989). The soil properties are as follows: saturated hydraulic conductivity in vertical direction, K_s = 6.25x10^{-3} cm/sec; θ_s = 0.3658; θ_r = 0.0286; ϕ = 0.3658; S_s = 1.0x10^{-5}. For one-dimensional case the domain size was 10x10x200 cm. The spatial discretization was set to 10 cm. in all directions. Initial pressure head was set to h = -2400 cm at each node to make the soil column at its residual saturation state. Zero flux boundary conditions are imposed on all sides of the boundary except top and bottom boundary. Bottom boundary condition remains the same as the initial condition.

4.1.1 Infiltration

The experiments reported here simulated flow during infiltration of water from top boundary in response to the top boundary condition. Two types of boundary conditions have been explored to examine the effect of boundary condition on the mean movement of the moisture plume.

4.1.1.1 Constant head boundary condition

In the first series of simulations a fixed head boundary condition was imposed on the top boundary of the domain. Total 7 simulations were run with a range of n (2.0-8.25) keeping all other parameters constant. By examining the results of location of center of mass it appears that location of center of mass of the moisture plume varies linearly with time and that slope of the relationships between z_c and t in each of these simulations increases with increasing n. Therefore, velocity of the center of moisture plume is increasing with increasing value of n in unsaturated soil. As we know, higher n represents soil with more uniformity in pore size distribution. This result is consistent with the expectation that water will move faster through a soil with more uniform pore size distribution than through a soil with less uniform pore size distribution, when all other soil properties are identical.

To verify whether velocity of moisture plume in unsaturated soil under constant head boundary condition is always increasing with increasing n or it depends on some other factors such as α and the magnitude of top boundary condition, some additional

series of simulations were run using different α for each series of simulations. The range of value of α used in the above mentioned series of simulations was from 0.028 cm^{-1} to 0.098 cm^{-1}. It was found that the velocity of moisture plume was not always increasing with increasing value of n. The response of the velocity of moisture plume to increasing n, changes slowly in the opposite direction as the value of α increases. That means, when higher values of α value was used in the simulation, water moves faster through soil with lower value of n. This change of response of the velocity of moisture plume to increasing n may be caused by the amount of infiltrated water, which depends on relative permeability at boundary and relative permeability at boundary, is a function of n, α and magnitude of boundary condition at the top.

Figure 4.1 shows the effect of n on relative permeability functions of soil at several given values of water pressure head. It appears that relative permeability at boundary is increasing with n at a given boundary condition pressure head (BCh), only when BCh is smaller than inverse of the α. On the other hand, when the boundary value of pressure head is greater than the inverse of the α, the relative permeability at boundary decreases with increasing n. Since, inverse of α relates to entry pressure, it might be concluded that the ratio of magnitude of entry pressure and boundary pressure head controls whether relative permeability at boundary is increasing or decreasing with increasing n. By analyzing all the simulation results, we arrive at the conclusion that the ratio of entry pressure and magnitude of the top boundary condition (in case of fixed head boundary condition only) dictates whether velocity of the moisture plume in unsaturated soil is increasing or decreasing with increasing n. In support of our conclusion, some

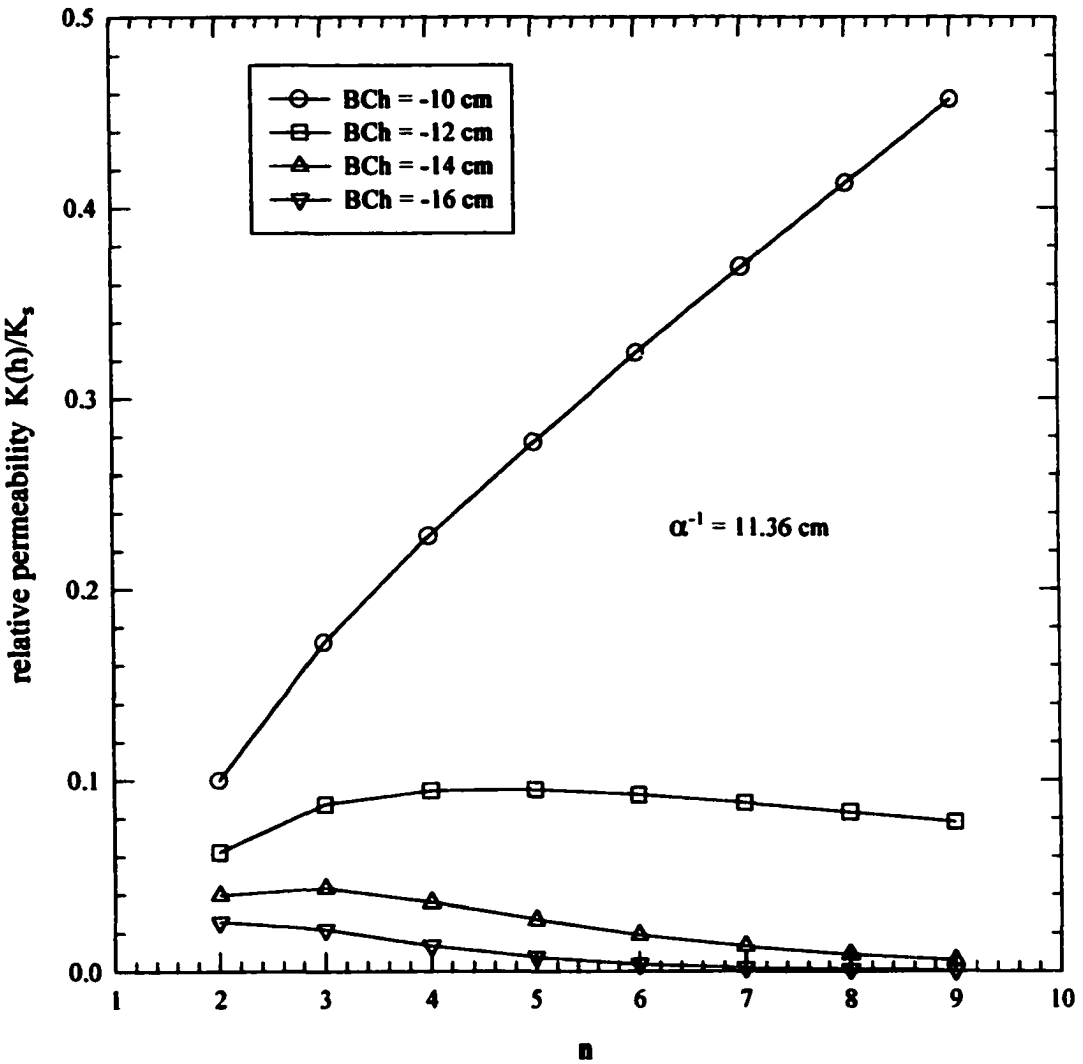

Figure 4.1 Influence of n on the relative permeability function at the top layer for different value of boundary pressure head; $\alpha = 0.088\ cm^{-1}$.

additional simulation experiments were run. From Figure 4.2 it is apparent that velocity of the moisture plume through unsaturated soil is not always increasing with n. It depends on the ratio of inverse of α and magnitude of top boundary pressure head.

Again, for the purpose of analyzing the results of second spatial moments, vertical spreading of the moisture plume is plotted against the vertical distance traveled by the center of moisture plume. As we defined earlier the change of vertical spreading per unit distance traveled by the moisture plume as vertical spreading index (which is equivalent to diffusivity in transport phenomena), n has no significant effect on vertical spreading index. One reason of this result might be the type of boundary condition used on the top of the soil column. Since we use constant head boundary condition on the top through out the simulation period, there is no drying front at the top of the moisture plume. Therefore, spreading of the moisture plume is observed only on the wetting front side. Calculation of second moment does not capture well the effect of n on vertical spreading index when fixed head boundary condition is used. The effect of n on vertical spreading index would probably be observed after the source of water is removed from top of the soil column.

Now to understand the effect α on the moisture plume movement, plots (Figure 4.3) of the ratio of velocity to saturated conductivity vs. α are made for a range of n value. It appears that rate of soil water movement is higher, when lower α was used in the simulation experiments. And these trends are consistent regardless of the value of n. Since low α represents soil with high capillary rise and high capillary rise corresponds to

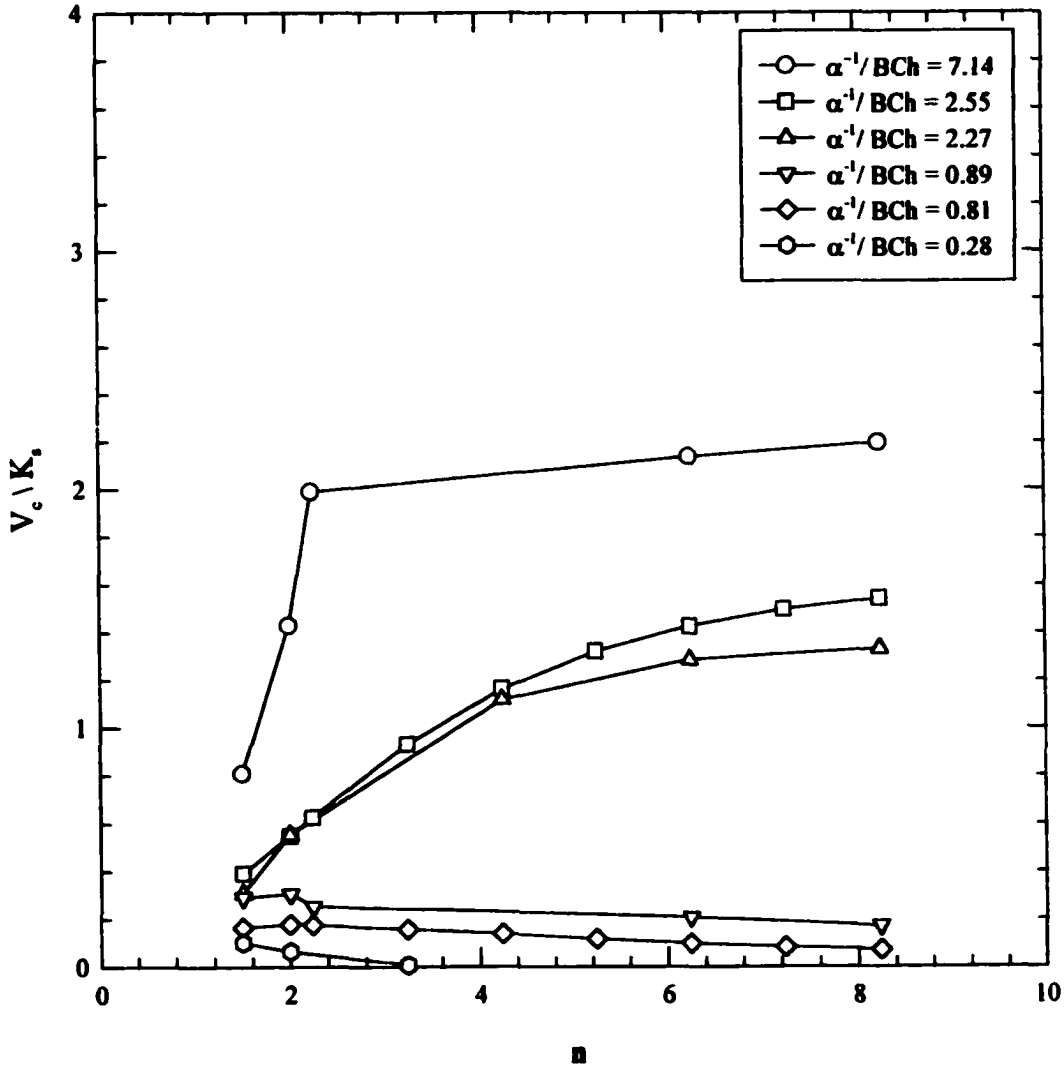

Figure 4.2 Influence of n on velocity of the moisture plume standardized by saturated conductivity, when constant head boudary condition (BCh) is imposed on the top.

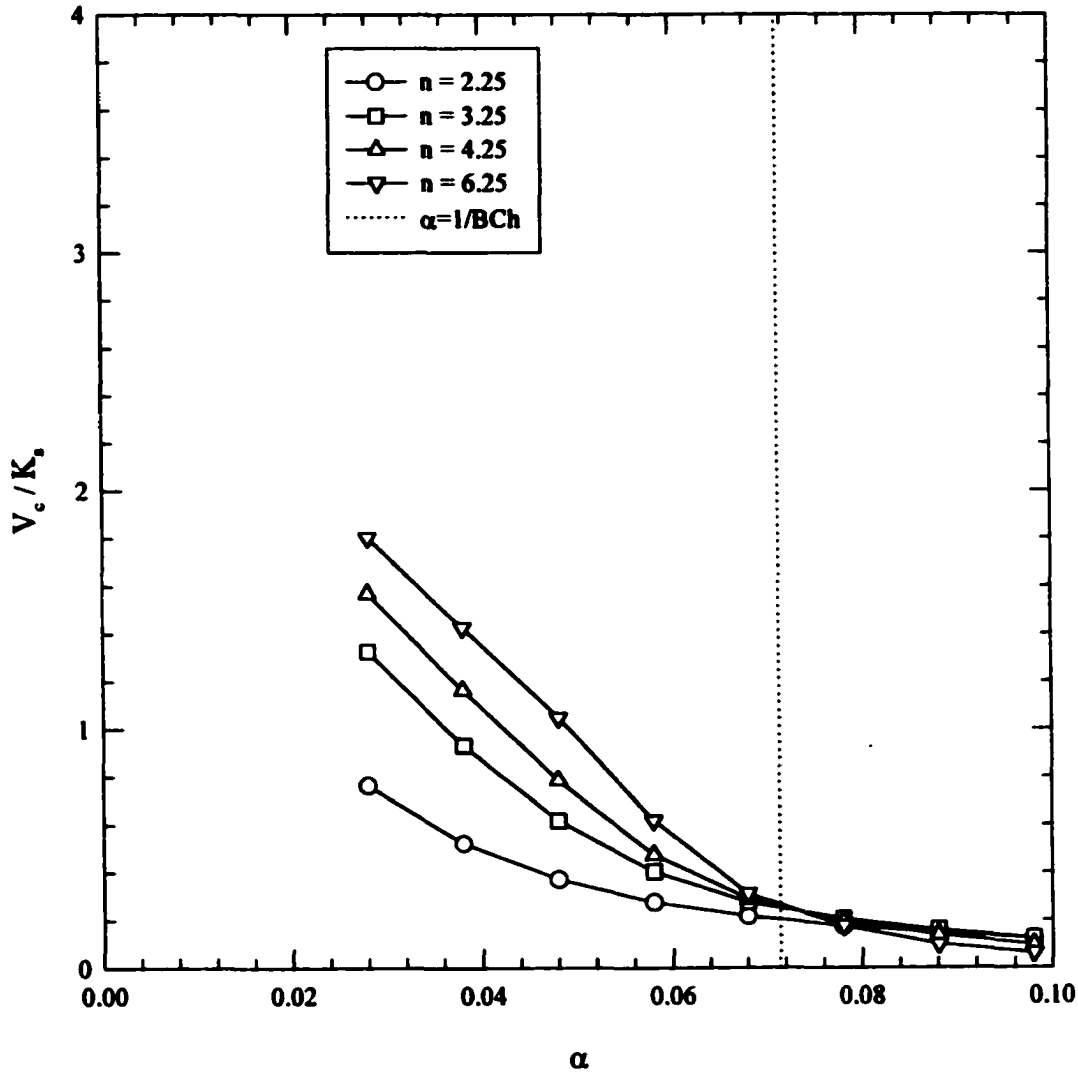

Figure 4.3 Influence of α on velocity of moisture plume standardized by saturated conductivity, when constant head boundary condition is imposed on the top.

Fine-grained soil such as clay or silt, perceptibly the results of the simulation experiments was found counter-intuitive. The expectation was opposite that means water should have moved slower through fine-grained soil (with low value of α). We don't see such characteristic of water movement through unsaturated soil because of the type of boundary conditions being used. For a particular value of fixed head boundary condition at top of the soil column, relatively more water infiltrates to the soil column if it is composed of finer grained soil (with smaller α), and consequently, overall relative permeability is higher at the top boundary of the soil column. As a result, higher average velocity is observed in soil with smaller α when constant head boundary condition is imposed on the top. In essence, the amount of infiltrating water controls the magnitude of average velocity. In other words, higher the rate of infiltration into the soil column, higher the average velocity is. And for a particular fixed head at the top boundary of the soil column, higher rate of infiltration is always occurred when the soil is finer (with smaller α). The spreading of moisture plume in vertical direction seems insensitive to α.

4.1.1.2 Constant flux boundary condition

Another series of computational experiments were conducted with a constant infiltration rate, 1.67×10^{-2} cm/sec on the top boundary of the domain. The simulation period for these experiments is 7200 sec. It was found that the velocity of center of mass of moisture plume while constant flux is imposed on the top of the soil column is entirely controlled by the boundary condition. Figure 4.4 illustrates the effect of n on the velocity of the moisture plume. From this plot, no significant effect of variability of n on the

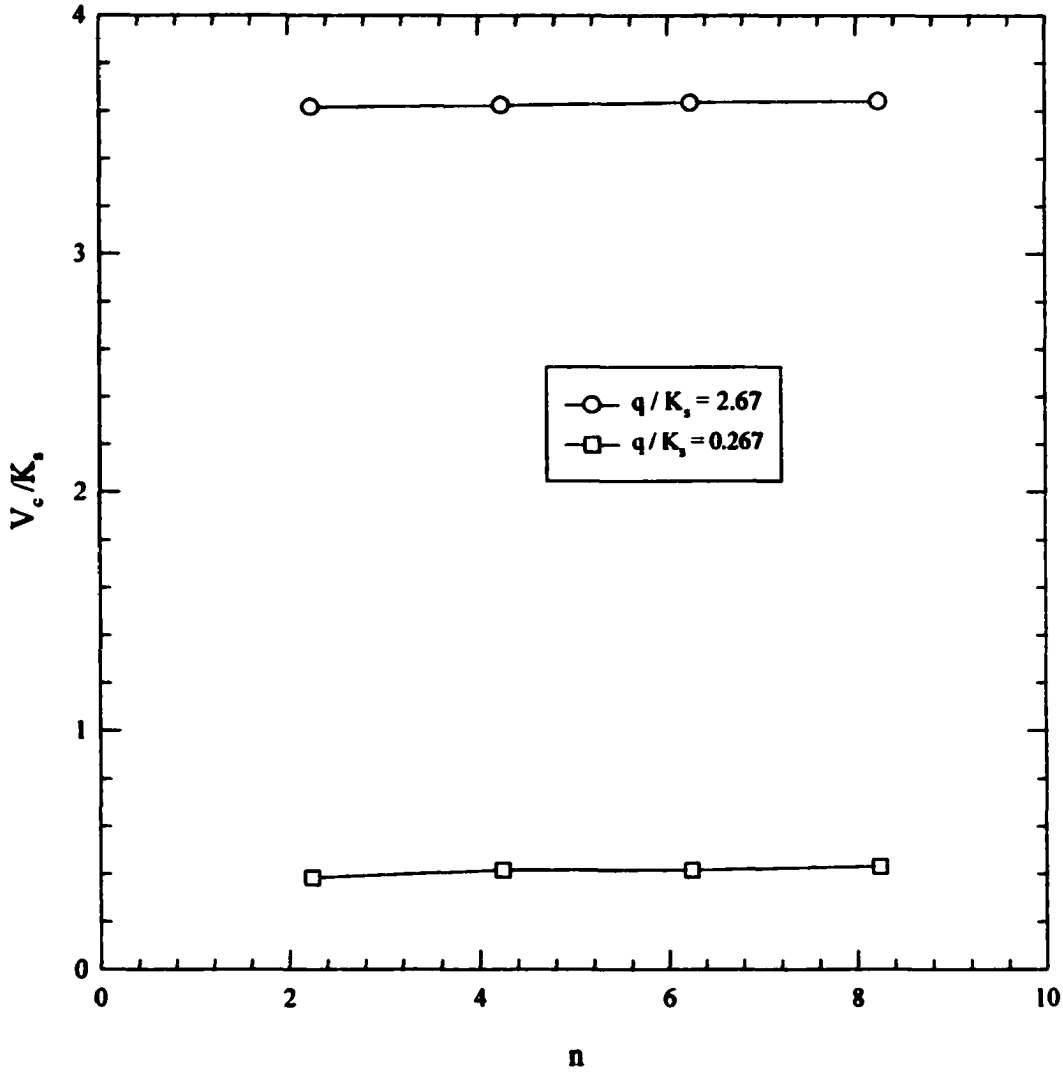

Figure 4.4 Influence of n on velocity of the moisture plume standardized by saturated conductivity, when constant flux boundary condition is imposed on the top.

change of first moment with time is apparent. To check whether this trend is independent of the magnitude of incoming flux, another set of simulations were run with relatively drier conditions. This time, fixed flux q was selected to 1.67×10^{-3} cm/sec. No effect of the magnitude of flux on the trend is observed. There is no effect of n on the vertical spreading of the moisture plume. Similar to the velocity of the moisture plume, the vertical spreading of the moisture plume remained the same irrespective of n. It is clear from the analysis results (Figure 4.5) that α has no impact on the rate of moisture plume movement. This is valid for a range of n value. Similarly, α has no effect on the vertical spreading of the moisture plume.

It is observed from this set of simulation results that at the very beginning of the simulation, negative water pressure (tension) at the top part of the soil column becomes very small. And after 400 seconds the node-pressure becomes positive, which means the soil behaves essentially as a saturated soil on the top part. Since equal amount of water is forcing into the system continuously, the top portion of the soil column became saturated after a very short period of time. Once the soil becomes saturated, there are no effects of VG parameter on the soil water movement. The insensitivity of velocity and vertical spreading of the moisture plume to VG parameters can also be explained from the moisture retention curves and relative permeability relationship. At the low tension, no significant variation of moisture content is found for different VG parameters. And relative permeability at such small tension is basically same for different VG parameters. Since saturated conductivity remained the same for each of this simulation experiment,

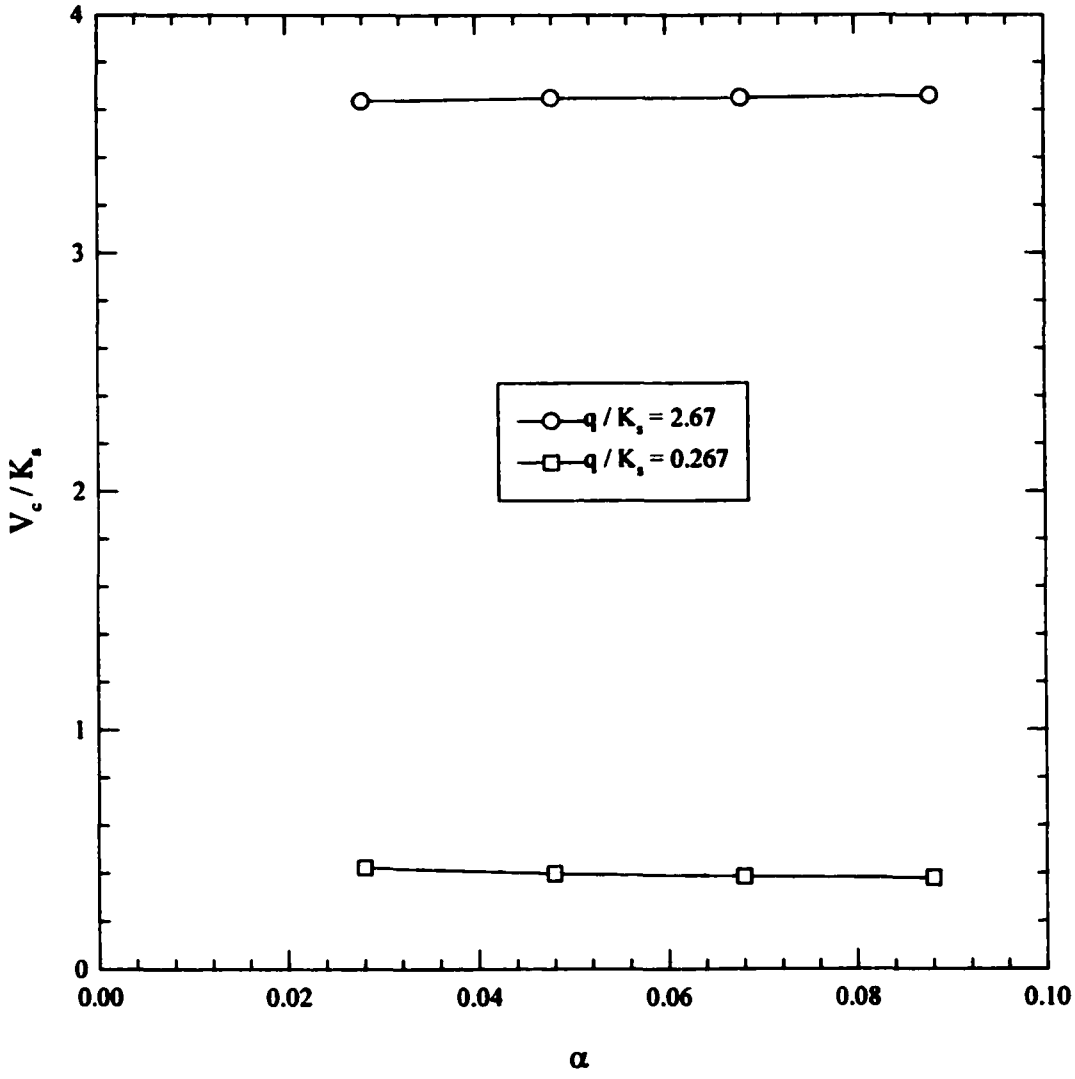

Figure 4.5 Influence of α on velocity of the moisture plume standardized by saturated conductivity, when constant flux boundary condition is imposed on the top.

same rate of moisture movement has been observed for different VG parameters.

4.1.2 Infiltration and redistribution

The purpose of using time varying head boundary condition is to see whether the type of boundary condition has any effect on the pattern of water movement after the boundary condition has been turned off, especially on spreading in the vertical direction. The same domain size and spatial discretization was selected as in previous simulations.

4.1.2.1 Time varying head boundary condition

At top boundary, a fixed pressure head, h = 1.0 cm was specified for 10 minute. After that, zero flux was applied on all sides for the rest of the simulation period. Bottom boundary condition remains the same as initial condition. Initial pressure head was set to h = -2400 cm at each node to make the soil column dry.

By analyzing the results of this set of numerical experiments run with different combinations of n and α, it was found that the velocity of center of mass of the moisture plume is higher through soil with higher n during infiltration ($t \leq 600$ sec). Figure 4.6 is a plot of velocity of the moisture plume standardized by saturated conductivity of the soil versus time during the simulation. Figure 4.6 shows an example of effects of n on velocity of the moisture plume for a particular α both during infiltration and

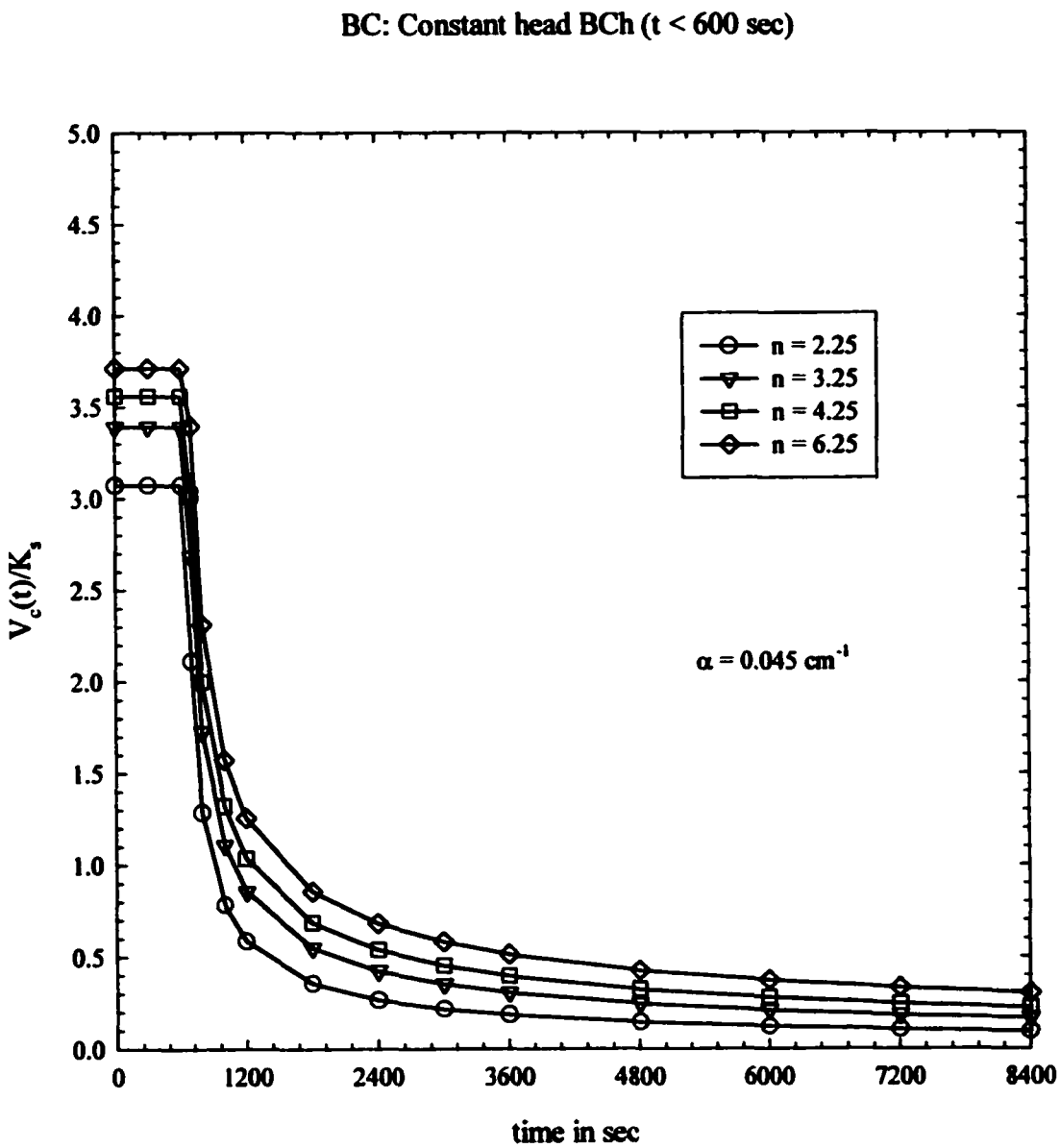

Figure 4.6 Effect of n on velocity of moisture plume standardized by saturated conductivity; when $\alpha = 0.045\ cm^{-1}$; Top BCh = 1 cm for 600 seconds.

redistribution. During infiltration, velocity is constant and higher velocity is observed in soil with higher n. This trend remains the same for all α. That means whatever value of α is used in the numerical experiments, water moves faster through soil with higher value of n. But this is not the case when the constant head boundary condition is imposed on the top boundary. In the numerical experiments using constant head boundary condition at top, water moves faster through soil with higher value of n, only when the ratio of α^{-1} and boundary value of pressure head is greater than unity. As it is mentioned in section 4.1.1.1, this inconsistency in trend is because of the magnitude of top boundary condition. Since top boundary condition was chosen to be h = 1.0 cm instead of h = -14 cm in this set of numerical experiments, the top portion of the soil column was always wetter when the pore size distribution is more uniform (higher n). Since, boundary pressure head is less than the inverse (α^{-1} / BCh > 1.0) of the value of α, relative permeability of soil at boundary is increasing with increasing n. As a result, during infiltration higher constant velocity of moisture plume is observed in soil (for all value of α) with more uniform pore size distribution.

During redistribution period ($t \geq 600$ sec), time dependent velocity of moisture plume gradually reduces with increasing time to a constant velocity. It is observed that the velocity of moisture plume in soil with more uniform pore size distribution is higher throughout the redistribution period. This characteristic of moisture plume movement may be explained by the fact that during infiltration greater amount of water infiltrates into the soil column, which has more uniform pore size distribution. Therefore, just after turning off the source of infiltration (t = 600 sec), mass and velocity of moisture plume is

greater in soil, which has more uniformity in pore size distribution. Magnitude of momentum of moisture plume at the end of infiltration period might contribute to the higher velocity of the moisture plume in soil with more uniform pore size distribution.

Since during infiltration VG parameters has no effect on vertical spreading, vertical spreading of moisture plume is plotted against the vertical distance traveled by the center of mass of moisture plume during redistribution only in Figure 4.7. It is found that spreading of moisture plume in the vertical direction is higher as the value of n decreases. The following two mechanisms may account for higher spreading of moisture plume. More water is held up in the drying front of the moisture plume in soil that has less uniform pore size distribution. While at the wetting front, water flows through preferential path due to more variation in pore size that causes moisture plume to spread out more. When the vertical distance traveled by the center of mass of moisture plume is same in two soil columns, higher vertical spreading is observed in soil that has less uniform pore size distribution. The effect of pore size distribution on vertical spreading of moisture plume remains the same irrespective of the texture (low \or high α) of soil.

Again, velocity standardized by saturated hydraulic conductivity is plotted against time for several different α and for a particular n in Figure 4.8. It appears from Figure 4.8 that during infiltration, water moves faster when lower α is used in the simulation experiments. For the constant boundary (pressure head) condition at top, more water infiltrates into the medium while lower α is used in the simulations. Therefore, because of higher relative permeability at the boundary, velocity of center of mass is higher in soil

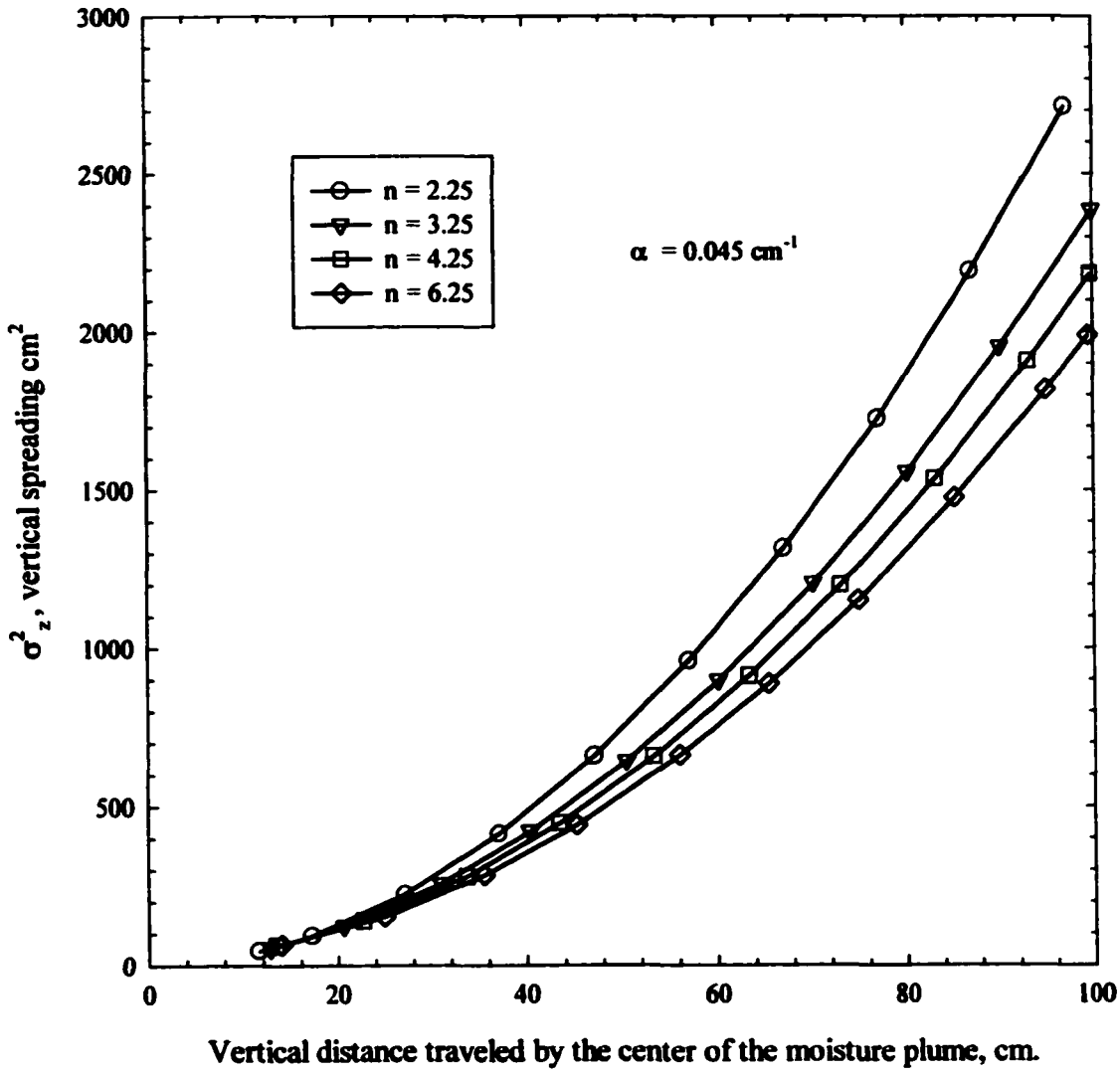

Figure 4.7 Vertical spreading of moisture plume as a function of vertical distance traveled by the center of the moisture plume; when $\alpha = 0.045\ cm^{-1}$; Top BCh = 1.0 cm for 600 seconds.

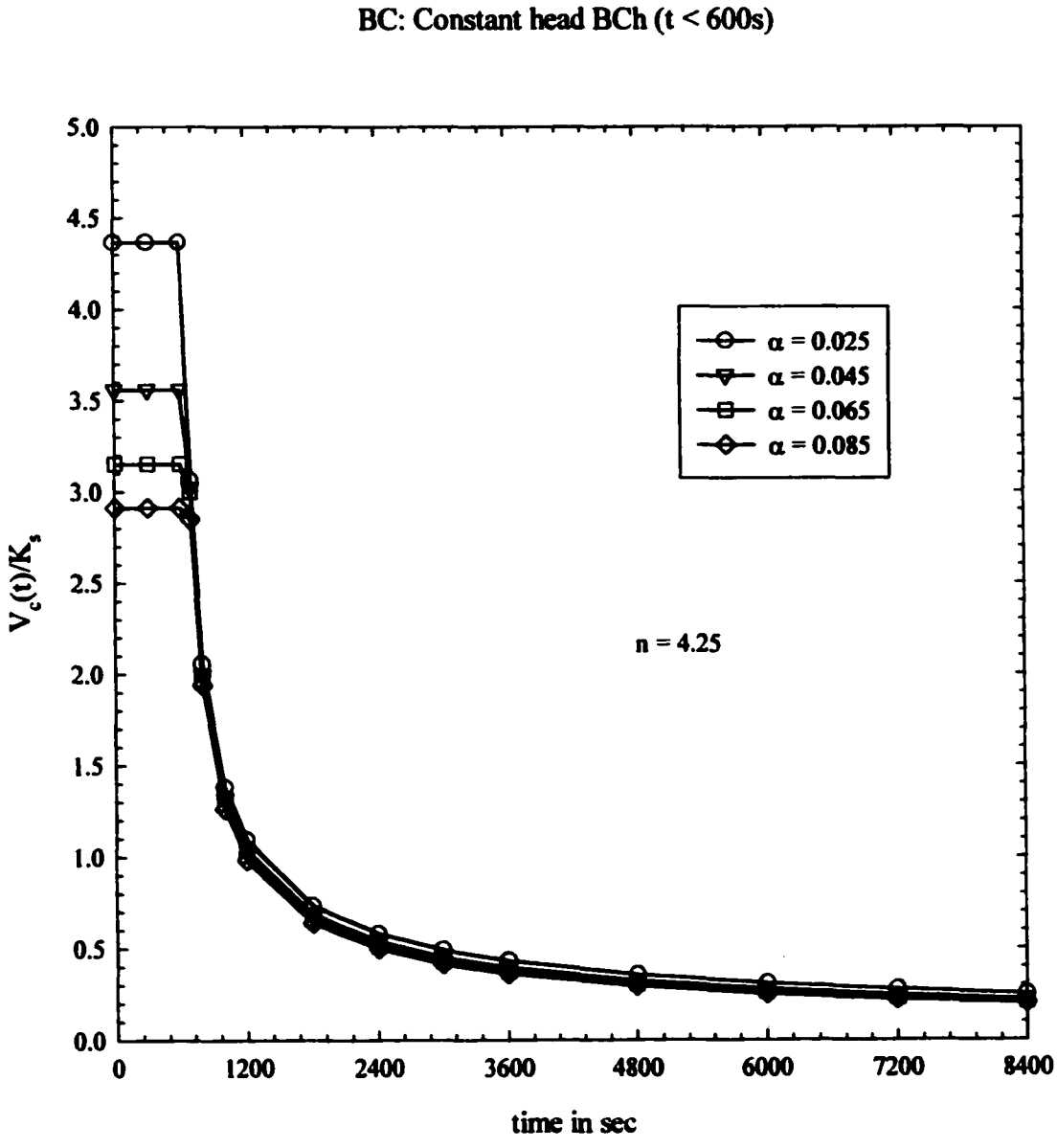

Figure 4.8 Effect of n on velocity of the center of the moisture plume standardized by saturated conductivity, when $\alpha = 0.045\ cm^{-1}$; Top BCh = 1 cm for 600 seconds.

with smaller α. There is no significant effect of variability of α on velocity of moisture plume during redistribution. During redistribution, water is expected to move slower in soil with lower α because of the steeper slope of moisture retention function. During infiltration velocity is higher in soil with smaller α and during redistribution only velocity is lower in soil with smaller α. These two opposite effects of α on velocities of the moisture plume cancel out the effect of variability of α when the water flow enters into redistribution mode. To distinguish the effect of α on velocity during redistribution, the initial velocity for all soils should be the same, which is impossible, if the magnitude of top boundary condition (pressure head) remains same. To overcome this problem, time varying flux boundary condition can be imposed on top of the domain for all simulation experiments.

α has no effect on vertical spreading during infiltration. Figure 4.9 illustrates the effect of α on spreading of moisture content in the vertical direction after boundary pressure head is removed. It appears from the Figure 4.9, spreading is comparatively higher in soil with lower α. Lower α is a characteristic of fine grain soil and it is expected that the extent of spreading is larger in fine grain soil than in coarse grain soil. It can be explained by the moisture retention functions. The retention function of finer soil is steeper, as a result higher moisture content is held up in the drying front of the moisture plume. On the wetting front of the moisture plume, more water enters into the dry zone in finer soil because of higher permeability.

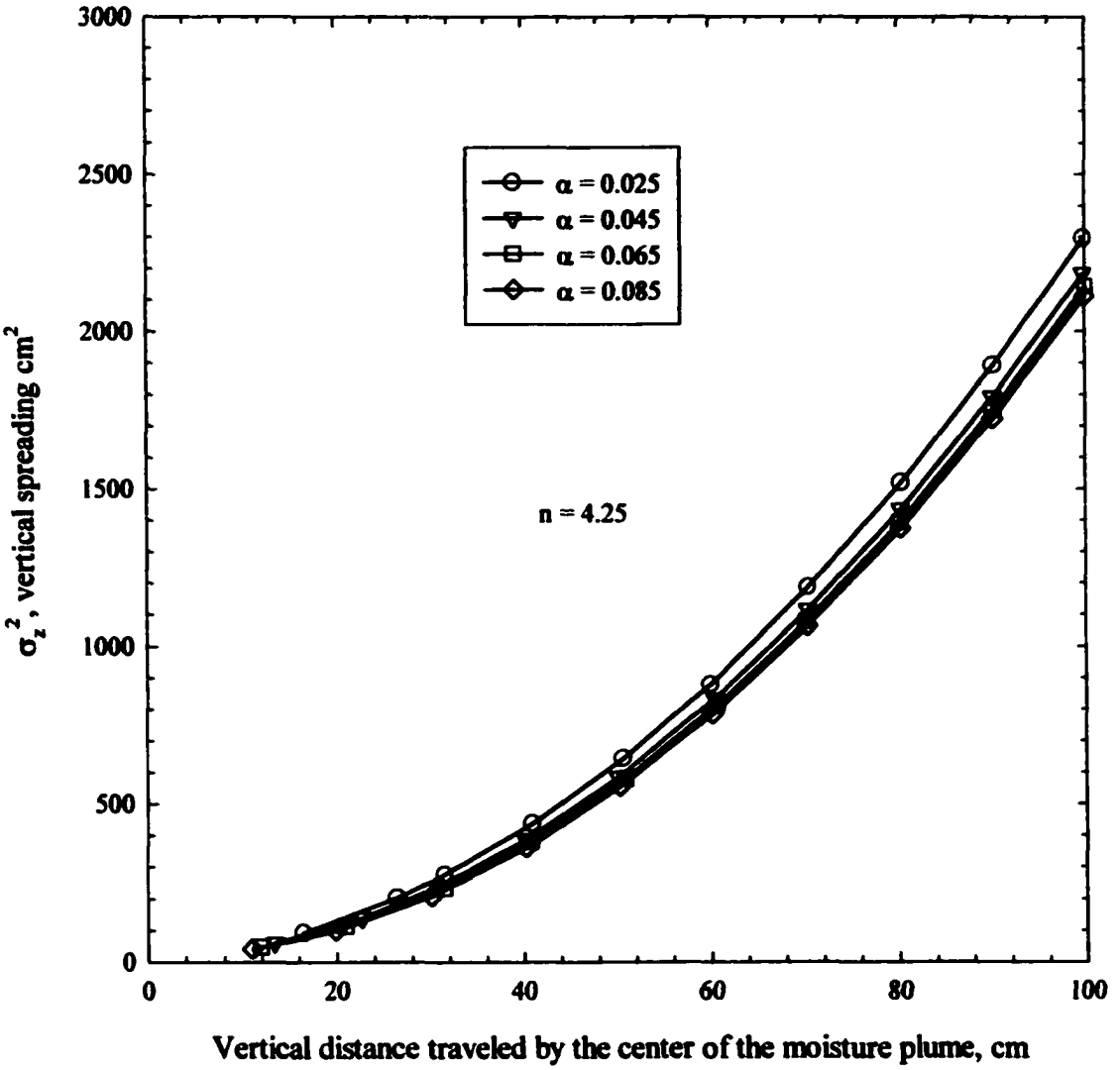

Figure 4.9 Vertical spreading of the moisture plume as a function of vertical distance traveled by the center of the moisture plume; when n = 4.25; Top BCh = 1 cm for 600 seconds.

4.1.2.2 Time varying flux boundary condition

The purpose of using a time varying flux boundary condition is to verify whether the type of boundary condition has any effect on the pattern of moisture movement after the source is removed. The same domain size and spatial discretization was selected as in previous simulations. At top boundary, a constant flux q = 1.67×10^{-2} cm/sec was imposed for 10 minute. After that, zero flux was applied on all sides for the rest of the simulation period. Bottom boundary condition remains the same as initial condition. Initial pressure head was set to h = -2400 cm at each node to force all soil columns to reach at its residual saturation while varying n and α.

Figure 4.10 illustrates the effect of n on the standardized velocity of the moisture plume. It appears from these results that velocity is constant during infiltration and the magnitude is same for all n. But during redistribution, higher velocity is observed in soil with higher n. This behavior is what we expected. Since an equal amount of water is forced into all soil columns during infiltration velocity is constant and n has no effect on it. The mass of water is same for all soil columns when infiltration stops. Higher n represents coarser grained soil. The slope of moisture retention function of coarser grained soil is flatter. For a small increment or reduction of tension larger amount of water are expelled from or entered into a soil volume.

The change in vertical spreading with respect to the travel distance of the center of moisture plume is shown in Figure 4.11 for four different n. It can be seen from these plots that higher spreading of moisture plume occurs in soil with smaller n. Once again,

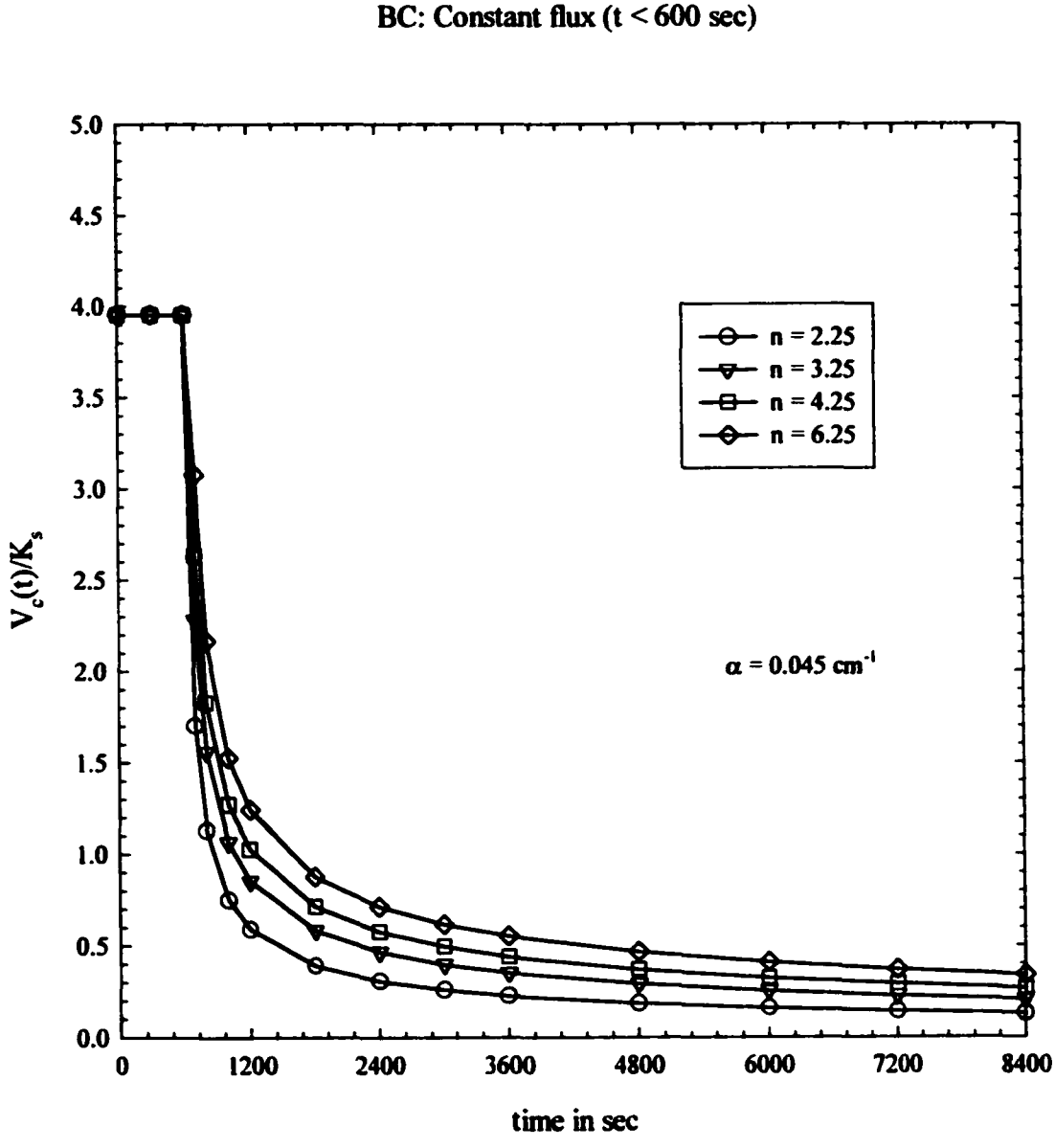

Figure 4.10 Effect of n on velocity of the center of the moisture plume standardized by saturated conductivity when $\alpha = 0.045\ cm^{-1}$; Top BC: $q = 1.67 \times 10^{-2}$ cm/sec for 600 seconds.

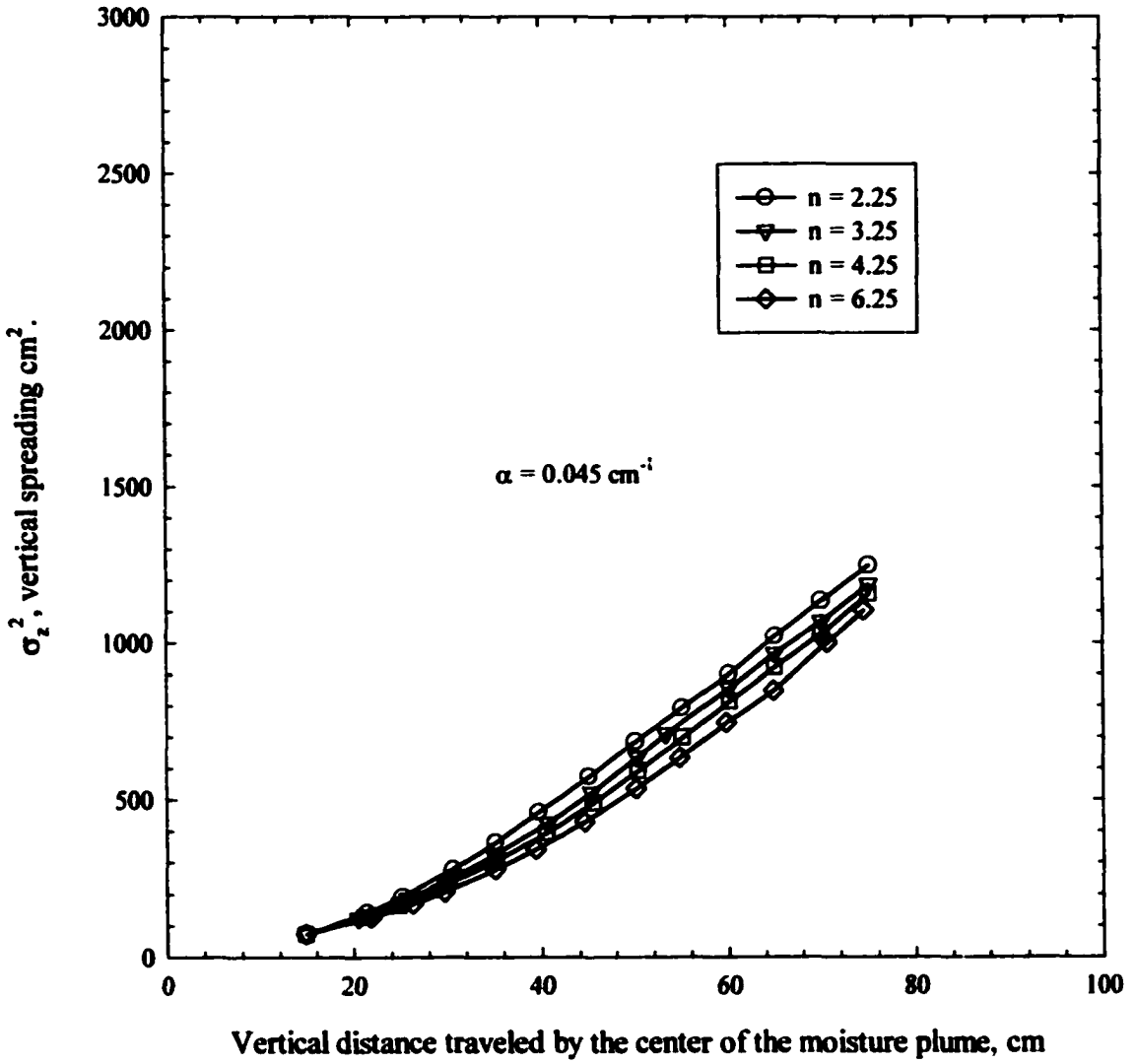

Figure 4.11 Vertical spreading of the moisture plume as a function of vertical distance traveled by the center of the moisture plume; when $\alpha = 0.045\ cm^{-1}$; Top BC: $q = 1.67 \times 10^{-2}$ cm/sec for 600 seconds.

the higher spreading is due to slower drainage of water from the drying part of the moisture plume and faster imbibition in the wetting region of the moisture plume because of preferential flow path.

Figure 4.12 presents the effect of α on the standardized velocity of the moisture plume. Again, there is no significant effect of α on standardized velocity. Therefore, this type of boundary condition will not be useful in simulations design to investigate the effect of soil properties.

Vertical spreading as a function of vertical travel distance during redistribution is plotted in Figure 4.13. It is found from these results that higher spreading is observed in soil with smaller α. In other words, higher vertical spreading is observed in finer grained soil. This trend is consistent with the simulation results with time varying constant head boundary condition.

4.1.3 Redistribution

It has been found from previous simulation results that the velocity (time rate of change of first spatial moment standardized by mass) of the moisture plume decreases with increasing α for both fixed head and time varying head boundary condition (both situation while boundary flux is "on" or "off"). We don't notice any effect of α in the case of constant flux boundary condition. In case of time varying flux boundary condition, the trend is opposite i.e. velocity increases with increasing α, but the effect of variability of α on velocity is very insignificant. This irregular trend of moisture

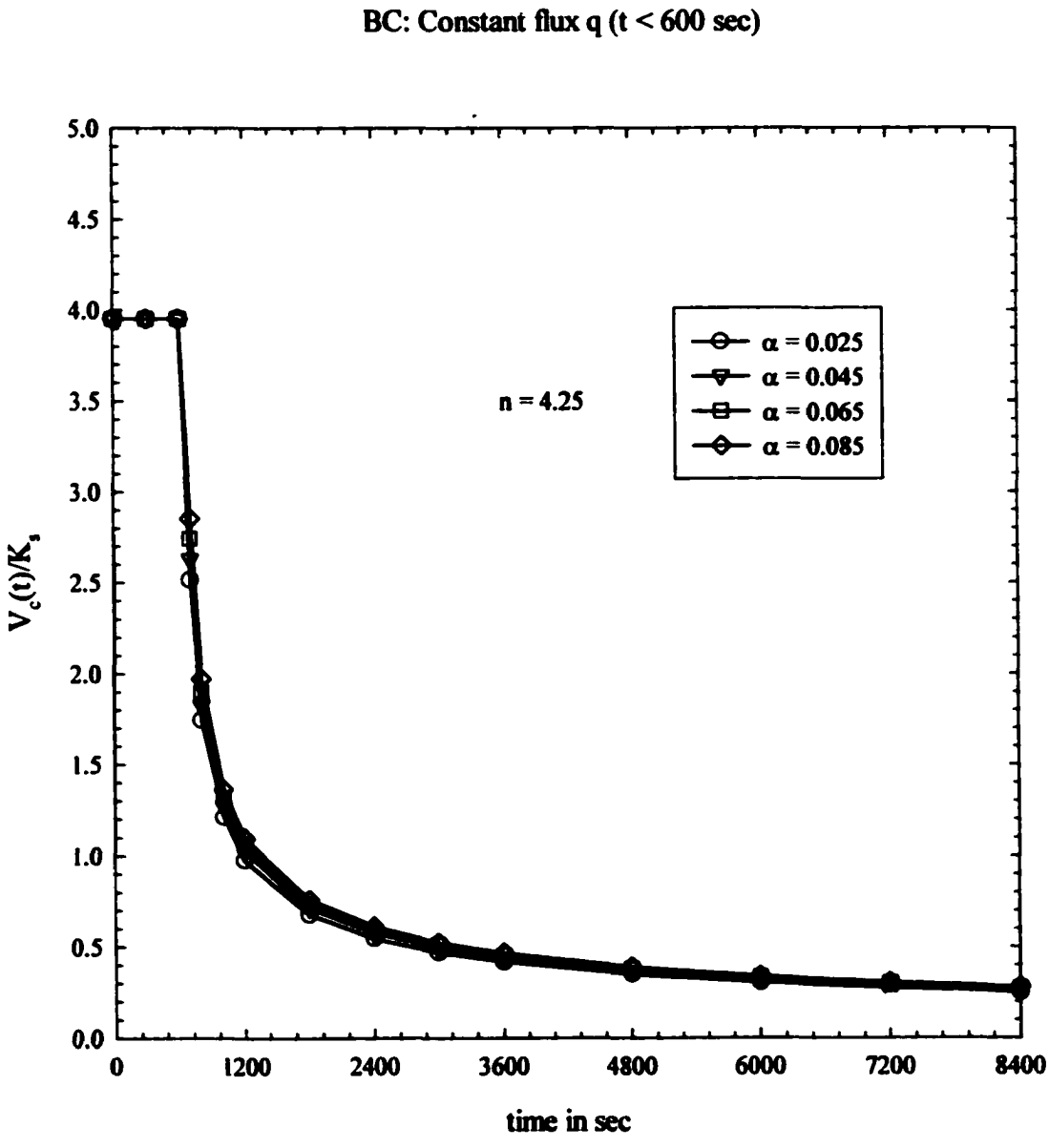

Figure 4.12 Effect of α on velocity of the center of the moisture plume standardized by saturated conductivity, when n = 4.25; Top BC: q = 1.67×10^{-2} cm/sec for 600 seconds.

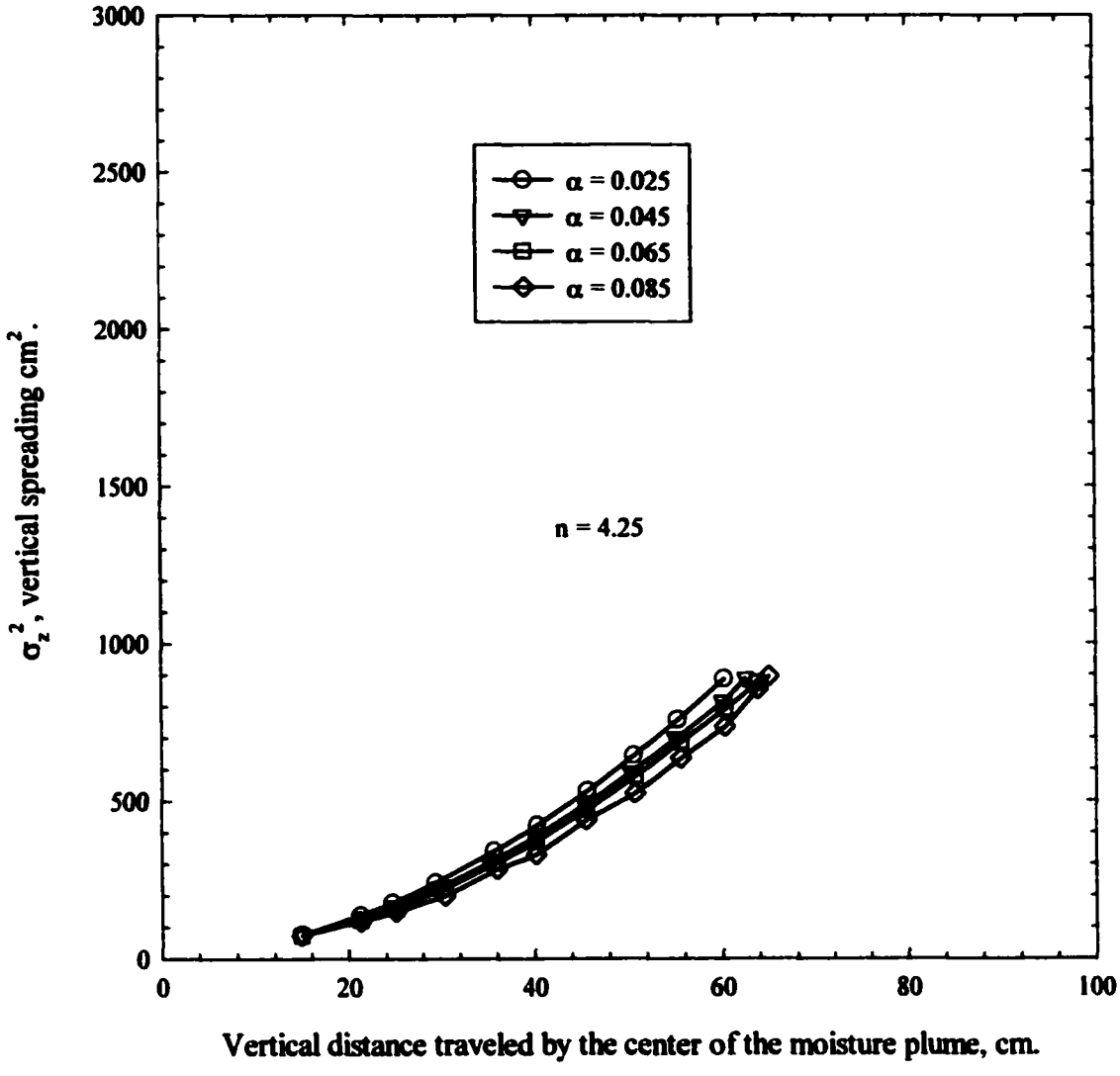

Figure 4.13 Vertical spreading of the moisture plume as a function of vertical distance traveled by the center of the moisture plume; when n = 4.25; Top BC: q = 1.67×10^{-2} cm/sec for 600 seconds.

movement came up because of the different moisture content distribution when infiltration stops. Therefore it can be concluded that type and magnitude of boundary condition has a vital impact on the mean behavior of plume movement and that they may interact with n and α to affect moisture flow. This already suggests that the search for effective parameters may be futile. However we pursue our investigation by eliminating the effect of initial and boundary conditions on the average movement of the plume. To do so we carry out some additional numerical experiments with same initial moisture distribution and zero-flux boundary condition on all sides of the column except on the bottom. We observed from the results of previous experiments that during infiltration, second spatial moment is insensitive to parameter. This could be because there is only wetting front of the infiltrating moisture plume. But during redistribution after infiltration, the moisture plume develop both drying and wetting front. We found that second spatial moment is significantly sensitive to VG parameters. Therefore, we decided to run simulation experiments to estimate transient first and second spatial moment during redistribution only with the same initial moisture distribution. Simulations results will be used to estimate the parameters of the fitting equations for velocity as a function of time and spreading as a function of vertical travel distance. Further calculations are required to estimate average velocity of the moisture plume using fitting parameters. Now, the average velocity and the rate of change of spreading with unit distance traveled by the center of moisture plume will be plotted against n for different α. These curves will determine the selection of appropriate effective parameters when average velocity and rate of change of spreading in heterogeneous soil is known. The parameter values corresponding to the average velocity and rate of change of

spreading in heterogeneous soil will be considered as the effective parameter for that heterogeneous soil.

4.1.3.1 Models for transient spatial moments

As we learned from the simulation experiments described in section 4.1.2 that first spatial moment standardized by total mass of moisture plume varies linearly with time during infiltration. But during redistribution, the relationship between first spatial moment standardized by total mass of the moisture plume and time is not linear. It approximately follows power law equation (3.10).

In the computational approach used in this research work, we concentrate on the effects of spatial variability in the α and n. The effective parameters of heterogeneous soil system can be derived by conceptualizing the heterogeneous system as an equivalent homogeneous medium. Under the same initial moisture distribution and same boundary condition, the equivalent homogeneous soil should give the same location of the center of mass (first spatial moment standardized by total mass of the moisture plume) and the same spreading (standardized second spatial moment) of the moisture plume at any given time. In other words, velocity and rate of change of spreading with respect to distance traveled by the moisture plume in heterogeneous soil should be equal to that of equivalent homogeneous soil. One approach to get effective parameters will be to attempt to minimize the difference in velocity and spreading for heterogeneous and equivalent or effective homogeneous simulations.

4.1.3.2 Calculation of average velocity

To achieve this goal, first a series of transient spatial moments for a range of α, n pairs for homogeneous soils was developed. Next simulation data can be fitted to the power law model during redistribution. It has been found that redistribution velocity starts declining with time and then approaches zero, when redistribution time tends to infinity. Since we are interested in some type of average behavior of moisture plume movement, average velocity of the moisture plume over redistribution time will be estimated. Based on average velocity, effective n and α will be estimated. This will simplify the problem a great deal. For comparison purposes average velocity can be estimated over the time length during which center of moisture plume reaches at the middle point of the soil column. Integrating equation (3.12) over the time period from 0 to t_{end}:

$$V_{avg} = \frac{1}{t_{end}} \int_0^{t_{end}} k_1 \tau^{-k_2} \qquad (4.1)$$

Where t_{end} is the time taken by the center of moisture plume to reach at the mid-depth of the soil column and V_{avg} is average velocity of the moisture plume over the redistribution time.

After integration,

$$V_{avg} = \frac{1}{t_{end}} \left[k_1 \frac{\tau^{-k_2+1}}{-k_2+1} \right]_0^{t_{end}} \qquad (4.2)$$

or

$$V_{avg} = \frac{1}{t_{end}} \left[\frac{k_1}{1-k_2} (t_{end})^{1-k_2} \right] \qquad (4.3)$$

After simplification equation (4.3) becomes

$$V_{avg} = \left[\frac{k_1}{1 - k_2} (t_{end})^{-k_2} \right] \qquad (4.4)$$

Now comparison of the two parameters (V_{avg}, VSI) between heterogeneous simulation and homogeneous simulation will be done. It is anticipated that this comparison will enable us to formulate relationships between measures of soil heterogeneity and effective hydraulic parameters.

4.1.3.3 Relationship between flow properties and soil properties

In this paragraph, we will see how these two parameters (V_{avg}, VSI) relate to VG parameters. Plots of V_{avg} vs. n (Figure 4.14) are made for a range of α. It appears that average velocity of moisture plume is increasing with increasing n. Since higher n corresponds to a soil where pore size distribution is more uniform, moisture plume moves faster in soil with larger n. Similarly, it has been found that average velocity of moisture plume is increasing with increasing α. Higher α corresponds to soil with smaller entry pressure, which makes the slope of moisture retention function flatter on the middle portion of the curve. In another words, small increase or decrease of tension, force more water to drain out of soil (drainage cycle) or penetrate to soil (imbibition) with higher α. Therefore, average velocity of moisture plume becomes higher in soil with higher α.

Again Figure 4.15 illustrates the effect of parameters on VSI. This plot shows that VSI is decreasing with increasing n. Comparatively less vertical spreading of

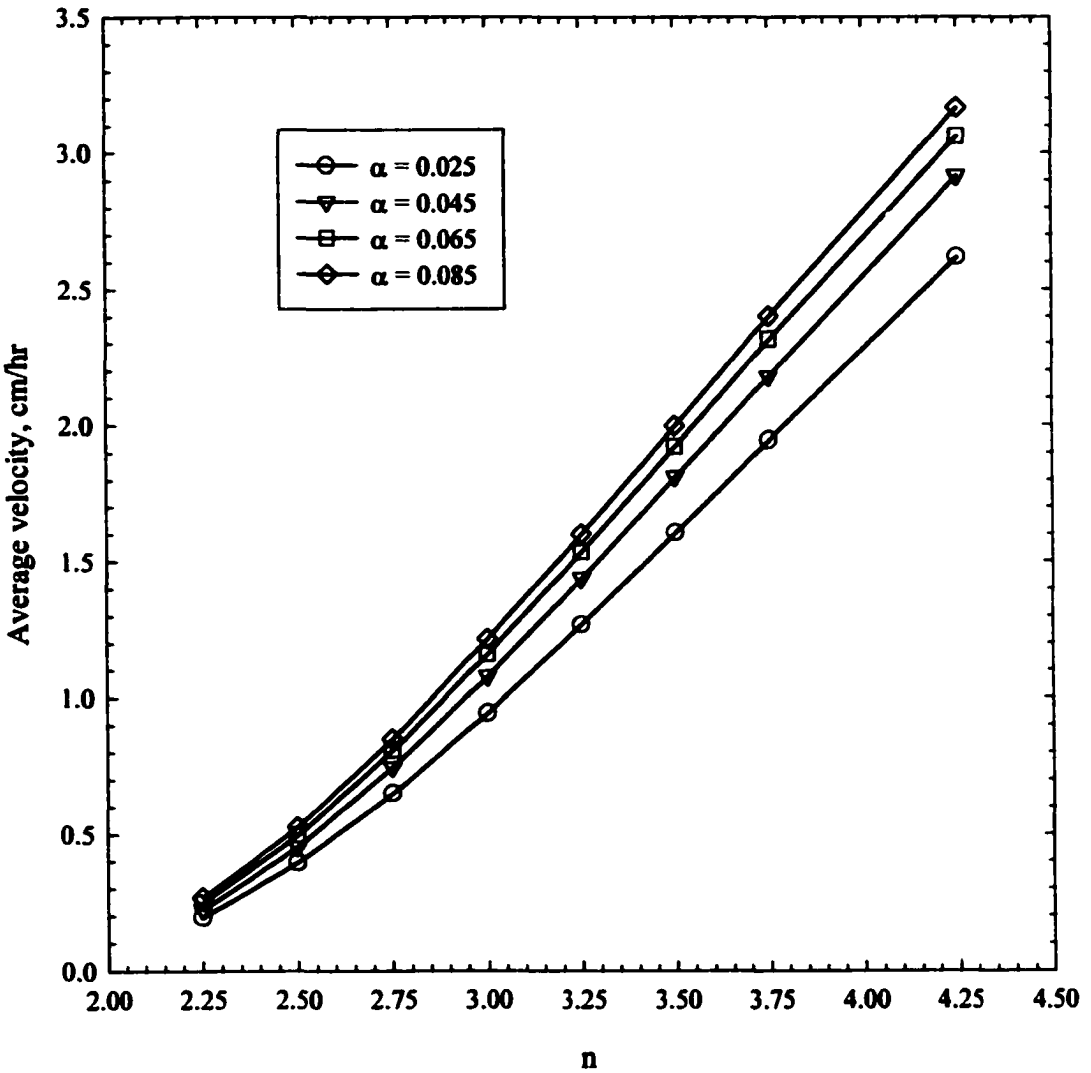

Figure 4.14 Effect of VG parameters on average velocity of the moisture plume in 1D homogeneous simulations.

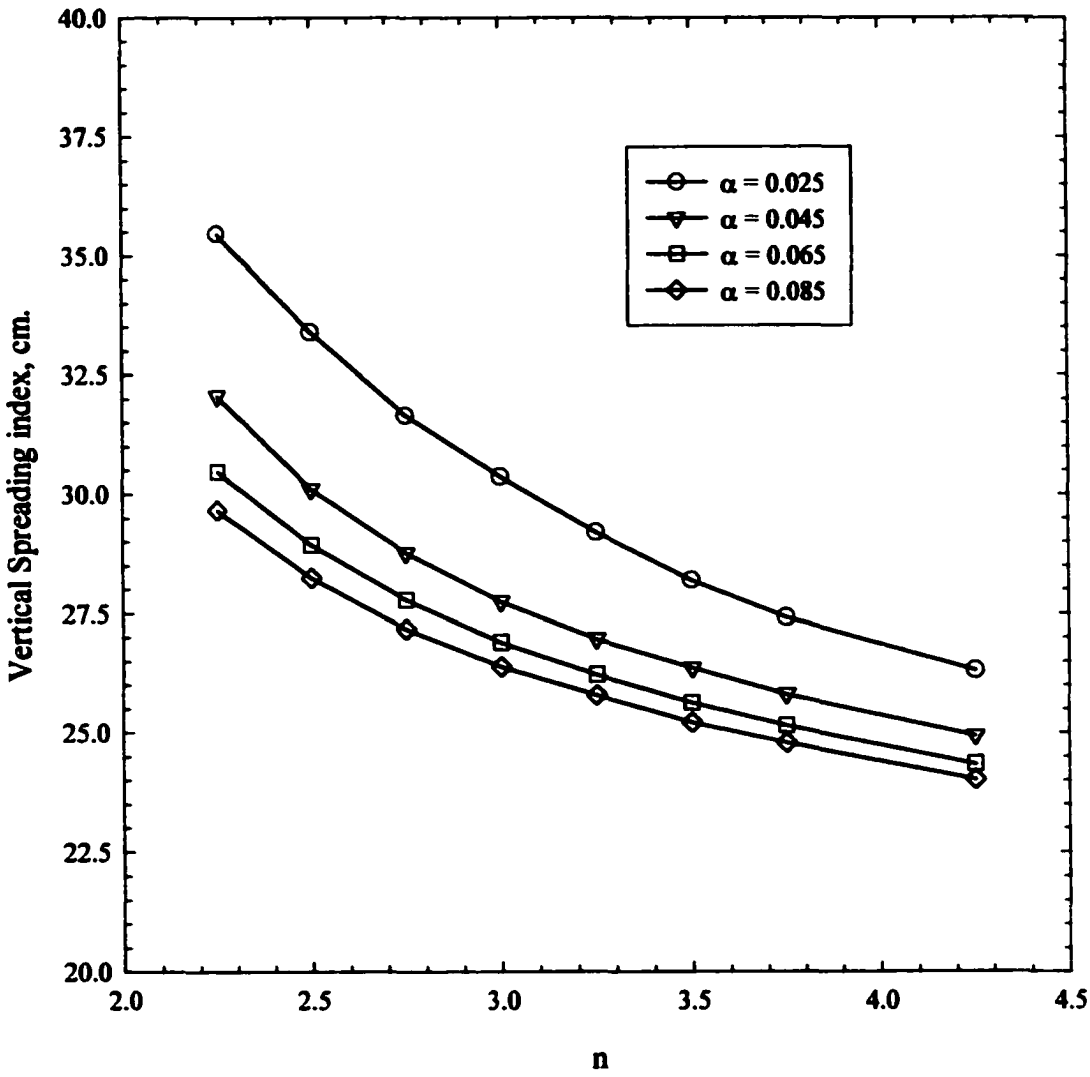

Figure 4.15 Effect of VG parameters on Vertical Spreading Index (VSI) of the moisture plume in 1D homogeneous simulations.

moisture is observed in soil with higher n. More uniformity in pore size distribution contributes this lesser extent of spreading. It has also been found from the same plot that VSI is decreasing with increasing α. Higher α is a characteristic of coarse grain soil (smaller entry pressure) and less spreading of moisture is anticipated in coarse grain soil. Figure 4.14 and Figure 4.15 are termed as standard type curves for 1D flow simulation.

4.2 Two-Dimensional flow simulations

4.2.1 Redistribution

Two-Dimensional flow simulation experiments are done to see the effect of variability of VG parameters on lateral movement of moisture plume, mainly lateral spreading. For two-dimensional flow simulations the domain size was selected as 100×10×100 cm. The horizontal and vertical discretizations are 10 cm and 2.5 cm respectively. Soil properties used in 2D flow simulations are same as that used in 1D flow simulations. In two-dimensional cases, we simulate the flow when time varying boundary condition is applied only on the central portion of the top boundary of the domain. As we learned from one-dimensional flow experiments, to eliminate the effect of type and magnitude of boundary condition and initial moisture content distribution on moisture plume movement, we need to apply zero flux boundary condition on all sides of the domain and use same initial moisture content distribution for all simulations. For all simulations with different VG parameters, equal amount of moisture is introduced on the top specified part of the domain and then let it redistribute both vertically and horizontally as long as the center of mass reaches the mid-depth of the soil domain. The

top central strip of size 20×30 cm is fully saturated at the beginning of the simulation. All other input parameters remain the same for all 2D simulations.

4.2.2 Transient spatial moments

In addition to transient first and second spatial moment in vertical direction, we need to calculate first and second spatial moment in transverse direction. Because of symmetry and homogeneity in material properties, center of mass of moisture plume does not move horizontally at all for homogeneous simulations. Therefore, we will focus only on transverse second spatial moment not the transverse first spatial moment.

4.2.3 Calculation of transverse spreading index.

Similar to 1D case, second spatial moment in horizontal direction as a function of distance traveled vertically by the center of mass can be modeled by the following linear equation:

$$\sigma_x^2 - \sigma_{xin}^2 = k_4 (z_c - z_{cin}) \qquad (4.5)$$

where, σ^2_x = spreading in vertical direction.

σ^2_{xin} = spreading in horizontal direction when redistribution starts.

k_4 = constant of proportionality

Since k_4 is a measure of spreading at a particular distance traveled by the center of mass, k_4 may be termed as transverse spreading index (TSI). This parameter is equivalent to dispersivity in solute transport phenomena in transverse direction. Now comparison of three parameters (V_{avg}, TSI, VSI) between heterogeneous simulation and

homogeneous simulation will be done. It is anticipated that this comparison will enable us to formulate relationships between measures of soil heterogeneity and effective soil hydraulic parameters.

4.2.4 Relationship between flow properties and soil properties

Now we will investigate how these three parameters (V_{avg}, TSI, VSI) relate to soil properties (VG parameters). Figure 4.16 illustrates the relationship between VG parameters and average velocity. The results suggest that average velocity of moisture plume is increasing with increasing n for any α. Again, from the same results it can be said that average velocity is increasing with increasing α. This trend is more pronounced when n is on the higher side. It is evident from Figure 4.16 that the highest average velocity is observed when both VG parameters are highest. Note that the soil with this combination of VG parameters has the moisture retention curves with flattest slope. Similarly, lowest average velocity occurs in soil when both VG parameters are lowest.

It is apparent from the Figure 4.17 that Transverse Spreading Index is decreasing with increasing n for any α. Increasing uniformity of pore size results in less spreading of moisture plume in transverse direction. From the same plots, it is evident that TSI is decreasing with increasing α. Generally, water in coarse grain soil is likely to spread less and this result is consistent to our anticipation.

Figure 4.18 shows the relationship between Vertical Spreading Index and VG parameters. It appears from the plots that VSI is also decreasing with increasing n. Soil

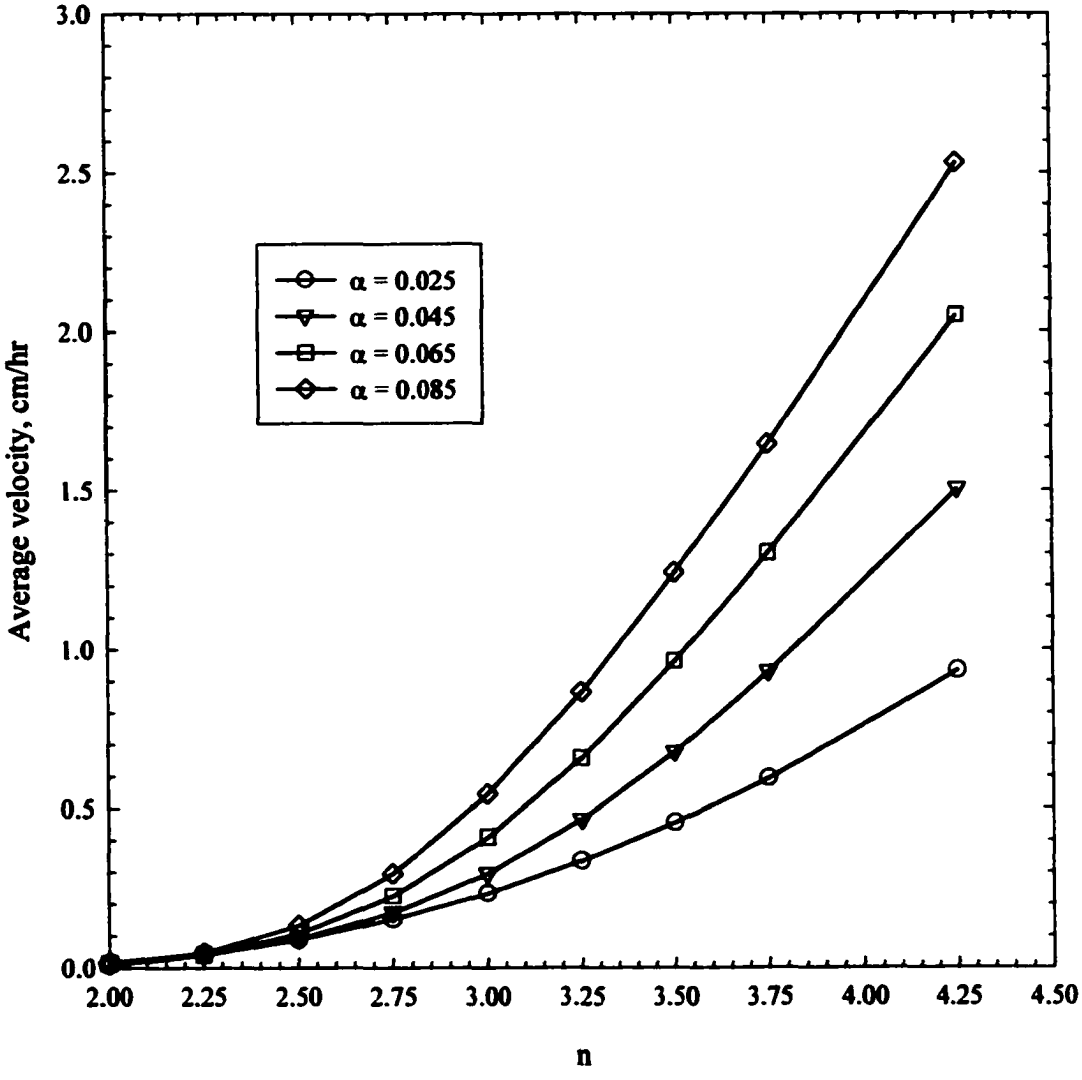

Figure 4.16 Effect of VG parameters on the average velocity of the moisture plume in 2D homogeneous simulations.

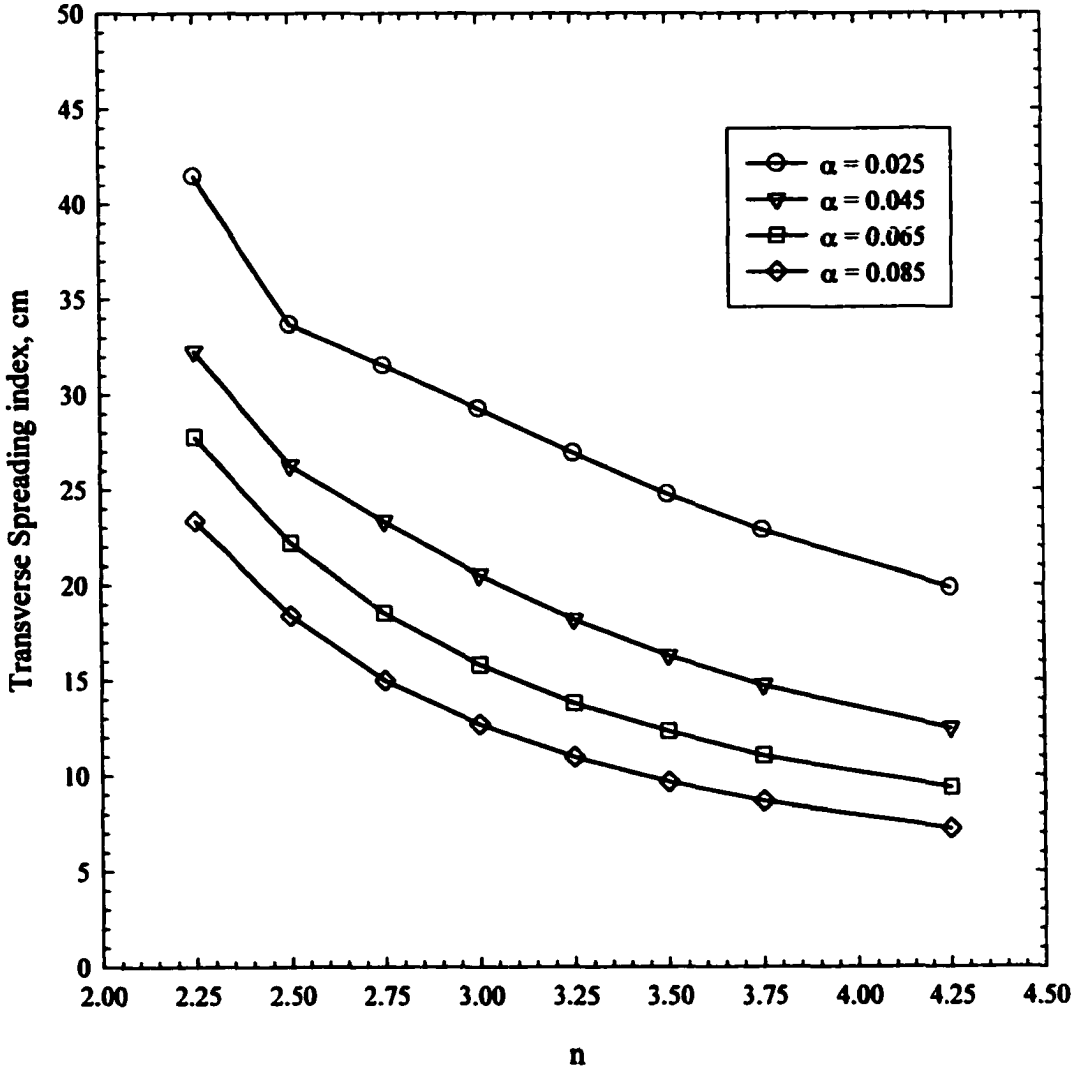

Figure 4.17 Effect of VG parameters on Transverse Spreading Index (TSI) of the moisture plume in 2D homogeneous simulations.

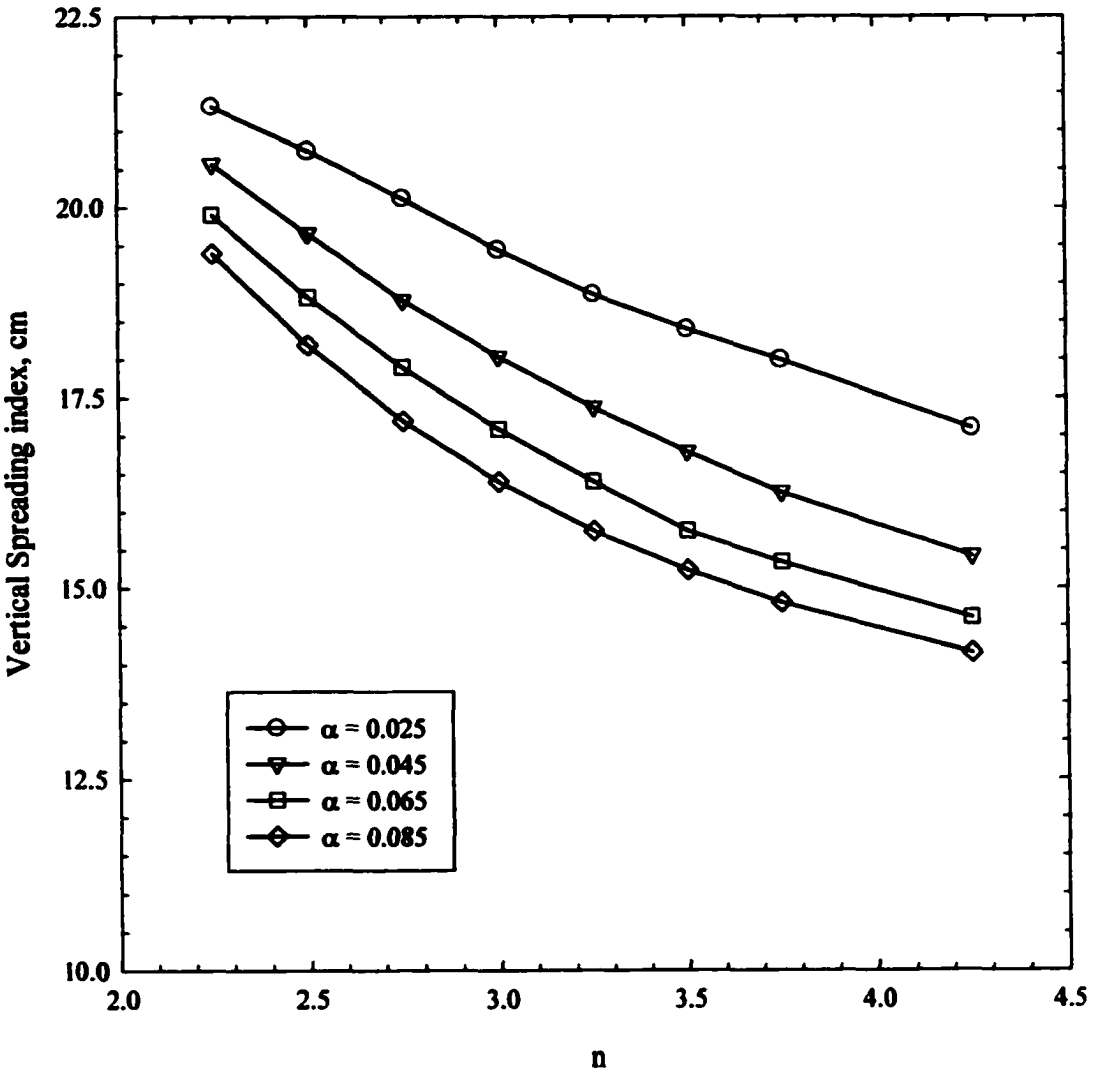

Figure 4.18 Effect of VG parameters on Vertical Spreading Index (VSI) of the moisture plume in 2D homogeneous simulations.

with higher n, which represents soils with more uniformity in pore size, has smaller spreading of moisture plume. Again, from the same plots it is observed that VSI decreases as α increases. Therefore, spreading of moisture plume in vertical direction is smaller, same as in the transverse direction, in coarser grain soil.

4.3 Summary

The effects of unsaturated soil properties on moisture movement in homogeneous soils are summarized in this section. It is revealed through a series of homogeneous infiltration simulation that interaction between boundary condition and soil properties probably make it improbable to define effective properties to capture the infiltration behavior. We then went on to explore the effect of unsaturated soil properties on soil water movement during redistribution.

Same initial condition and zero-flux boundary condition were selected for all homogeneous simulation experiments during redistribution period. So that there would be no effect of initial moisture content and type of boundary condition on the moisture plume movement. It has been found that the average vertical velocity of the moisture plume increases with increasing VG parameters in both 1D and 2D simulation experiments. Higher velocity of the moisture plume in unsaturated soil was observed when the soil is coarser grained or more uniformed in its pore size distribution, i.e., when. the moisture retention function has flatter slope at middle saturation section. Increments

in water pressure head over a small interval drive out more water from such soil during drainage cycle.

Spreading of the moisture plume is decreases in both transverse and vertical direction with increasing VG parameters. Smaller spreading of the moisture plume in unsaturated soil was observed when the soil is coarser grained or more uniformed in its pore size distribution. Because of the shape of moisture retention curve of coarser grained soil or more uniformed soil in pore size distribution, comparatively less water is held up in the drying part of the moisture plume. On the wetting front side of moisture plume, comparatively less water spreads out due to more uniformity of pore size distribution or due to coarser textural characteristics. On the wetting front side tension were very high as the soil in that region were at residual saturation. The slope of moisture retention function of the coarser soil or the soil with more uniform pore size distribution is steeper at dry region (where moisture content is close to residual saturation). As a result, equal drop in water pressure head drives in less water to surrounding dry soil.

Chapter 5: Heterogeneous simulations

5.1 Introduction

A primary objective of the simulation experiments described in this chapter is to observe the effect of heterogeneity on the average velocity, transverse and vertical spreading index of the moisture plume in 1D and 2D domain. The computational porous medium used in these numerical experiments consists of two soils (background and lens). These two soils are only different in their pressure-saturation-relative permeability functions. As it is discussed in previous chapters, these relationships can be parameterized by n and α. Therefore, mediums used in the experiments are heterogeneous only with respect to n or α or both. All other soil properties are same for both soils.

Descriptions of variables that can quantify the heterogeneity of the 1D medium are illustrated in Section 5.2.1. Section. 5.2.2. presents the variables, which can capture the overall movement of the moisture plume in 1D domain. Descriptions of the 1D numerical simulations (Domain size, time step, vertical and horizontal discretizations, boundary condition, initial condition etc.) are presented in Section 5.2.3. Resulting data and their analysis are summarized in Section 5.2.4. Similarly, Section 5.3.1 to Section 5.3.4 describes the same for 2D simulations.

5.2 1D Simulations

5.2.1 Controlled variables

5.2.1.1 Heterogeneity

The heterogeneity of a soil can be quantified by the degree of contrast between soil properties, volumetric proportion of different soil and correlation length or lens aspect ratio. In 1D simulations, only layered heterogeneity is possible. Degree of contrast is the only controlled variable, the effect of which on estimated variable would be evaluated in 1D heterogeneous simulations. When only two soil types are present, heterogeneity index (Φ_β) can be defined as

$$\Phi_\beta = \frac{\beta_B - \beta_L}{\beta_B} \qquad (5.1)$$

where β_B = background soil property of interest; β_L= lens soil property of interest.

5.2.2 Estimated variables in 1D domain

Two variables that describe the average behavior of moisture plume movement in 1D medium are average velocity and vertical spreading index. These two variables are estimated from the transient moisture distribution during redistribution. In theory, the estimated variables of heterogeneous simulation could be compared to the respective variables estimated from homogeneous simulation results to identify effective parameters for a particular heterogeneous medium.

5.2.3 Descriptions of 1D simulations

We now consider a redistribution problem in a layered system, consisting of horizontal layers with alternating material properties (α and/or n). In the following experiments the initial and boundary conditions for flow were essentially identical to those for the homogeneous case. Zero flow boundary condition is applied on all sides of the domain. Initial pressure head distributions are selected in such a way, so that all the nodes of the top 30 cm are at full saturation and rest of the nodes are at residual saturation or close to residual saturation. For comparative analysis, our choice of initial pressure head distribution guarantees that total initial mass of water in the domain is equal for all simulations. At the same time, location of the center of mass and spreading around the center of mass of moisture plume at the beginning of redistribution are same for all cases. To avoid the effect of bottom boundary, all simulations are allowed to run till the center of the moisture plume reaches the middle depth of the domain.

Size of the computational domain was 10×10×200 cm. The domain was discretized using a nodal spacing of 2.5 cm in the vertical direction. A time step of 5 seconds was used throughout the simulation. For the heterogeneous cases, $(K_s)_x$, $(K_s)_z$, θ_s, θ_r had the same average values as in the homogeneous simulations, but Van Genuchten parameters α and n were treated as spatially variable. To isolate the effect of these two parameters, all simulations were divided into two categories. First, we consider only n was variable in space and second, only α was variable in space. The background soil used in this set of simulation experiments is loamy sand. The parameters are

reported by Hills et al. (1989). Grid setup and material properties used in heterogeneous simulations are summarized in Table 5.1.

Table 5.1 1D Heterogeneous model: grid setup and material properties

Number of nodes in x-direction	2
Number of nodes in z-direction	81
Node spacing in z-direction (cm)	2.5
Time step size (sec)	5.0
Saturated hydraulic conductivity, $(K_s)_x$ (cm/sec)	0.00625
Saturated hydraulic conductivity, $(K_s)_z$ (cm./sec)	0.00625
Saturated water content	0.3658
Residual water content	0.0286
Porosity	0.3658
Storativity	1×10^{-5}

5.2.4 1D Heterogeneous simulations results

The average velocity and vertical spreading index of the moisture plume in heterogeneous soil are normalized by the average velocity and vertical spreading index of the moisture plume in homogeneous medium that is composed of background soil. Average velocity of the moisture plume in homogeneous medium that is composed of background soil is denoted by V_{Bavg}. Similarly, vertical spreading of the moisture plume

in homogeneous medium that is composed of background soil is denoted by $(VSI)_B$. Normalized estimated variables of the moisture plume in heterogeneous soil are the measure of the impact of heterogeneity. For example, normalized velocity less than unity indicates that average velocity of the moisture plume in heterogeneous soil is reduced due to heterogeneity.

5.2.4.1 Heterogeneous with respect to n

Normalized average velocity is plotted against the degree of contrast (Φ_n) between n of background and lens soil in Figure 5.1. The graph shows two cases (1) when background n is larger than lens n ($\Phi_n > 0$) and (2) when background n ($\Phi_n < 0$) is smaller than lens n. It has been observed that average velocity is decreasing with increasing degree of contrast of n in both cases. However, the effect of degree of contrast on average velocity is less pronounced when background n is smaller than lens n. The average velocity of the moisture plume ($\Phi_n < 0$) in heterogeneous medium remains very close to the average velocity in homogeneous medium with background soil properties. In the other case ($\Phi_n > 0$), average velocity in the heterogeneous medium is significantly reduced with small increment of degree of contrast when $\Phi_n > 0$.

In the following two paragraphs, attempt is made to explain why normalized average velocity in heterogeneous medium is more sensitive to the degree of heterogeneity when $\Phi_n > 0$ than when $\Phi_n < 0$. It is established in previous chapter that moisture plume moves faster in homogeneous soil with higher n. Therefore, when lens

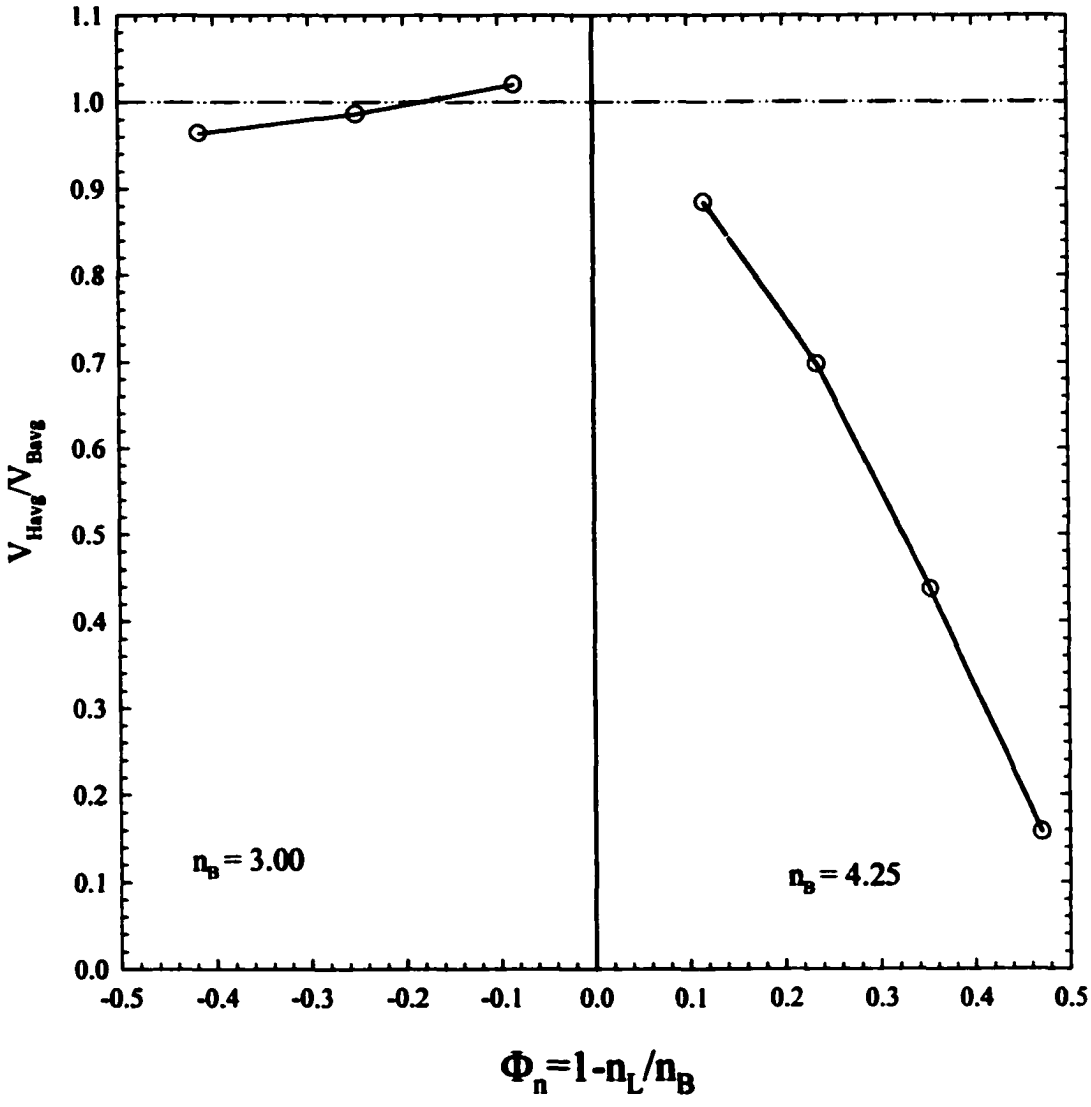

Figure 5.1 Effect of heterogeneity index on normalized average velocity of the moisture plume when $\alpha_B = \alpha_L = 0.045$.

with smaller n is introduced in background soil with higher n ($\Phi_n > 0$), it was expected that the average plume movement in heterogeneous soil would be retarded. Two mechanisms work behind this. First, because of the nature of moisture retention curve, more water is held up in lens soil for a particular capillary pressure, which makes the overall movement of moisture plume slow. Soil, with less uniform pore size distribution, retains more water for a particular water pressure provided the water pressure is higher than the entry pressure of the soil ($h > 1/\alpha$). This feature is illustrated in constitutive relationships curves (Figure 5.2). Second, water from lens soil penetrates very slowly to background soil because of reduced relative permeability of background soil. Since, both mechanisms work in the same direction, average velocity of moisture plume in heterogeneous medium ($\Phi_n > 0$) is significantly reduced.

On the other hand when $\Phi_n < 0$, it is expected that average velocity of moisture plume in heterogeneous soil with lens having larger n will be higher than the velocity in homogeneous soil. But it appears from Figure 5.1 that it is not always true and it depends on degree of contrast. As the degree of contrast is increasing, average velocity is decreasing. But in comparison to previous case ($\Phi_n > 0$), the reduction in normalized average velocity is not significant when $\Phi_n < 0$. In this case, water drains out faster from lens soil, which contribute to increment of overall velocity. Again, the lens soil with reduced relative permeability acts as a blockade and because of that, water bypass the lens soil and moves in the transverse directions, which contribute to reduction of average vertical velocity. Thus, two mechanisms work in opposite direction and the total effect is

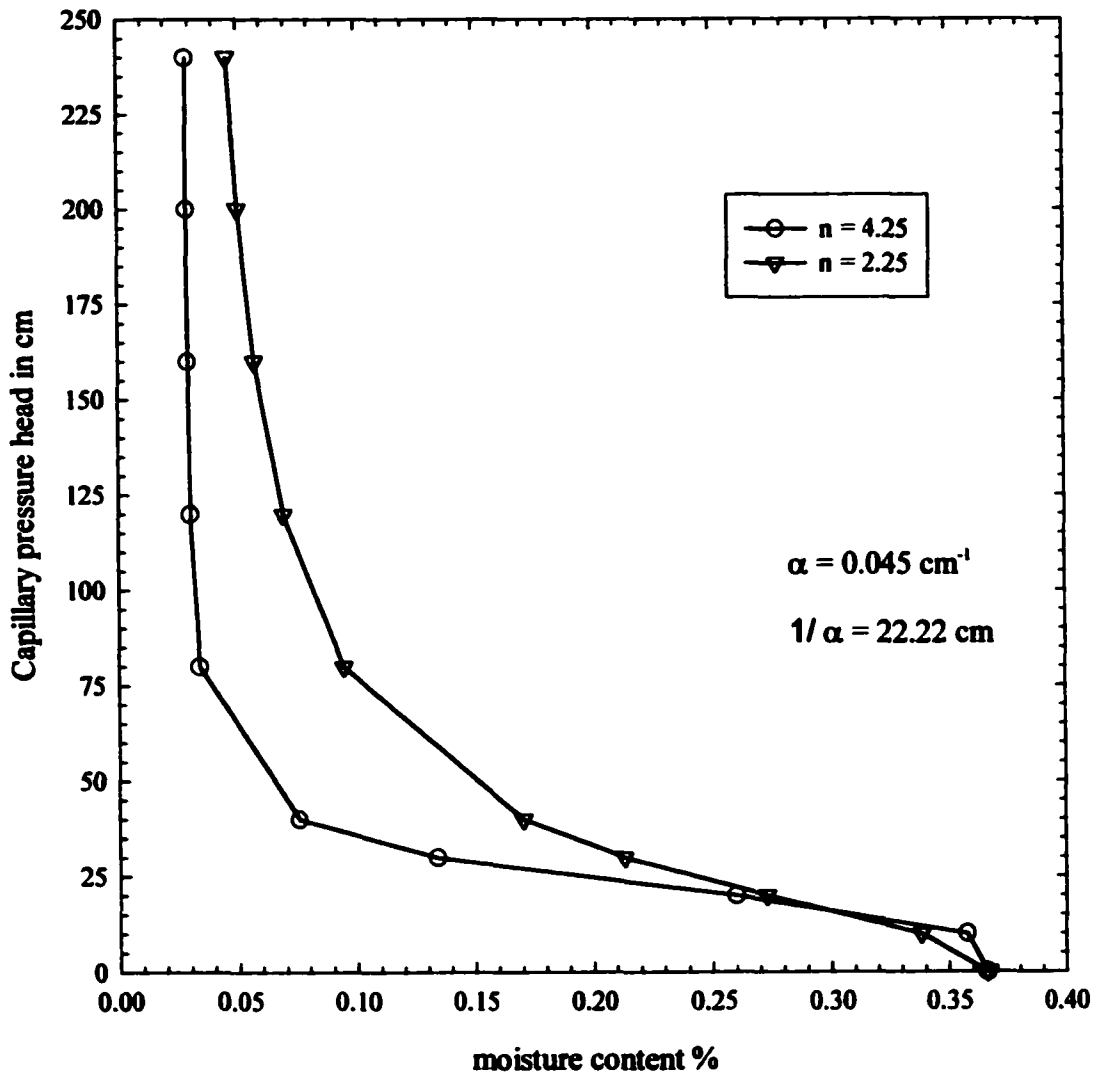

Figure 5.2 Capillary pressure ~ moisture relationship in two unsaturated soil with different n but equal $\alpha = 0.045\ cm^{-1}$

to some extent cancelled. That explains the insensitivity of average velocity of the moisture plume when background n is smaller than lens n.

Figure 5.3 shows the effect of heterogeneity index on normalized VSI for an alternating layering 1D system. It has been found that VSI is decreasing with heterogeneity index when $\Phi_n > 0$ and increasing when $\Phi_n < 0$. It has been observed from homogeneous simulation results that spreading index is smaller in soil with more uniform pore size distribution (higher n). In heterogeneous medium ($\Phi_n > 0$), because of the reduced relative permeability of background soil, soil water movement is slowed down. Consequently, vertical spreading of moisture plume is also restricted.

Vertical spreading in heterogeneous medium ($\Phi_n < 0$) is found to be increasing with increasing degree of contrast. Since normalized VSI of the moisture plume in heterogeneous medium is grater than unity, VSI in heterogeneous medium is higher than that in homogeneous medium, with same soil properties as background soil. This time, lens soil acts as a blockade, thus delaying water to drain from the top part of the column, which is made up with background soil. This entrapped water at the top of the column shown in Figure 5.4, contributes to the higher vertical spreading index in heterogeneous soil.

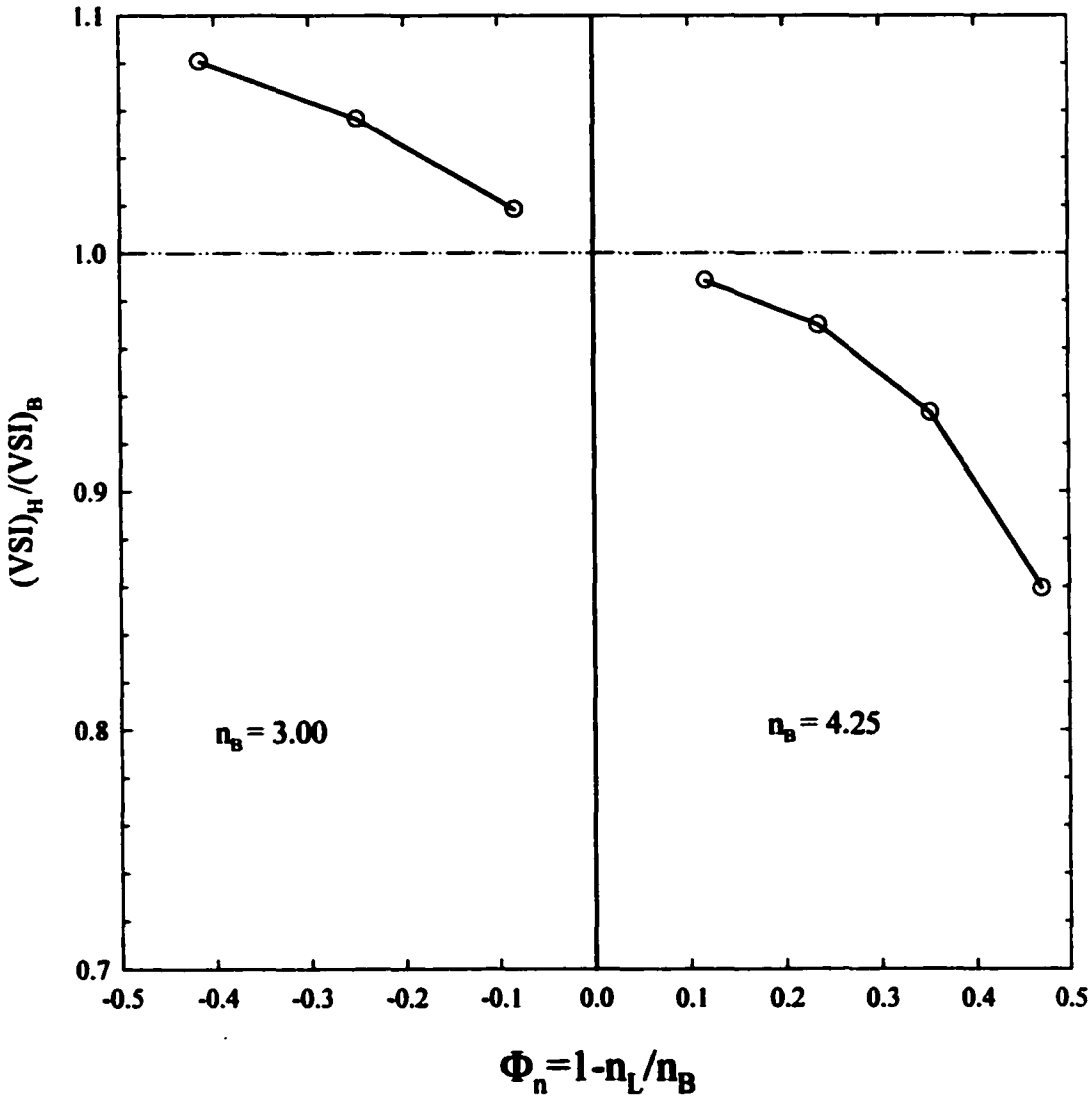

Figure 5.3 Effect of heterogeneity index on normalized vertical spreading index of the moisture plume when $\alpha_B = \alpha_L = 0.045$.

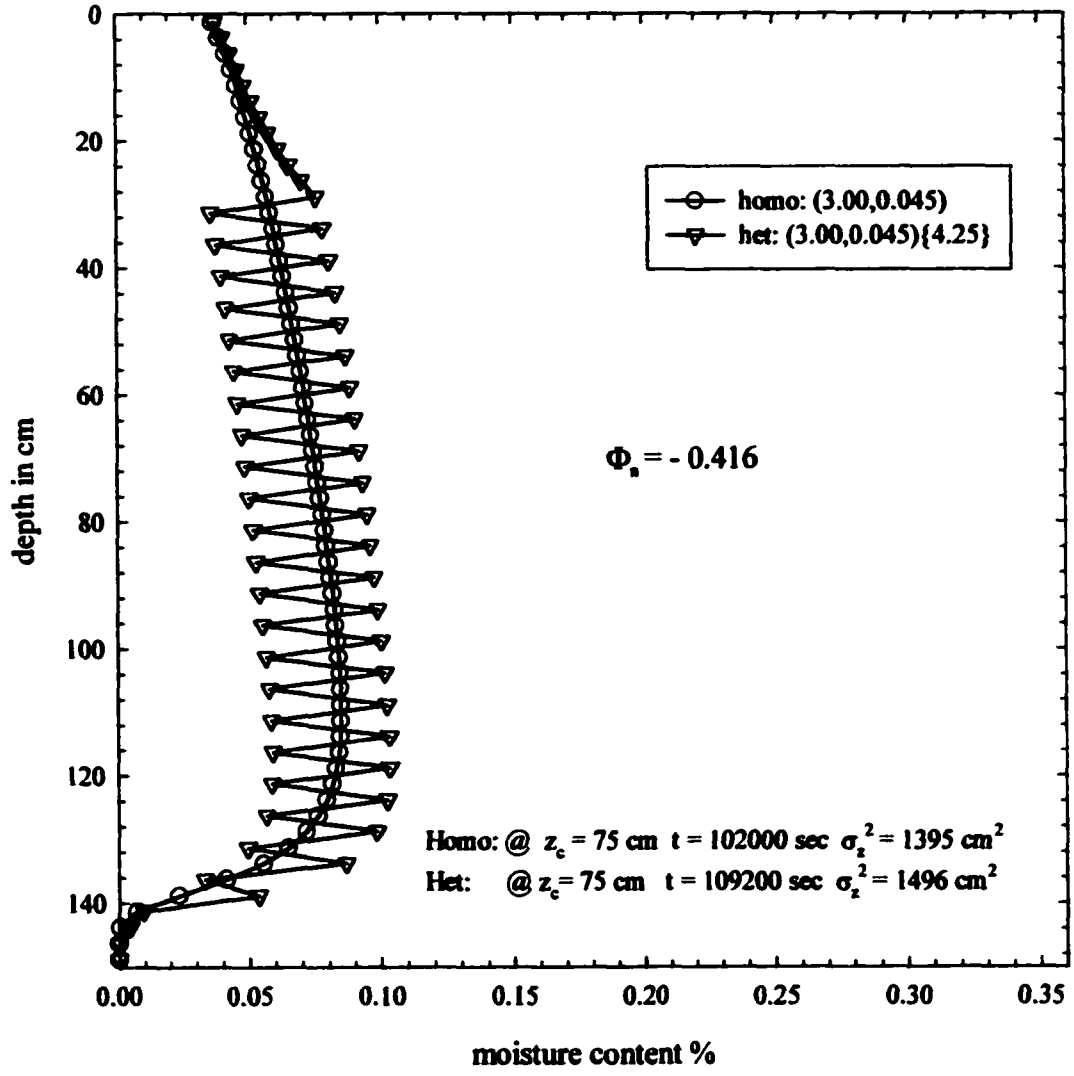

Figure 5.4 Moisture profile in homogeneous and heterogeneous soil, Φ_n for heterogeneous soil is -0.416, where $\alpha_B = \alpha_L = 0.045$.

5.2.4.2 Heterogeneous with respect to α

Figure 5.5 illustrates the effect of heterogeneity index Φ_α on the normalized velocity of the moisture plume. It has been observed that average velocity in heterogeneous medium is significantly reduced as the heterogeneity index increasing for both $\Phi_\alpha > 0$ and $\Phi_\alpha < 0$. When $\Phi_\alpha > 0$, background soil has higher α than that of lens soil and therefore has a smaller entry pressure which is a characteristic of coarse-grained soil. From homogeneous simulation results it has been shown that average velocity of moisture plume is higher in soil with higher α. This is because the moisture retention curve for this type of soil is flatter than that of soil with smaller α. Therefore, it is expected that introduction of lens soil with smaller α reduces the average velocity of the moisture plume. Another factor, which is responsible for the reduced average velocity in heterogeneous medium, is the reduced relative permeability of background soil. Relative permeability of background soil approaches to zero as time increases and water remains entrapped in the lens soil. As a result, the average velocity of the heterogeneous soil, with higher α in background and smaller α in lens material, turn out to be smaller than the velocity through the homogeneous medium with background material properties.

Also in heterogeneous medium with smaller background α ($\Phi_\alpha < 0$), average velocity is becoming smaller with increasing heterogeneity index (Figure 5.5). The general perception based on homogeneous simulation results is, average velocity in heterogeneous soil with lens material with higher α should be higher than the

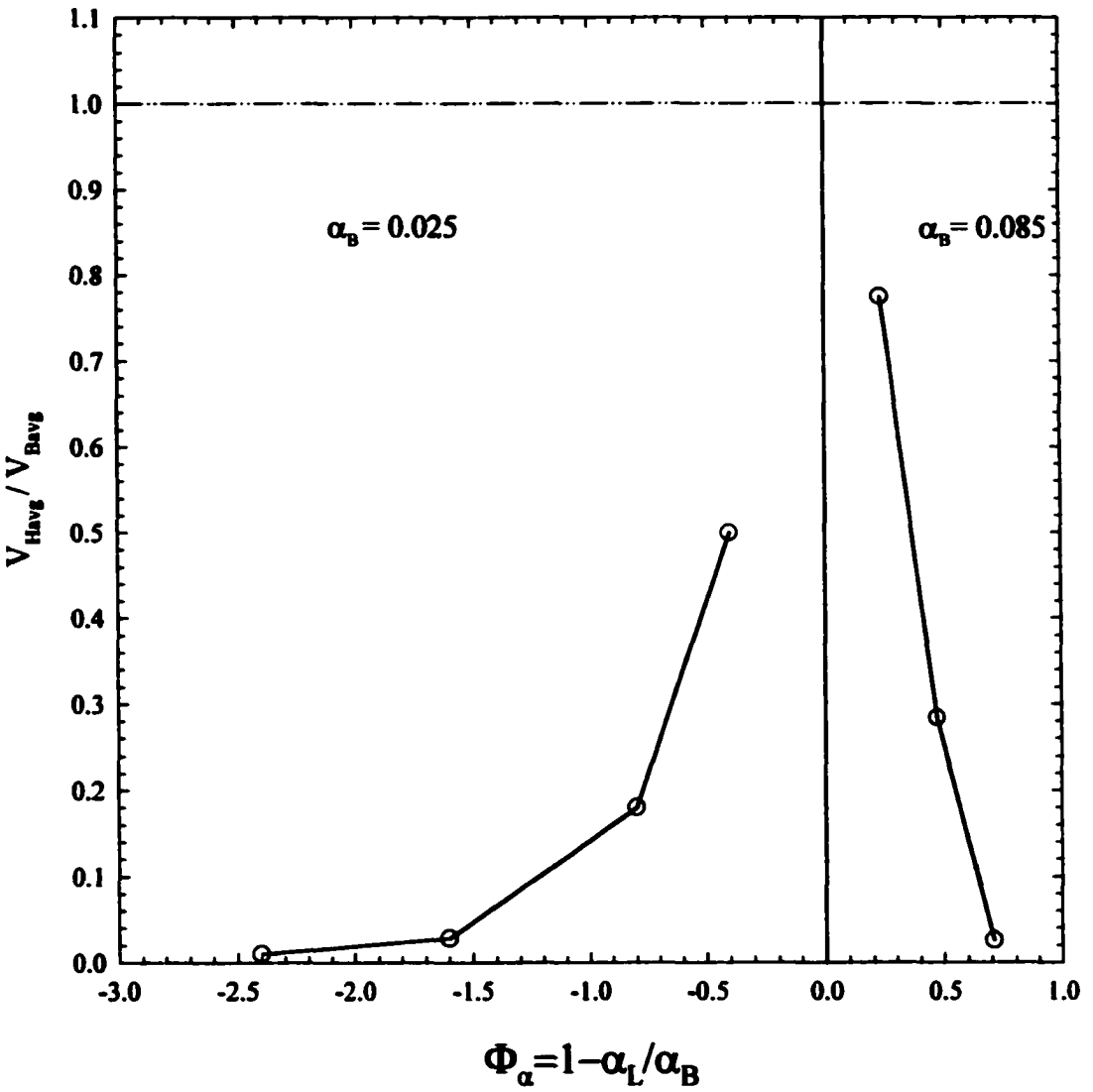

Figure 5.5 Effect of heterogeneity index on normalized average velocity of the moisture plume when $n_B = n_L = 2.75$.

homogeneous velocity. But from the Figure 5.5, it appears that it is not true. In this scenario, 'blockade' (reduced relative permeability) effect of lens soil surpass the effect of shape of moisture retention curves. It is evident from the moisture profiles (Figure 5.6) bulk of the initial moisture content remains entrapped in the top part of the soil column.

Figure 5.7 shows the effect of heterogeneity index on standardized VSI for an alternating layering 1D system when only α is the spatially variable material properties. It has been observed that VSI is decreasing with heterogeneity index when $\Phi_\alpha > 0$. From soil moisture profile (Figure 5.8) along the depth of the column, it is evident that moisture content distribution at upper most part of the heterogeneous column is a factor for reduced spreading in vertical direction. Water from the uppermost part of the column drains fast and water pooling is observed in lens soil.

Again, it appears from the Figure 5.7 that VSI of the moisture plume in heterogeneous medium is increased due to heterogeneity and is increasing with heterogeneity index when $\Phi_\alpha < 0$. In another words increased vertical spreading was observed when background soil α was smaller and it was increasing with increasing degree of contrast between background soil and lens parameter. Smaller α corresponds to soil with higher entry pressure; water starts draining at comparatively high capillary pressure. When that critical capillary pressure is attained, all waters drain out from lens soil with higher α and relative permeability in lenses approaches zero. Consequently, lens material acts as a barrier here and water trapped in background soil. It has been

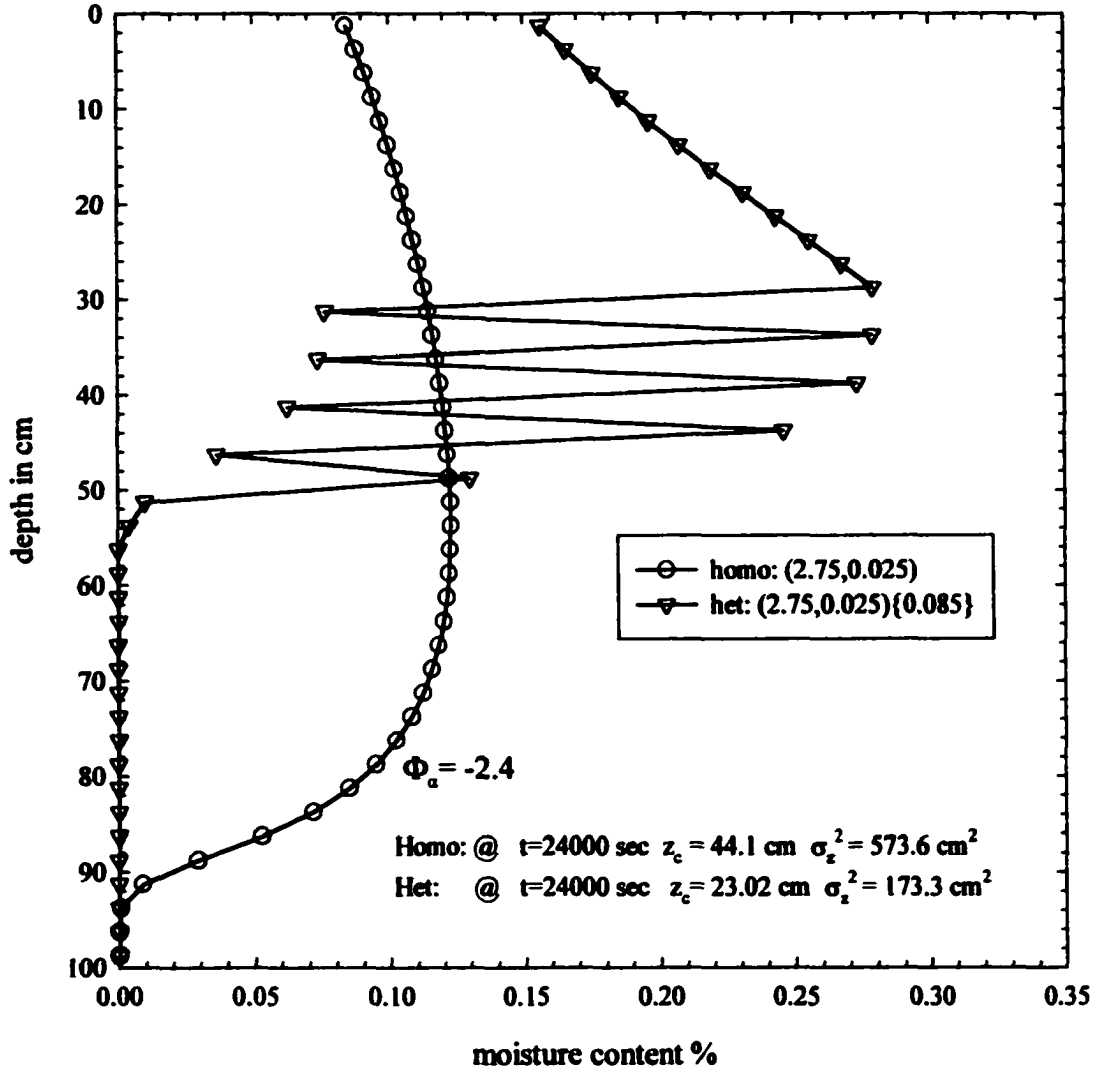

Figure 5.6 Moisture profile in homogeneous and heterogeneous soil, Φ_α for heterogeneous soil is - 2.4, where $n_B = n_L = 2.75$.

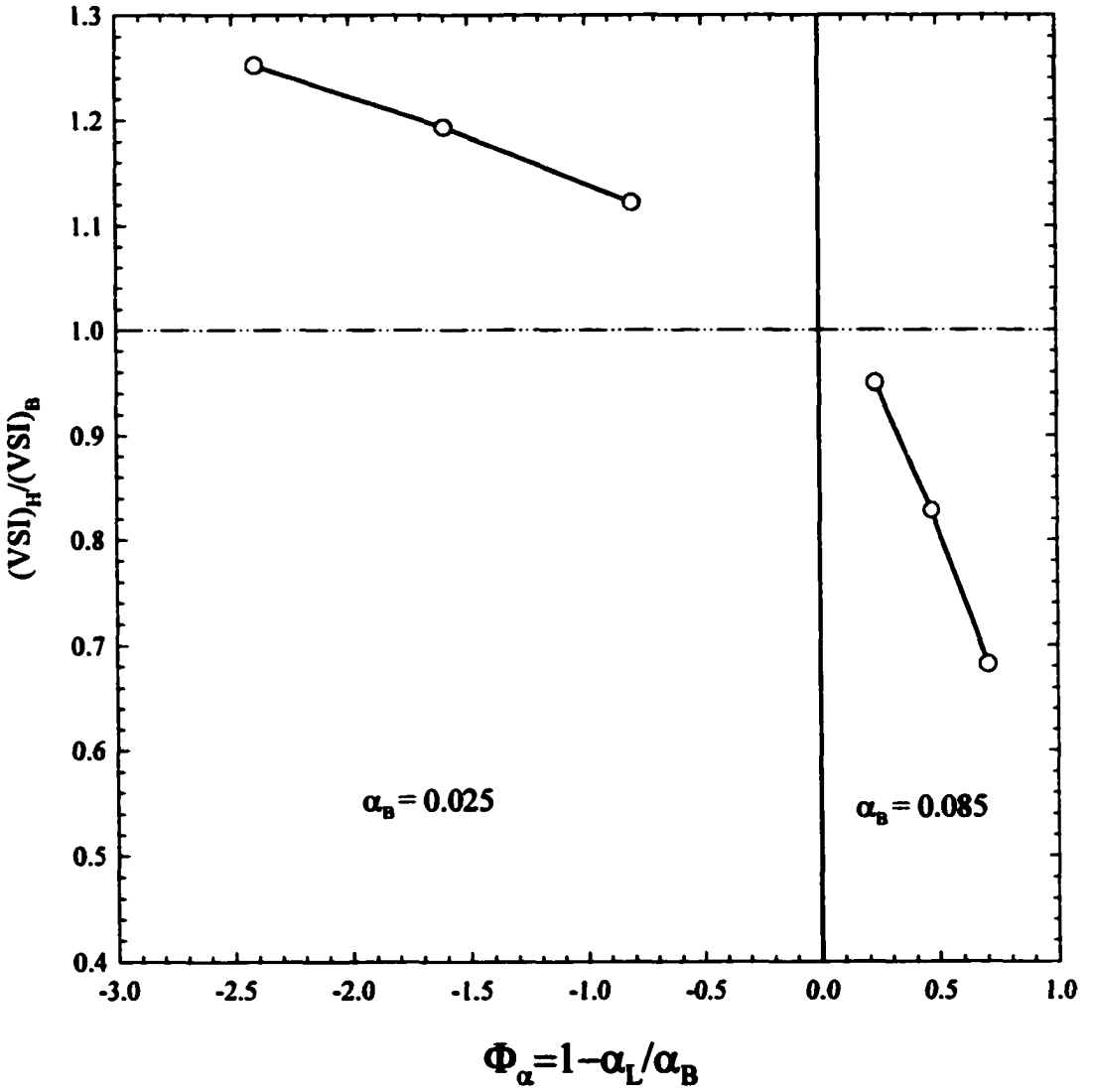

Figure 5.7 Effect of heterogeneity index on normalized vertical spreading index of the moisture plume when $n_B = n_L = 2.75$.

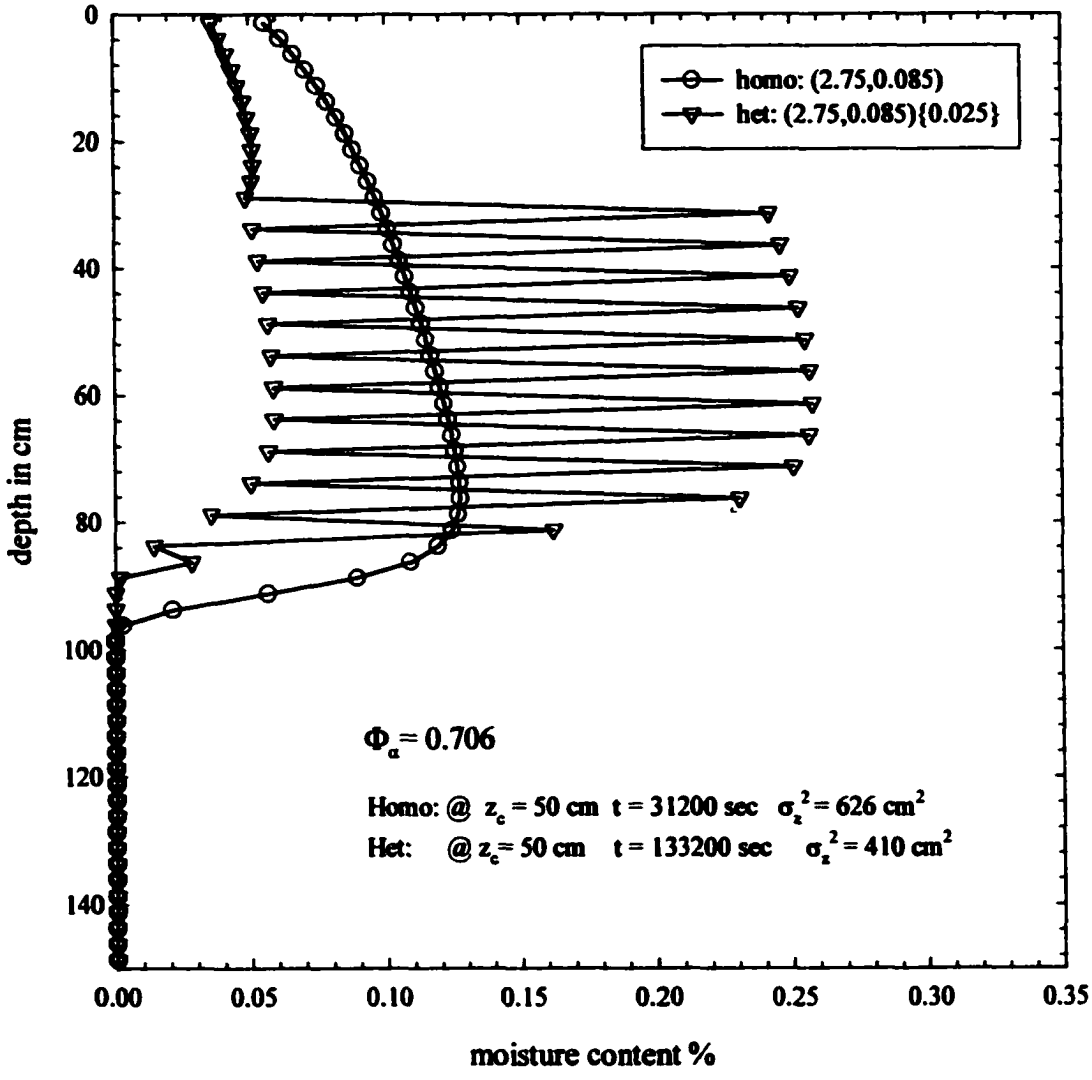

Figure 5.8 Moisture profile in homogeneous and heterogeneous soil, Φ_α for heterogeneous soil is 0.706, where $n_B = n_L = 2.75$.

observed in Figure 5.9 that higher proportions of moisture content are held up by the background soil at the top part of the soil column. This moisture content contributes to the higher spreading in vertical direction.

5.3 2D Simulations

5.3.1 Controlled variables

In addition to heterogeneity index, two more controlled variables are introduced in 2D simulations experiments: (1) volumetric proportion of lens material and (2) aspect ratio of lenses.

5.3.1.1 Volumetric proportion

The effect of volumetric proportion of lenses on the average movement of moisture plume will be explored. Three different proportion (10%, 20%, 30%) of lens material are considered for the following simulations to see the impact of the proportion of the lens material on soil water movement. Although the spatial distribution of lenses is random, we try to distribute lens material uniformly over the depth of the domain, i.e., each horizontal layer of grid elements contains a constant proportion of lens elements.

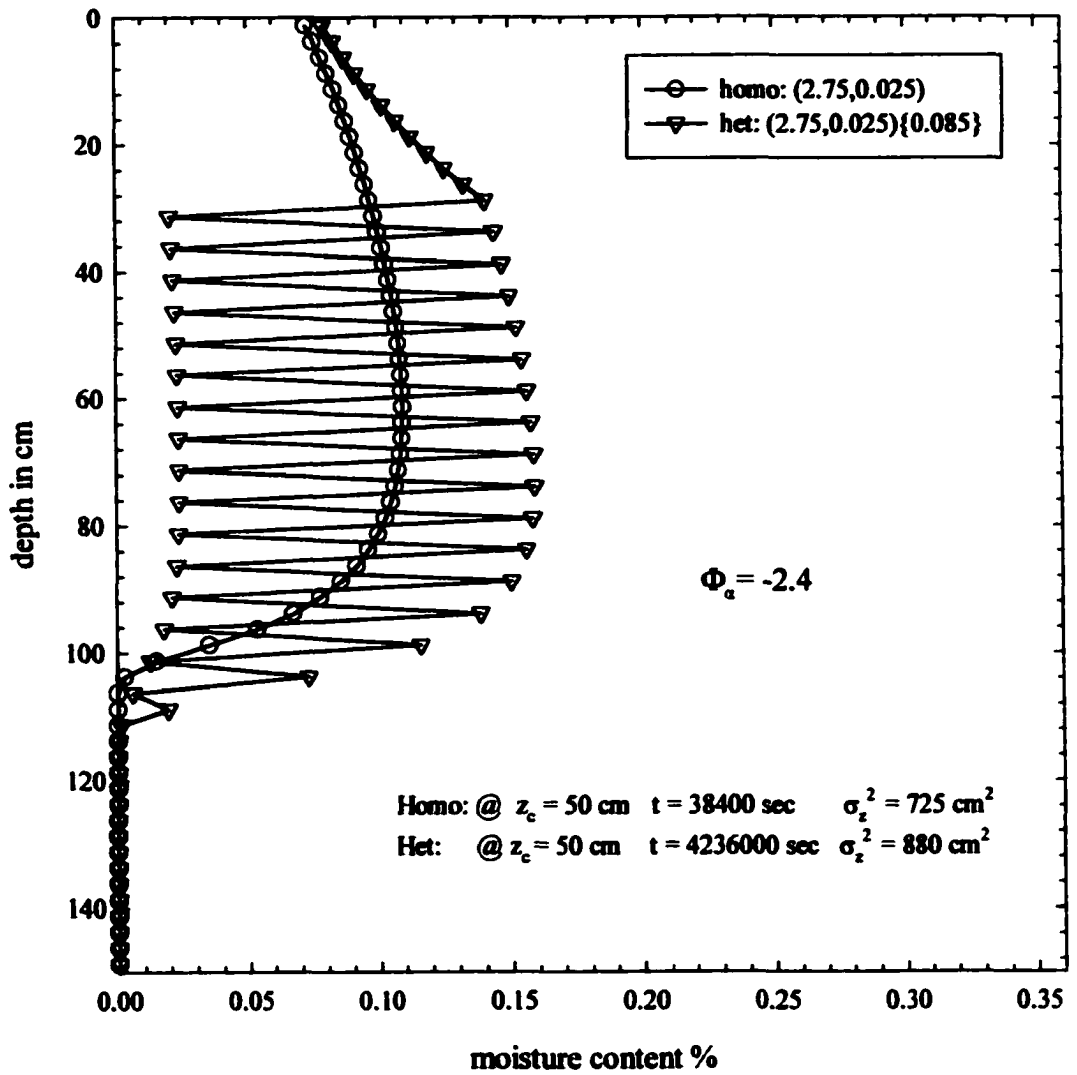

Figure 5.9 Moisture profile in homogeneous and heterogeneous soil, Φ_α for heterogneous soil is -2.4, where $n_B = n_L = 2.75$.

5.3.1.2 Aspect ratio of lens material

Aspect ratio of lens material is defined for this study as the ratio of horizontal length to vertical length of lenses. It is assumed that vertical correlation length (λ_v) is equal to one half of the layer thickness, the average distance over which the soil properties are correlated. Similarly, horizontal correlation length (λ_H) is one half of the length of lens material in transverse direction. Effect of three different aspect ratios ($\frac{\lambda_H}{\lambda_V}$ = 4, 8, 12) on average soil water movement, are evaluated when volumetric proportion of lens material is 30%.

5.3.1 Estimated variables in 2D domain

5.3.2.1 Transverse Spreading Index

In addition to average velocity and vertical spreading index, transverse spreading index (TSI) of the moisture plume may be estimated in 2D simulations. TSI can be estimated using equation (4.5). TSI of the moisture plume in heterogeneous soil is symbolized by TSI_H.

5.3.2 Description of 2D simulations

In the following experiments the initial and boundary conditions for flow were similar to those for 1D simulations. To allow spreading of the moisture plume in transverse direction, initial pressure head distributions are selected in such a way, so that

the top middle strip of nodes of size 20×30 cm are at full saturation and rest of the nodes are at residual saturation or close to residual saturation. Zero flow boundary condition is applied on all sides of the domain. For comparative analysis, our choice of initial pressure head distribution guarantees that total initial mass of water in the domain is equal for all simulations. At the same time, location of the center of mass and spreading around the center of mass of moisture plume at the beginning of redistribution are same for all simulations. In order to satisfy these criteria upper layers of the domain are not heterogeneous (Figure 10). To avoid the effect of bottom boundary, all simulations are allowed to run till the center of the moisture plume reaches the middle depth of the domain.

Size of the computational domain was 100×10×100 cm. The domain was discretized using a nodal spacing of 10 cm in horizontal and 2.5 cm. in vertical directions. Figure 5.10 shows a domain of heterogeneous soil with 30% lenses where lens aspect ration is 4. A time step of 5 second is used for all simulations. Same soil properties, which are used in 1D simulations, are used in 2D simulations.

5.3.4 2D Heterogeneous simulations results

5.3.4.1 Heterogeneous with respect to n

Figure 5.11 shows the normalized average velocity of center of mass of the moisture plume at different heterogeneity index for three different volumetric proportions. It is observed from the plot (Figure 5.11) that average velocity is reduced

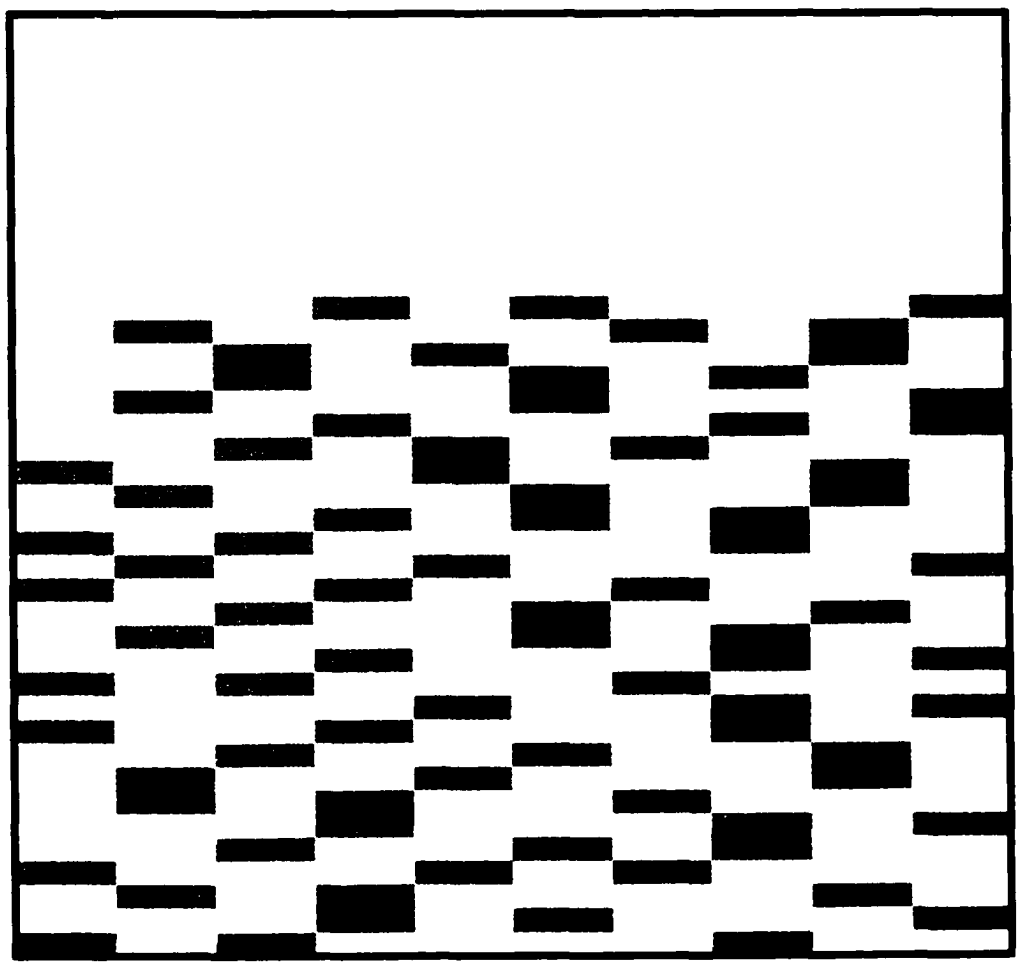

Figure 5.10 Heterogeneous soil domain with 30% lenses by volume; aspect ratio of lens size is 2 to 4.

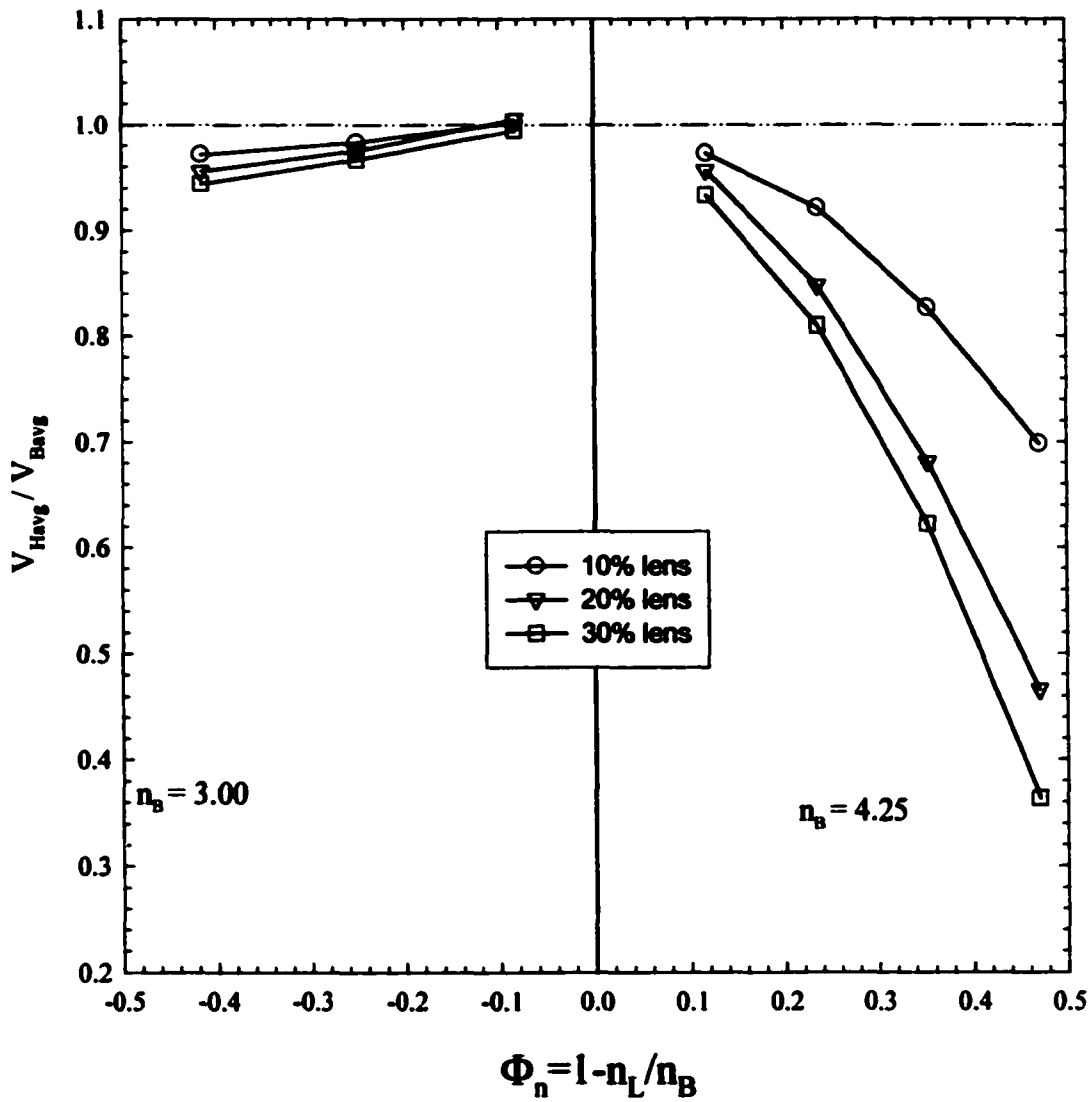

Figure 5.11 Effect of heterogeneity index on normalized average velocity of the moisture plume when $\alpha_B = \alpha_L = 0.045$.

because of heterogeneity. It is also observed that average velocity of the moisture plume is decreasing with increasing degree of contrast for both cases ($\Phi_n>0$ and $\Phi_n<0$). This effect is significantly more pronounced when $\Phi_n>0$. Average velocity is also decreasing with increasing volumetric proportion of lenses. Again, the effect of volumetric proportion of lenses on average velocity is more significant when $\Phi_n>0$.

In an attempt to explain the observed effect, we look into details of two examples. First example illustrates the movement of the moisture plume when background soil is more uniform in pore size distribution than lenses ($\Phi_n>0$) and comparative analysis between heterogeneous and homogeneous simulation results. Second example illustrates the movement of the soil moisture plume in heterogeneous soil where background soil is less uniform in pore size distribution ($\Phi_n<0$) than lenses and comparative analysis between heterogeneous and homogeneous simulation results. Homogeneous medium has the same soil properties as the background of heterogeneous soil has.

5.3.4.1.1 Example 1 (moisture content contour plots when $\Phi_n>0$)

Figure 5.12 and 5.13 show moisture content contour plots, which have been generated using homogeneous and heterogeneous simulations results respectively. Figure 5.14 and 5.15 represent the same results in different forms. The simulation time for both homogeneous and heterogeneous simulations are equal to 180 min. The medium is heterogeneous with respect to n only and background n is greater than lens n (Φ_n =0.47).

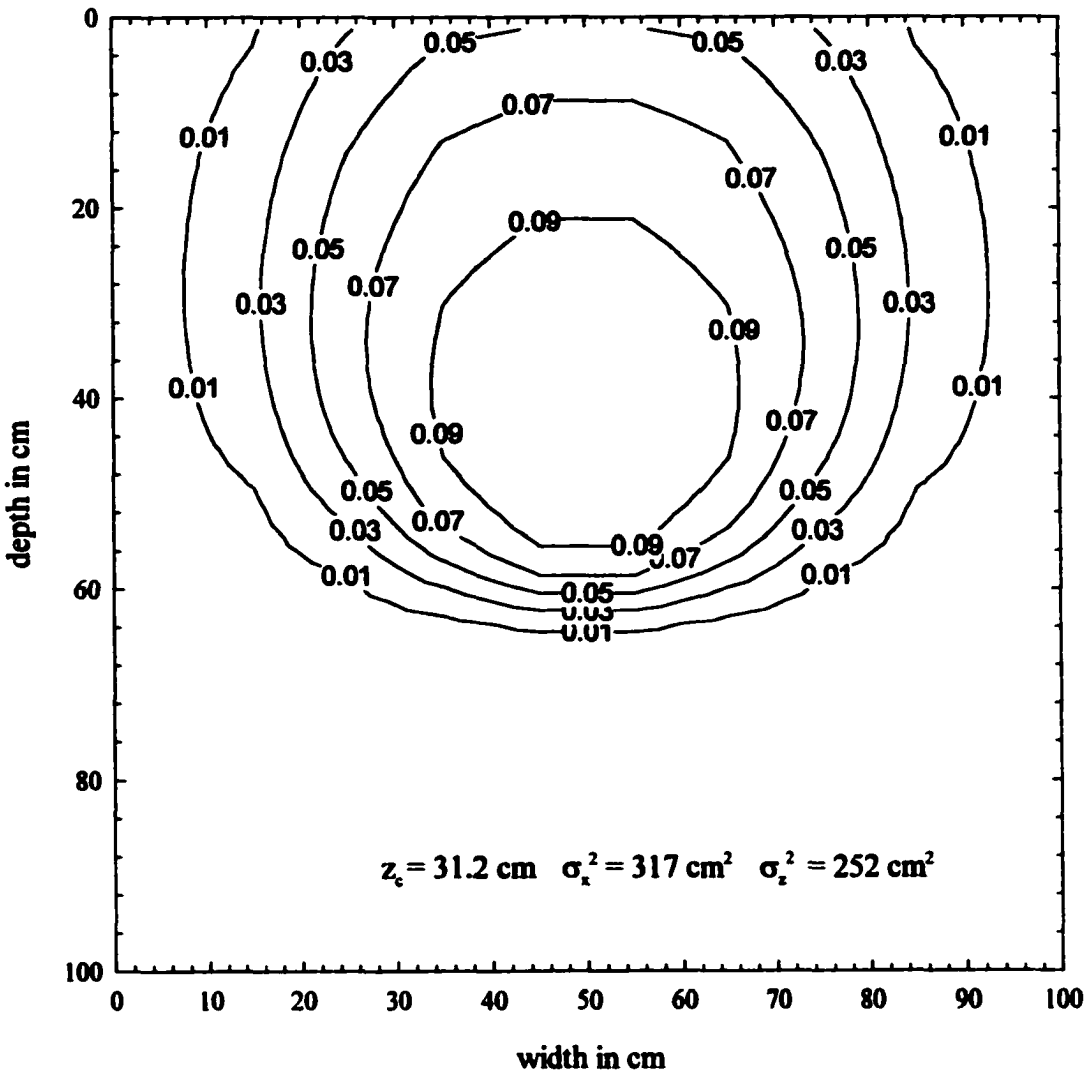

Figure 5.12 Soil moisture content contours when soil properties are homogeneous (n = 4.25, α = 0.045) at t = 180 minutes.

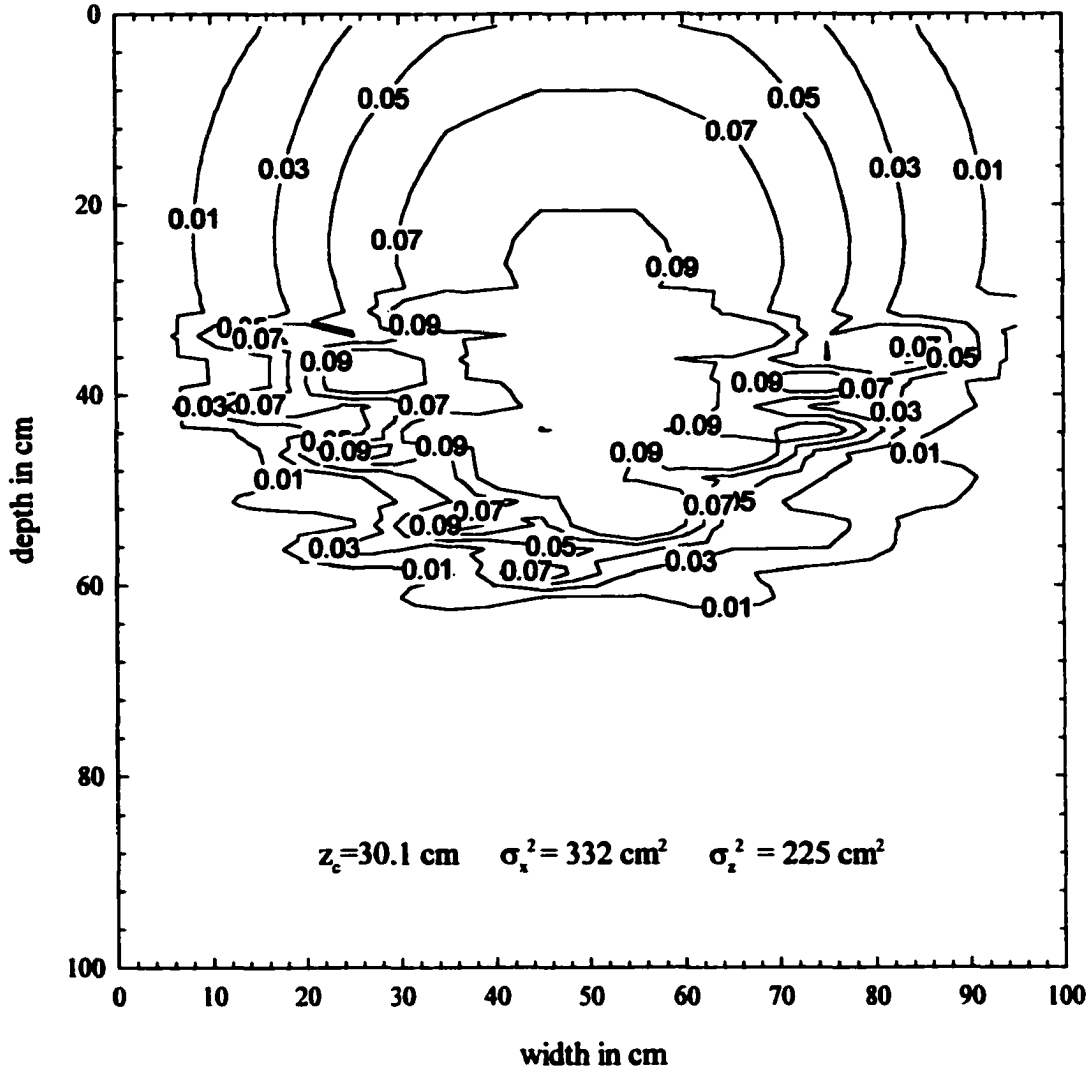

Figure 5.13 Moisture content contours when soil properties are heterogeneous (n_B= 4.25, n_L= 2.25 and α_B= α_L = 0.045) at t =180 minutes. Volumetric proportion of lens is 30% and aspect ratio is 4.0.

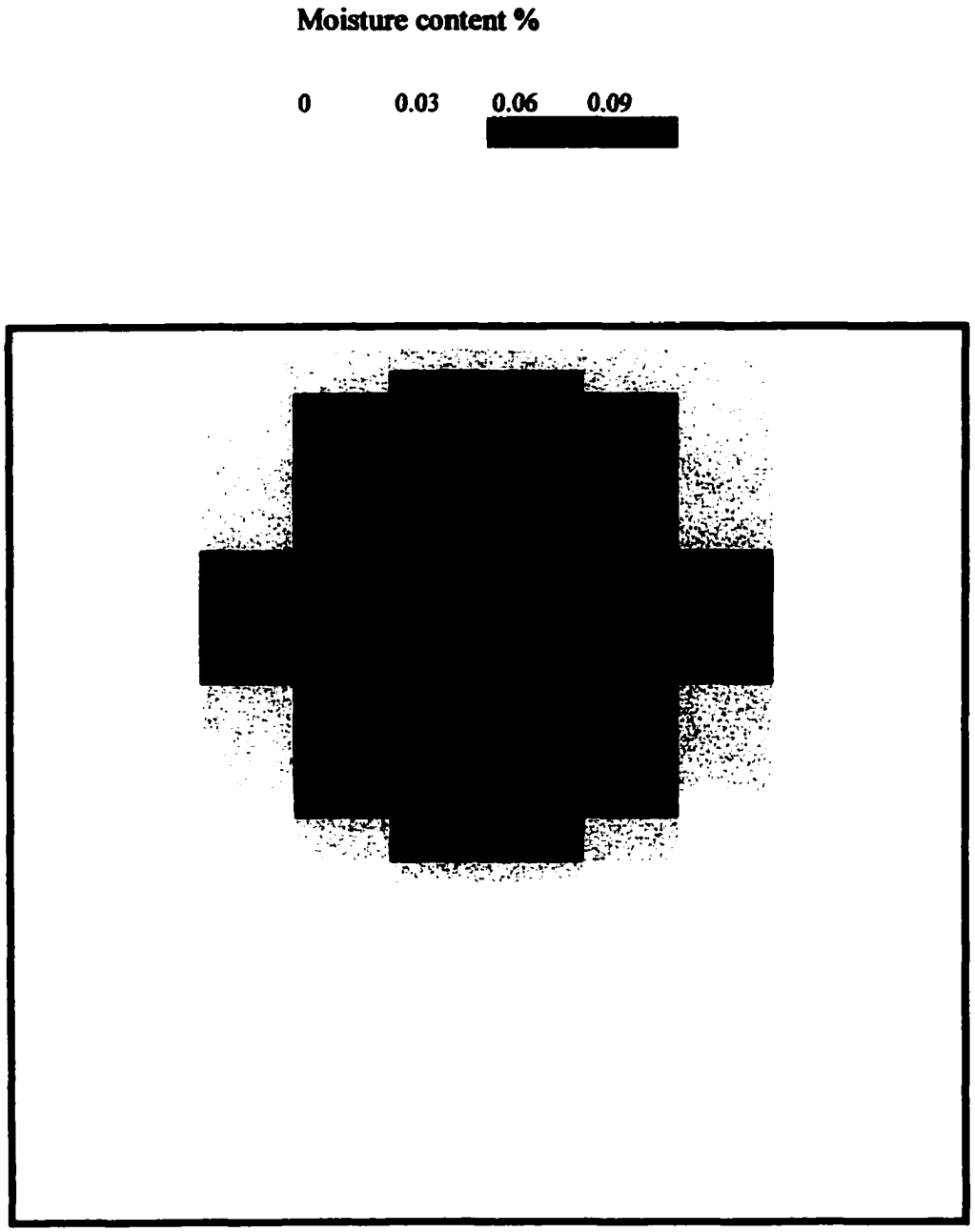

Figure 5.14 Moisture content distribution after 180 minutes in homogeneous soil when $n = 4.25$ and $\alpha = 0.045$.
$z_c = 31.2$ cm $\sigma^2_x = 317$ cm^2 and $\sigma^2_z = 252$ cm^2

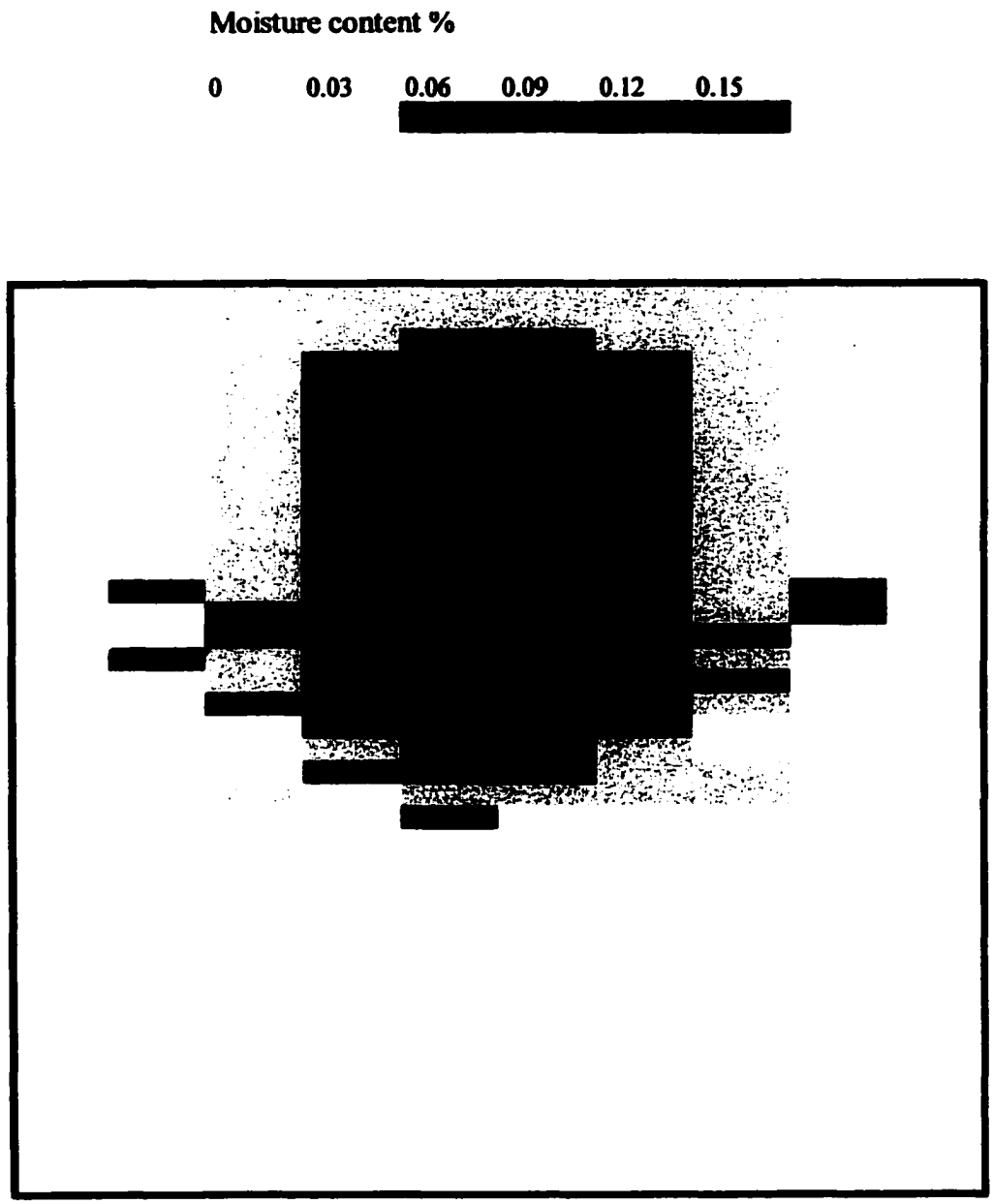

Figure 5.15 Moisture content distribution after 180 minutes in heterogeneous soil (n_B=4.25 n_L=2.25 and α_B=α_L=0.045) z_c = 30.1 cm σ^2_x = 332 cm^2 and σ^2_z = 225 cm^2

In other words, pore size distribution in background soil is more uniform than that in lenses. Since the slope of moisture retention function at the middle section is flatter in soil that has more uniform pore size distribution, water drains out much more abruptly from such soil, whereas relatively higher pressure is required to expel water from lenses with less uniform pore size distribution. As a result, water drains out at slower rate from lenses with less uniform pore size distribution. Another mechanism is account for the slower movement of water in such heterogeneous soil. Since water from background soil drains out faster, eventually moisture content in background soil reaches such a low point so that relative permeability in background soil approaches zero. The considerable amount of moisture content that is held up by lenses is practically trapped by the surrounding soil that has significantly reduced relative permeability. Hence, both the effect of the shape of the moisture retention function and relative permeability in soil contribute to the reduced average velocity of the moisture plume in heterogeneous medium. With the increasing degree of contrast between background soil and lenses, the weight of the two factors, which are responsible for reduced average velocity in heterogeneous soil, is also increasing. Obviously, the amount of trapped water in such configuration of soil ($\Phi_n>0$) is directly related to the volumetric proportion of lenses. Therefore, average velocity of the moisture plume in heterogeneous soil is decreasing due to increased volumetric proportion of lenses

A larger extent of the moisture plume (Figures 5.13 and Figure 5.15) in transverse direction is observed in heterogeneous soil while comparisons are made against the homogeneous simulation results (Figure 5.12 and Figure 5.14). Since the slope of the

moisture retention function of lenses (less uniform pore size distribution) in the vicinity of residual moisture content is flatter, during wetting cycle more water is absorbed by lenses. In addition to that since relative permeability in lenses is comparatively higher than that in background soil, more water flows into lenses. Because of scatter distribution of lenses, more water spreads out laterally, causing higher spreading of the moisture plume in heterogeneous soil.

A smaller extent of the moisture plume (Figures 5.13 and Figure 5.15) in vertical direction is observed in heterogeneous soil while comparisons are made against the homogeneous simulation results (Figure 5.12 and Figure 5.14). Since equal amount of water is allowed to redistribute both in homogeneous and heterogeneous simulation and larger fractions of water are held up by lenses in heterogeneous soil, reduced vertical spreading is observed when lenses are introduced. In another words, reduced relative permeability in surrounding soil retards water to move out from the lenses, which causes shrinkage of the moisture plume in the vertical direction.

5.3.4.1.2 Example 2 (moisture content contour plots when $\Phi_n < 0$)

Figure 5.16 and 5.17 show moisture content contour plots of homogeneous and heterogeneous simulation results respectively. The same results are presented in figure 5.18 and 5.19 in different form. This time heterogeneity index, $\Phi_n = -0.41$ i.e. medium is heterogeneous with respect to n only and background soil has less uniformity in pore size distribution than that in lenses ($\Phi_n<0$). Initial moisture contents are allowed to

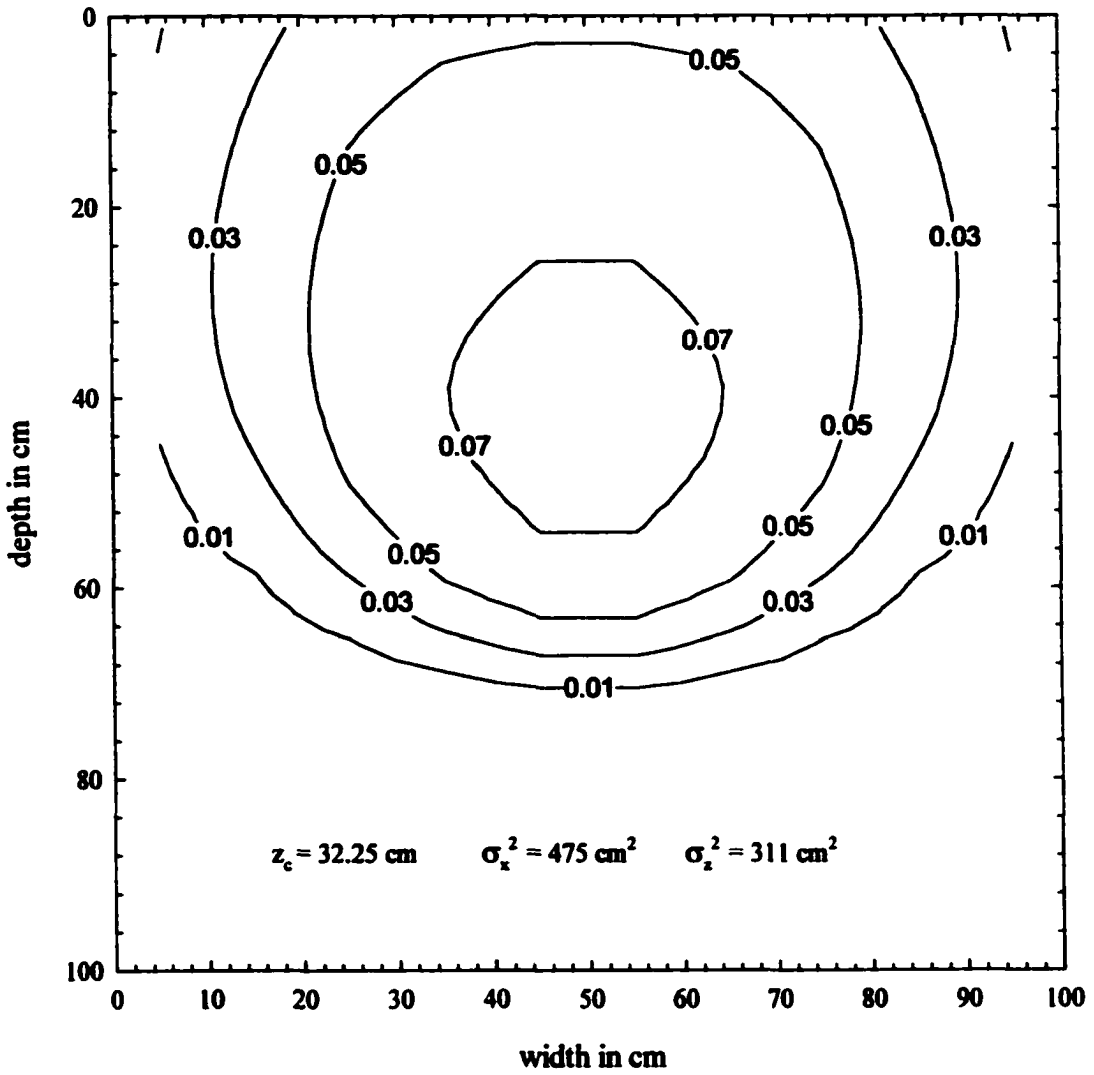

Figure 5.16 Moisture content contours after 720 minutes in a homogeneous soil, where n = 3.00 and α = 0.045.

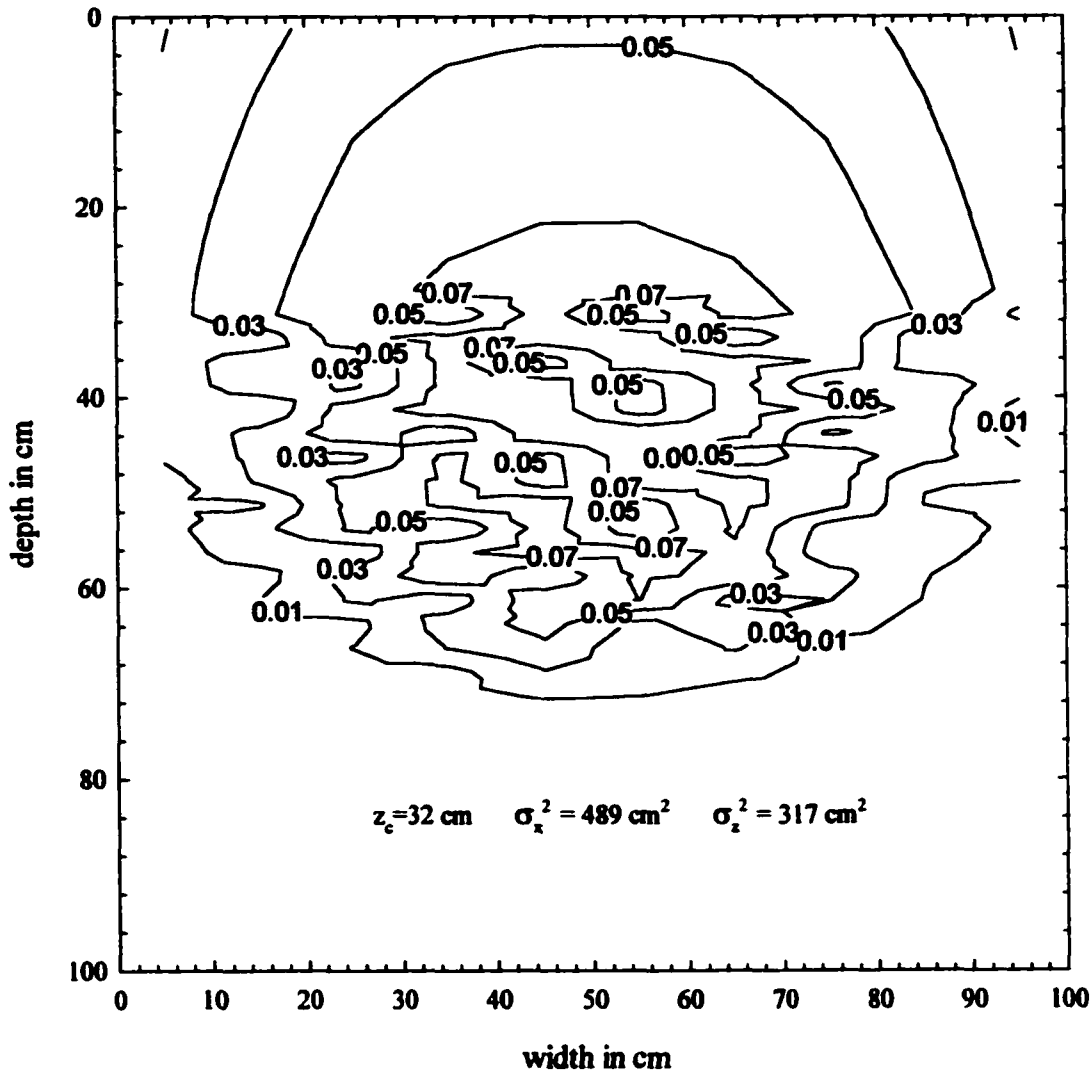

Figure 5.17 Moisture content contours when soil properties are heterogeneous; (n_B = 3.00, n_L = 4.25 and $\alpha_B = \alpha_L$ = 0.045) at t = 720 minutes. Volumetric proportion of lens is 30% and aspect ratio is 4.0.

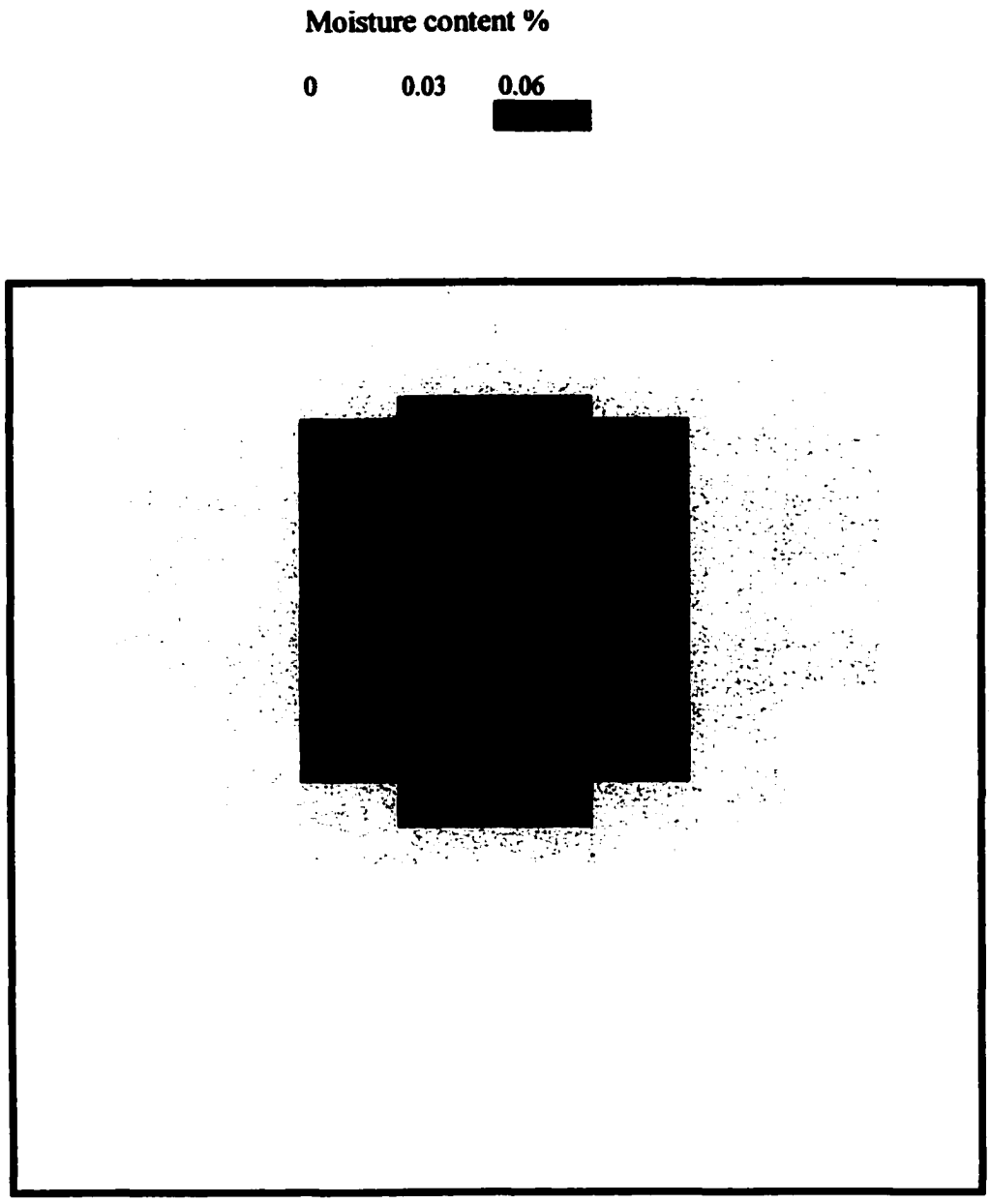

Figure 5.18 Moisture content distribution after 720 minutes in a homogeneous soil, where $n = 3.00$ and $\alpha = 0.045$.
$z_c = 32.25$ cm $\sigma^2_x = 475$ cm^2 and $\sigma^2_z = 311$ cm^2

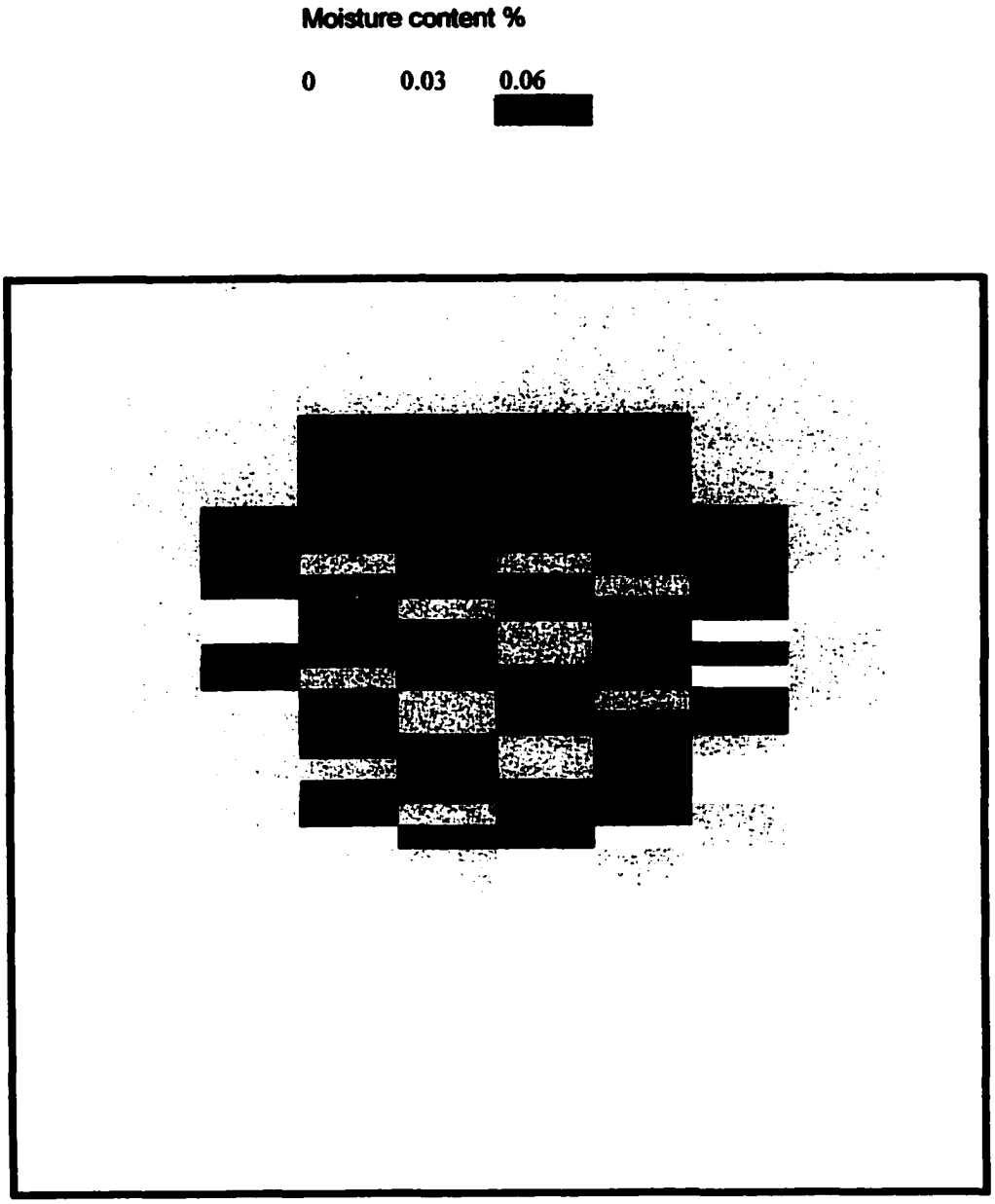

Figure 5.19 Moisture content distribution after 720 minutes in a heterogeneous soil, where $n_B = 3.00$ and $\alpha = 0.045$, $n_L = 4.25$ and $\alpha_L = 0.045$; $z_c = 32$ cm $\sigma^2_x = 489$ cm^2 and $\sigma^2_z = 317$ cm^2.

redistribute for 720 minutes both for homogeneous and heterogeneous simulations. Since the slope of the moisture retention function of soil with less uniform pore size distribution is flatter at the dry zone (capillary pressure is very high), more water infiltrates into the soil with less uniform pore size distribution. Consequently, relative permeability in the soil with less uniform pore size distribution becomes higher. Figure 5.19 shows, as the water encountered the lenses, low relative permeability of the lenses would tend to cause the water to flow around it, leading to relatively low moisture content in lens soil. This lateral movement of water causes reduced average vertical velocity of the moisture plume in heterogeneous soil. As it is evident from the Figure 5.11, the effect of heterogeneity on average velocity of the moisture plume is very small in comparison to the case where background soil has more uniform pore size distribution ($\Phi_n>0$). Due to reduced relative permeability in background soil, considerable amount of water is held up by lenses at the end of simulation when $\Phi_n>0$. Where as in simulation where $\Phi_n< 0$, due to reduced relative permeability of lenses water bypass the lenses and at the end of the simulation the difference between moisture content in background soil and lenses are very small. Therefore, the effect of heterogeneity on the average velocity of the moisture plume is small when background soil has less uniform pore size distribution.

A larger extent of moisture plume (Figures 5.17 and Figure 5.19) in the transverse direction is observed in the heterogeneous soil when a comparison is made with the homogeneous (in background soil properties) simulation results (Figure 5.16 and Figure 5.18). Because of the reduced relative permeability in lenses, water cannot penetrate lenses and travels in the transverse direction before finding a pathway through more

permeable background soil. As a result, increased transverse spreading index is observed in heterogeneous soil.

Larger extent of moisture plume (Figures 5.17 and Figure 5.19) in vertical direction is observed in heterogeneous soil while comparisons are made against the homogeneous simulation results (Figure 5.16 and Figure 5.18). Water drains out slowly from the top part of the domain because of the low relative permeability of water in lenses. Thus top part of the heterogeneous soil retains more water than homogeneous soil. On the wetting front of the moisture plume, water is inclined to penetrate into background soil, which is relatively more permeable to water. Consequently, increased vertical spreading index is observed in heterogeneous soil where background soil is less uniform in pore size distribution.

Figure 5.20 illustrates the effect of aspect ratio on average velocity of moisture plume. It has been observed that average velocity is decreasing with increasing aspect ratio. The effect is relatively more pronounced when $\Phi_n < 0$. This behavior is expected because as the correlation length of the lenses in transverse direction is increasing, water has to travel more distances laterally to bypass the relatively less permeable lenses. As a result, it causes overall slow down of the average vertical velocity of the moisture plume. But in the case when $\Phi_n > 0$, the amount of water entrapped in lenses depends on the volumetric proportion of lenses. Since, each layer of the soil domain contains constant proportion of lenses, the effect of correlation length in transverse direction is not prominent.

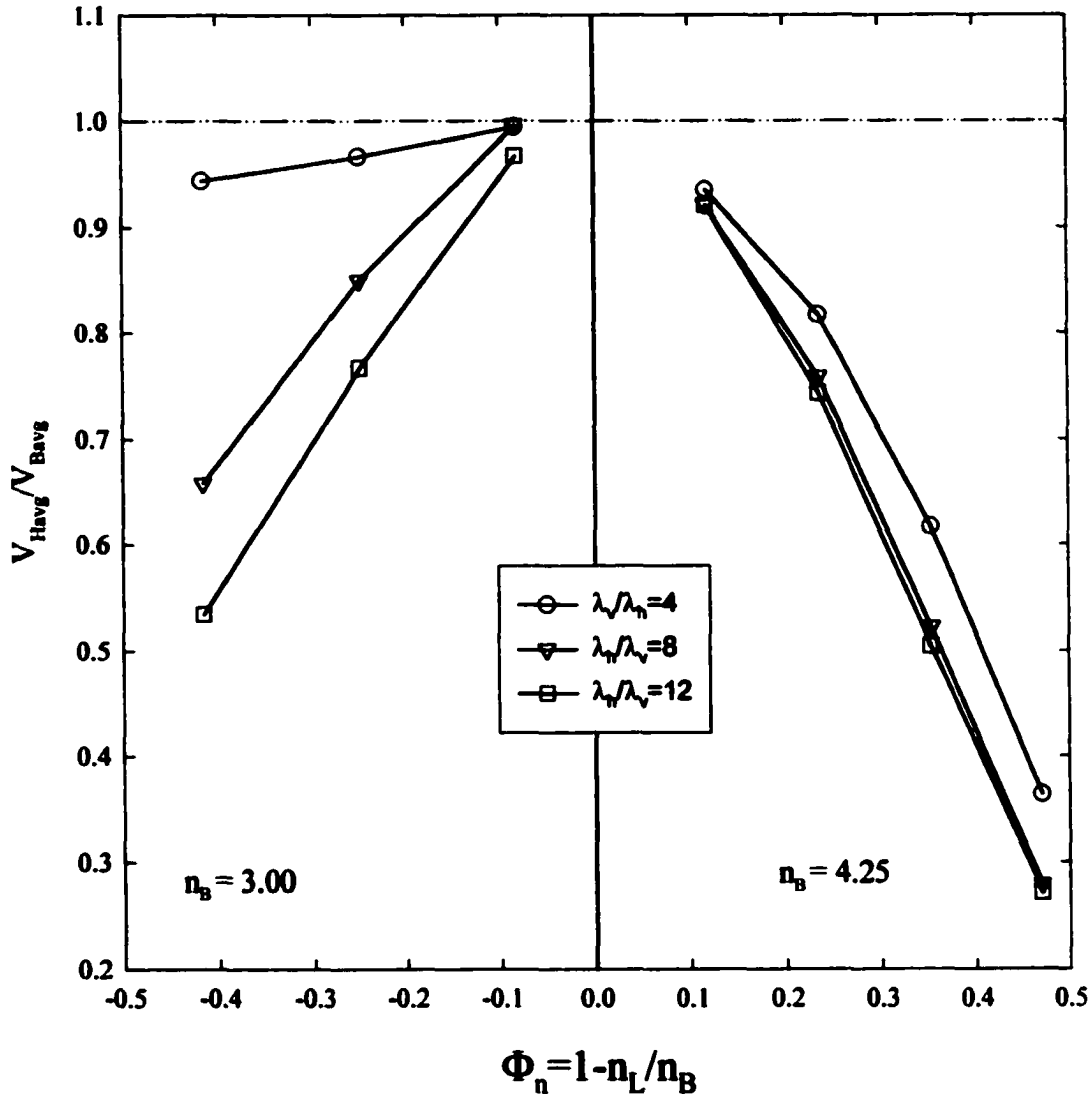

Figure 5.20 Effect of lens aspect ratio on normalized average velocity of the moisture plume when $\alpha_B = \alpha_L = 0.045$ and volumetric proportion of lens is 30%.

The effect of heterogeneity index and volumetric lens proportion on TSI is shown in Figure 5.21. Standardized TSI is found to be increasing with increasing degree of contrast for both cases when $\Phi_n > 0$ and $\Phi_n < 0$. But the effect is less prominent when $\Phi_n < 0$. Normalized TSI is increasing with increasing proportion of lens material for both cases when $\Phi_n > 0$ and $\Phi_n < 0$. Again the effect is less significant in case when $\Phi_n < 0$.

Figure 5.22 indicates that higher aspect ratio is causing higher transverse spreading for both cases, $\Phi_n > 0$ and $\Phi_n < 0$. But the effect is relatively more definite when $\Phi_n < 0$.

The effect of heterogeneity index and volumetric proportion of lenses on vertical spreading index (VSI) is presented in Figure 5.23. For $\Phi_n > 0$, vertical spreading index is decreasing with increasing degree of contrast. On the other hand, VSI is increasing with increasing degree of contrast when $\Phi_n < 0$. VSI decreases with increasing volumetric proportion when $\Phi_n > 0$. On the other hand, VSI is increasing with increasing lens proportion.

Figure 5.24 illustrates the effect of lens aspect ratio on VSI. It appears from the plot that VSI is decreasing with increasing aspect ratio. It happens in both cases when $\Phi_n > 0$ and $\Phi_n < 0$.

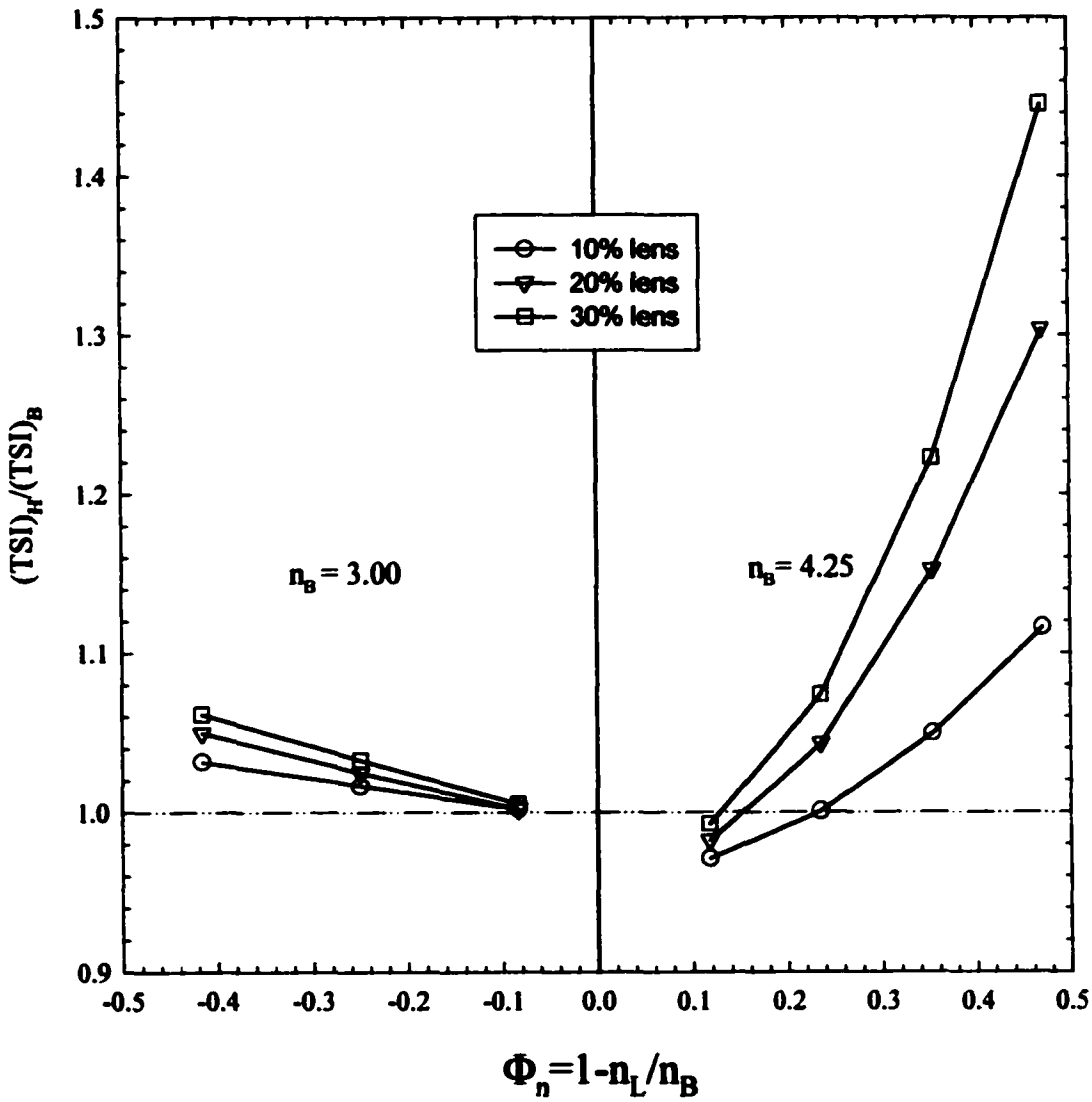

Figure 5.21 Effect of heterogeneity index on normalized transverse spreading index of the moisture plume when $\alpha_B = \alpha_L = 0.045$.

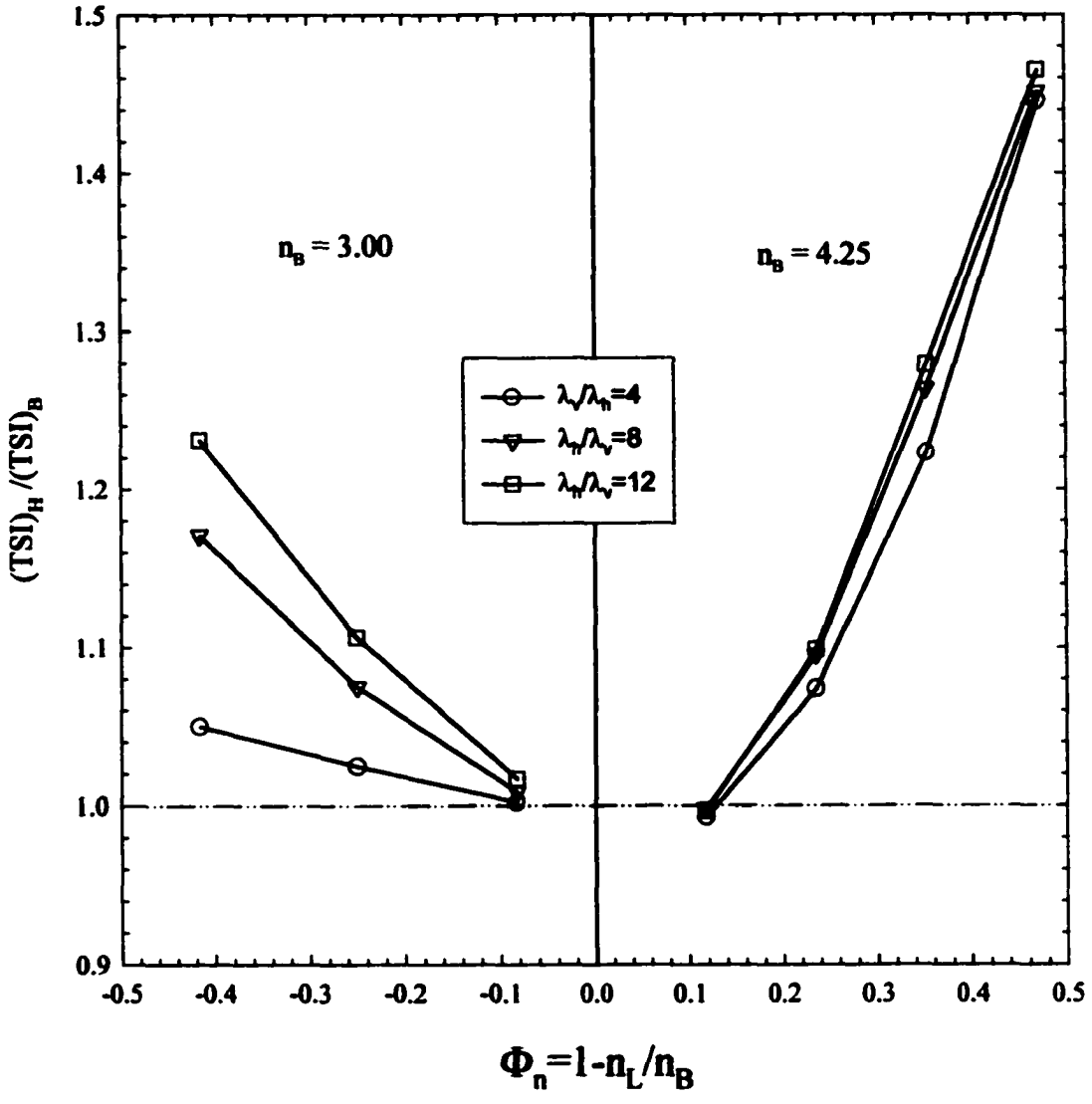

Figure 5.22 Effect of lens aspect ratio on normalized transverse spreading index of the moisture plume when $\alpha_B = \alpha_L = 0.045$ and volumetric proportion of lens is 30%.

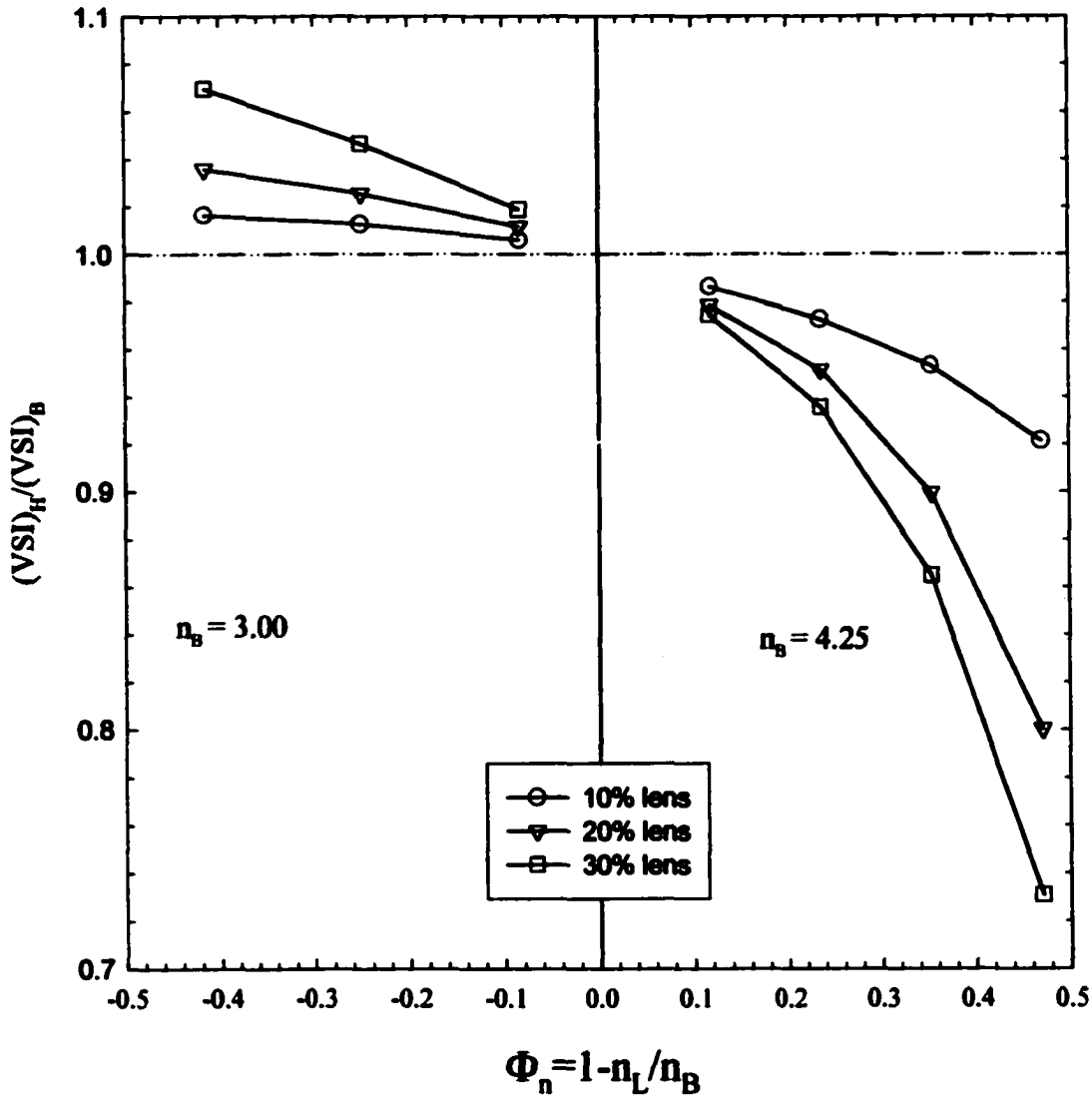

Figure 5.23 Effect of heterogeneity index on normalized vertical spreading index of the moisture plume when $\alpha_B = \alpha_L = 0.045$.

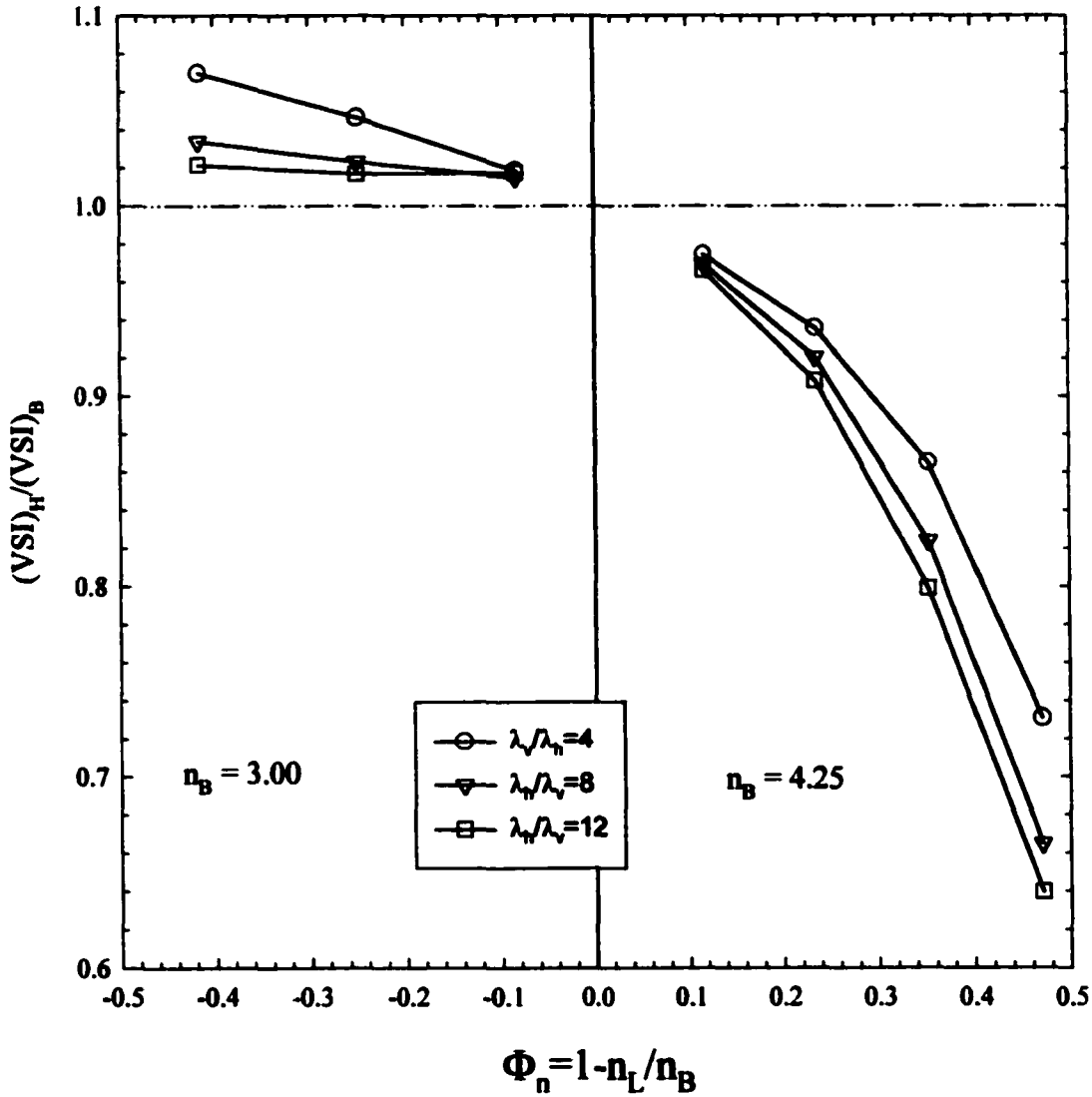

Figure 5.24 Effect of lens aspect ratio on normalized vertical spreading index of the moisture plume when $\alpha_B = \alpha_L = 0.045$ and volumetric proportion of lens is 30%.

5.3.4.2 Heterogeneous with respect to α

In this section, simulations results are presented when the medium is heterogeneous only with respect to α. Figure 5.25 shows the effect of heterogeneity index and volumetric proportion of lenses on the normalized average velocity. It is obvious from the plot that average velocity of the moisture plume is reduced in comparison to average velocity of the moisture plume in homogeneous (in background soil properties) soil because of heterogeneity. However, increasing degree of contrast does not have any effect on average velocity when background soil is finer than lenses ($\Phi_\alpha < 0$), specially when absolute value of heterogeneity index ($|\Phi_\alpha|$) become higher than 0.5. When coarser lenses are surrounded by finer soil, low relative permeability in coarser lenses slows down the vertical movement of water. Average velocity is decreasing with increasing degree of contrast when $\Phi_\alpha > 0$.

The moisture retention function of a finer soil has relatively flat slope at high capillary pressure in comparison to coarser soil. So when finer lenses are surrounded by coarser soil ($\Phi_\alpha > 0$), during wetting cycle more water enters into lenses. Since relative permeability in surrounding coarser soil is low, water inside lenses is trapped. As a result average velocity of the moisture plume is reduced. For both $\Phi_\alpha > 0$ and $\Phi_\alpha < 0$ cases, increasing heterogeneity and proportion of lenses reduces the average velocity.

Figure 5.26 demonstrate the effect of lens aspect ratio on normalized average velocity of the moisture plume in heterogeneous medium. It is apparent from these plots

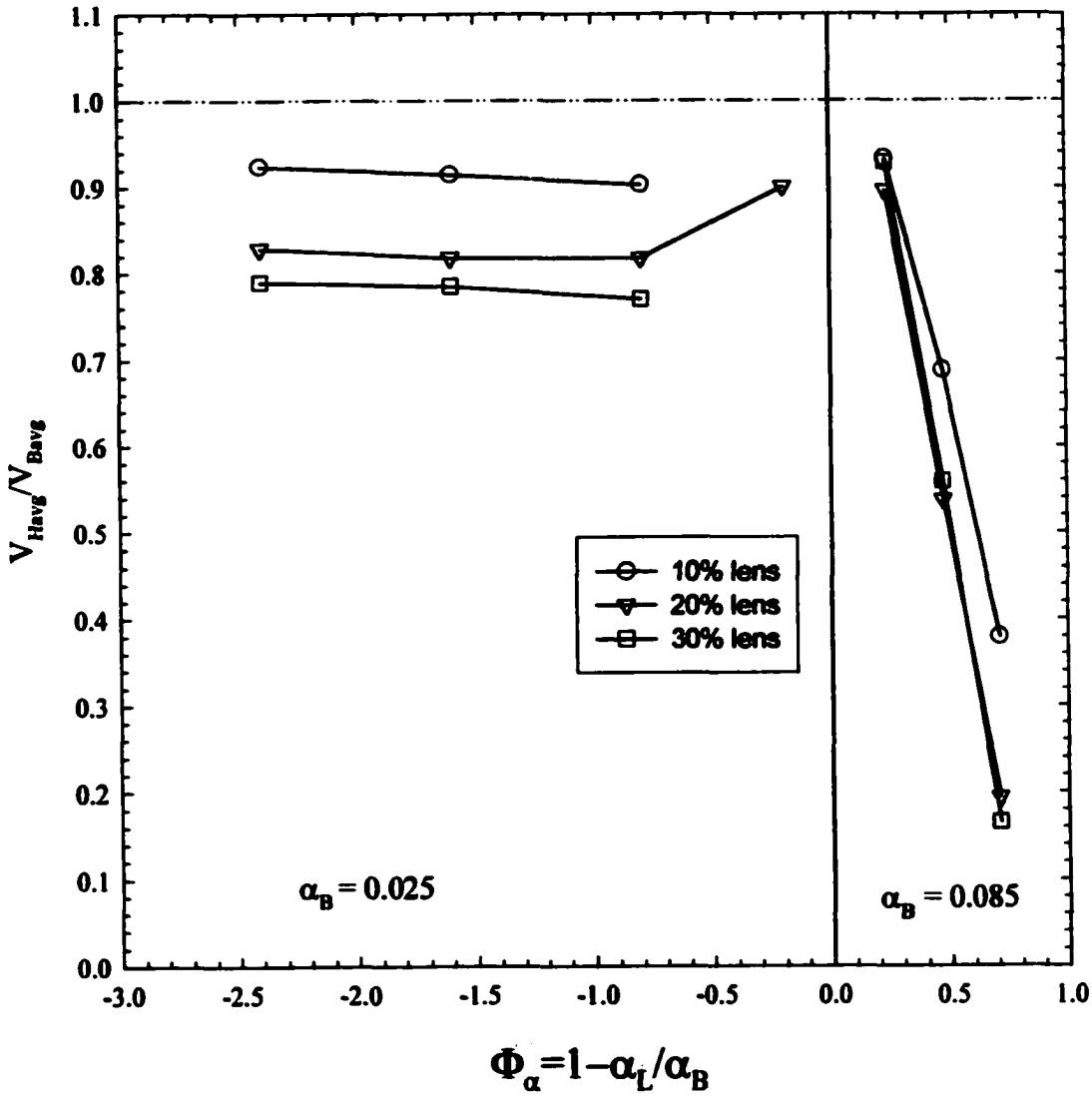

Figure 5.25 Effect of heterogeneity index on normalized average velocity of the moisture plume when $n_B = n_L = 2.75$.

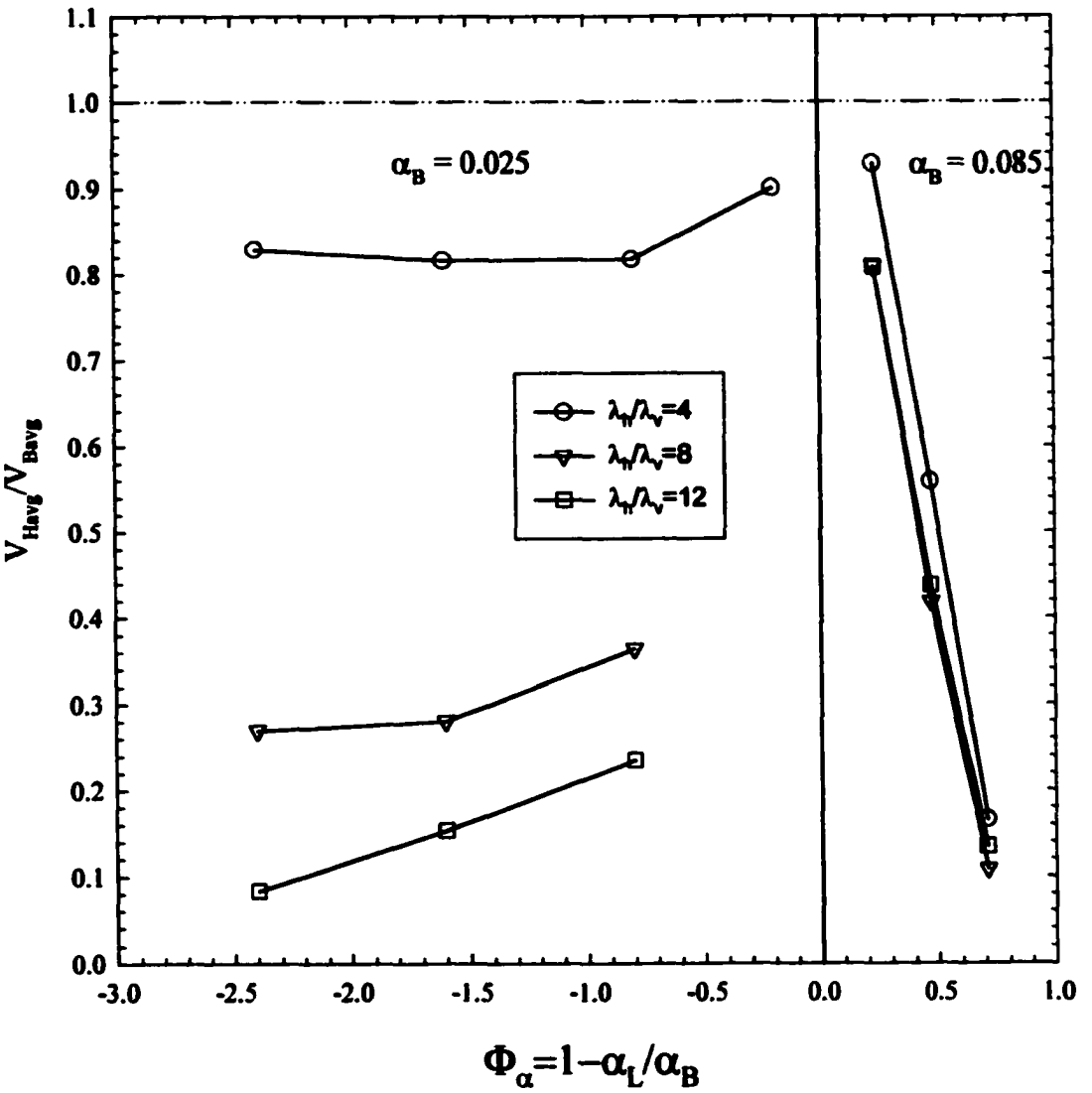

Figure 5.26 Effect of lens aspect ratio on normalized average velocity of the moisture plume when $n_B = n_L = 2.75$ and volumetric proportion of lens is 30%.

that lens aspect ratio has relatively more significant effect on average velocity when $\Phi_\alpha <$ 0. With the increasing correlation length in transverse direction, water has to travel more distance in transverse direction before entering into more permeable background soil. However, average velocity is decreasing as aspect ratio of lens increases for both cases.

Figure 5.27 shows the effect of degree of contrast and lens proportion on TSI of the heterogeneous medium. TSI is significantly increasing with degree of contrast when $\Phi_\alpha > 0$. On the other hand, no significant change of TSI with increasing degree of contrast when $\Phi_\alpha < 0$. Both cases, TSI is higher than that in homogeneous soil with background soil properties. It happened to be more sensitive when $\Phi_\alpha > 0$. Also, higher volumetric proportion of lenses results in higher TSI but this effect is less significant beyond 20% lenses. It could be due to limited lateral movement of moisture plume. Water does not reach to some of the lenses, which are located close to the transverse boundary. Therefore, adding lenses after certain proportion does not have any effect on TSI.

Figure 5.28 illustrates the effect of lens aspect ratio on TSI. It has been observed that TSI is increasing with increasing aspect ratio for both cases. But TSI is less sensitive to aspect ratio at smaller degree of contrast when $\Phi_\alpha > 0$.

From Figure 5.29, it has been observed that VSI is decreasing with increasing degree of contrast when $\Phi_\alpha > 0$. On the contrary, VSI is increasing with increasing degree of contrast when $\Phi_\alpha < 0$. Volumetric proportion of lens has the similar effect on

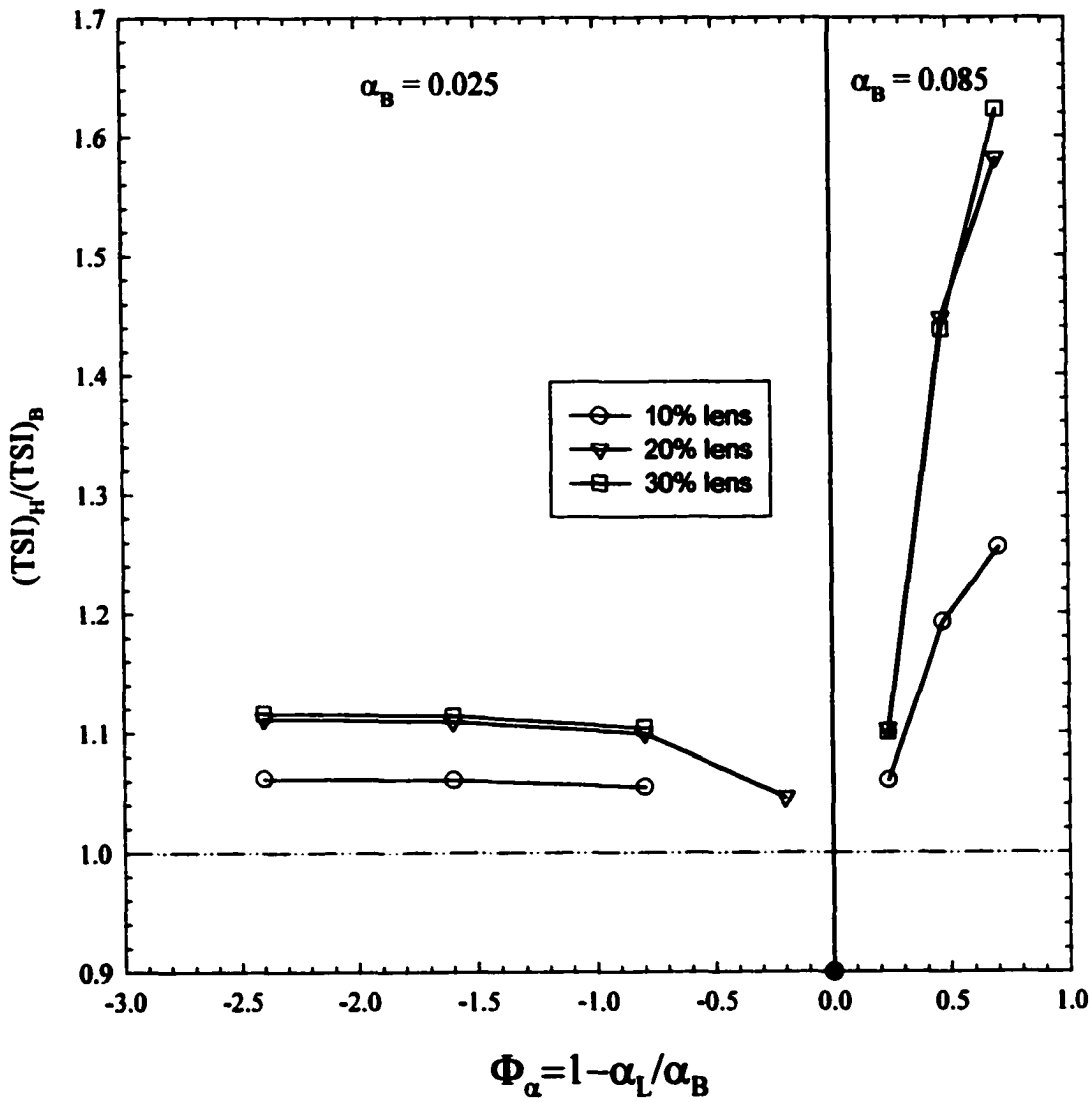

Figure 5.27 Effect of heterogeneity index on normalized transverse spreading index of the moisture plume when $n_B = n_L = 2.75$.

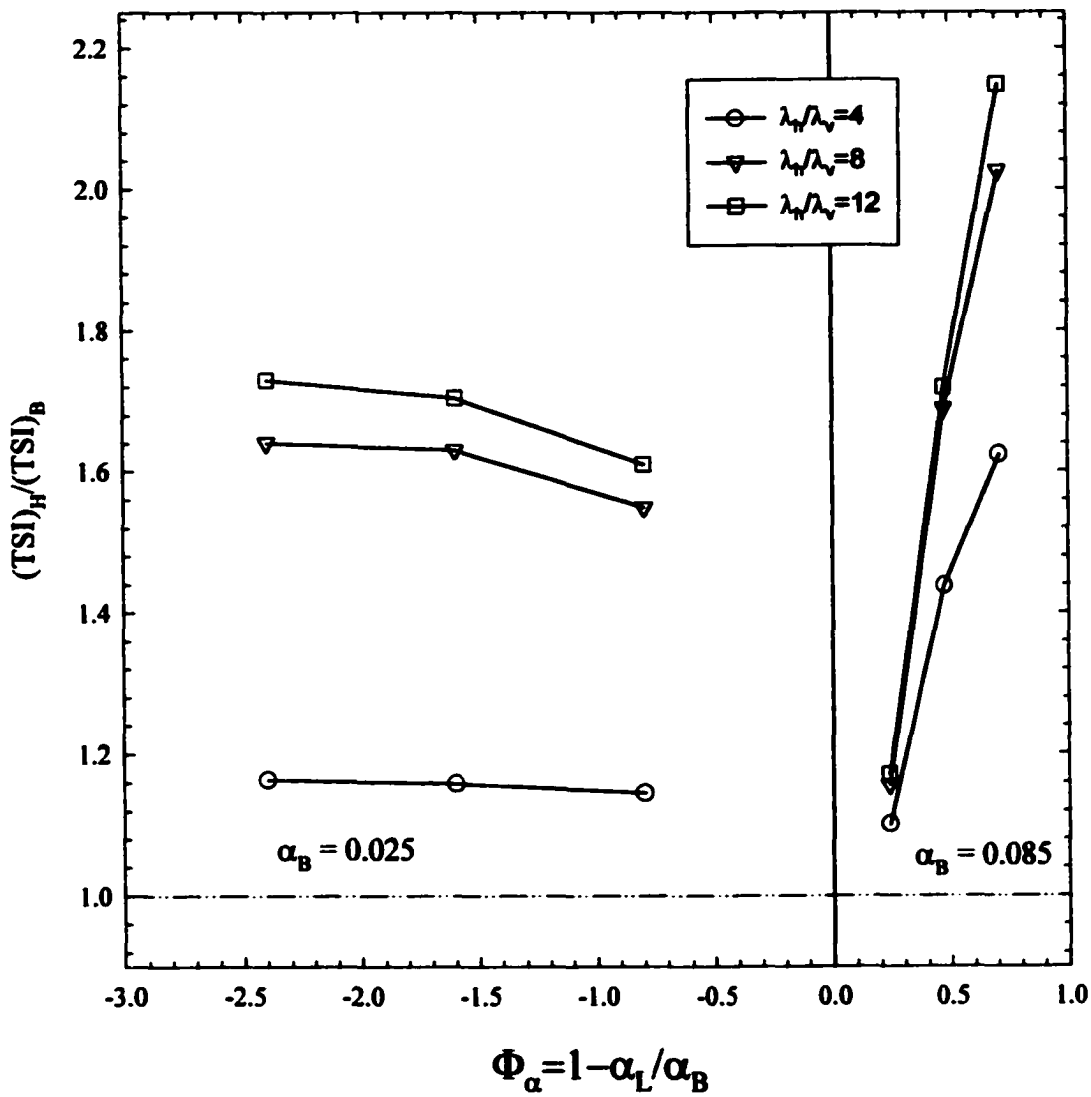

Figure 5.28 Effect of lens aspect ratio on normalized transverse spreading index of the moisture plume when $n_B = n_L = 2.75$ and volumetric proportion of lens is 30%.

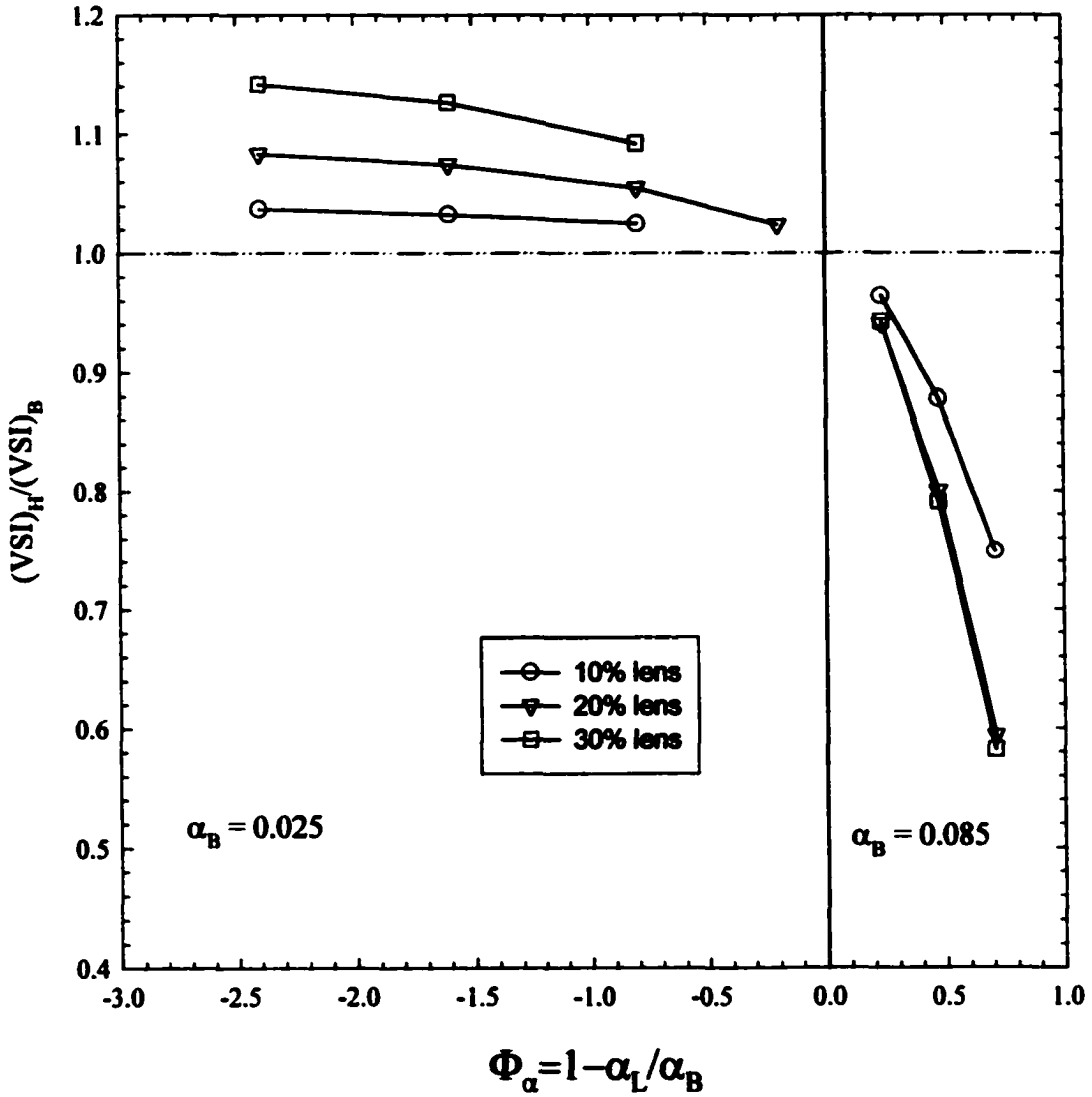

Figure 5.29 Effect of heterogeneity index on normalized vertical spreading index of the moisture plume when $n_B = n_L = 2.75$.

VSI. VSI is increasing with increasing proportion of lens when $\Phi_\alpha < 0$. But it is decreasing with increasing proportion of lens material when $\Phi_\alpha < 0$.

Figure 5.30 shows the effect of lens aspect ratio on vertical spreading index of heterogeneous medium. It has been observed that VSI is decreasing with increasing aspect ratio for both cases.

Table 5.2 summarizes qualitatively the effect of controlled variables (degree of contrast (Table 5.2(a)), volumetric lens proportion (Table 5.2(b)) and aspect ratio of lens (Table 5.2(c))) on the output variables (average velocity, TSI and VSI) for all heterogeneous simulations.

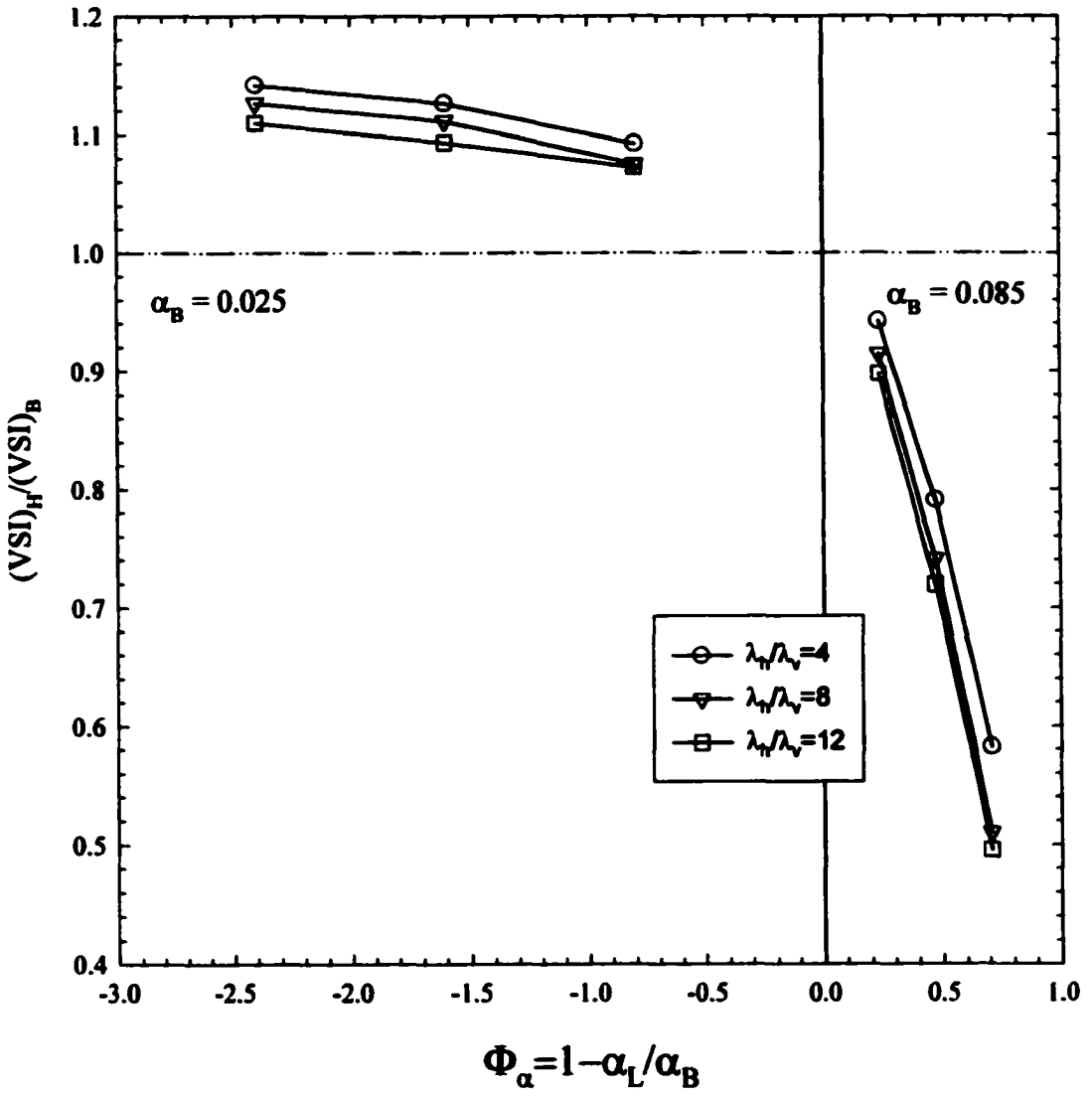

Figure 5.30 Effect of lens aspect ratio on normalized vertical spreading index of the moisture plume when $n_B = n_L = 2.75$ and volumetric proportion of lens is 30%.

Table 5.2 (a) Summary of effect of the heterogeneity index on output variables for 2D simulations.

	V_{avg}	TSI	VSI
$\Phi_n > 0$	↓	↑	↓
$\Phi_n < 0$	↓	↑	↑
$\Phi_\alpha > 0$	↓	↑	↓
$\Phi_\alpha < 0$	↓	↑	↑

Table 5.2 (b) Summary of effect of the volumetric proportion of lenses on output variables for 2D simulations.

	V_{avg}	TSI	VSI
$\Phi_n > 0$	↓	↑	↓
$\Phi_n < 0$	↓	↑	↑
$\Phi_\alpha > 0$	↓	↑	↓
$\Phi_\alpha < 0$	↓	↑	↑

Table 5.2 (c) Summary of effect of the aspect ratio of lenses on output variables for 2D simulations.

	V_{avg}	TSI	VSI
$\Phi_n > 0$	↓	↑	↓
$\Phi_n < 0$	↓	↑	↓
$\Phi_\alpha > 0$	↓	↑	↓
$\Phi_\alpha < 0$	↓	↑	↓

5.3.4.3 Heterogeneous with respect to both VG parameters

Two sets of simulation with different degree of contrast between background and lens properties were run to evaluate the effect of heterogeneity in both VG parameters on the movement of the moisture plume. We divided these sets of simulations into four groups depending on the characteristics of background soil properties relative to lenses. The results of first set of simulation are presented in Table 5.3. The results of second set of simulation are presented in Table 5.4. The second set of simulation results represent the state where degree of contrast between background soil and lens are higher than that in the first set of simulation results. Group 1 simulates flow through heterogeneous medium when background soil is finer and less uniform in its pore size distribution ($\alpha_B < \alpha_L$ and $n_B < n_L$). Group 2 simulates flow through heterogeneous medium when background soil is finer but more uniform in its pore size distribution ($\alpha_B < \alpha_L$ and $n_B > n_L$). Group 3 simulates flow through heterogeneous medium when background soil is coarser but less uniform in its pore size distribution ($\alpha_B > \alpha_L$ and $n_B < n_L$). Group 4 simulates flow through heterogeneous medium when background soil is coarser and more uniform in its pore size distribution ($\alpha_B > \alpha_L$ and $n_B > n_L$). Two extra simulation results are added in each group by varying only one VG parameter at a time to verify whether the effect of heterogeneity on the movement of the moisture plume is always cumulative.

5.3.4.3.1 Results of Group 1 simulations

Since background soil is finer and pore size distribution is less uniform than that of lenses, the slope of soil moisture retention functions of background soil is steeper than that of lens. Relative permeability of moisture in lenses is smaller than that in background soil. As a result, water encounters difficulty entering the coarser lenses. The reduced permeability in coarser lenses restricts vertical movement of water resulting reduced average velocity of the moisture plume. Although, average velocity of the moisture plume in heterogeneous soil is reduced but the effect of heterogeneity is not cumulative. The effect of heterogeneity on TSI and VSI is cumulative.

5.3.4.3.2 Results of Group 2 simulations

Here, background soil is finer grained but the pore size distribution is more uniform than that of lenses. Average velocity of the moisture plume is reduced considerably and the effect of heterogeneity on average velocity is not cumulative. TSI is increased due to heterogeneity but there is no cumulative effect of heterogeneity on TSI. VSI of the moisture plume in heterogeneous soil remains same as that in homogeneous soil because the effect of heterogeneity due to change one parameter almost cancels the effect of other.

5.3.4.3.3 Results of Group 3 simulations

In this group, background soil is coarser than lenses and is less uniform in its pore size distribution. The effect of heterogeneity on average velocity is partially cumulative. Although TSI is increased due to heterogeneity, there is no cumulative effect on TSI of the moisture plume. Effect of heterogeneity on VSI of the moisture plume is cumulative and reduced VSI is observed due to heterogeneity of both VG parameters velocity.

5.3.4.3.4 Results of Group 4 simulations

Here, finer lenses with less uniform pore size distribution are surrounded by coarser soil with more uniform pore size distribution. Both average velocity and VSI of the moisture plume are reduced significantly and TSI is increased considerably because of heterogeneity in both VG parameters. In this case, α has the most pronounced effect i.e. only changing α has almost the same effect as changing both n and α. This is the only group, where the effects of heterogeneity on all flow properties are partially cumulative.

Table 5.3 Results of simulation experiments when both VG parameters are variable

Volumetric proportion of lenses is 20% and aspect ratio ($\frac{\lambda_V}{\lambda_H}$) of lenses is 4.

		Norm. V_{avg}	Actual. V_{avg}	Norm. TSI	Actual TSI	Norm. VSI	Actual. VSI
Group 1 $\alpha_B < \alpha_L$ $n_B < n_L$ $\Phi_\alpha = -1.14$ $\Phi_n = -0.3$	Homo. Sim. $\alpha_B = 0.035$ $n_B = 2.50$	1	0.088.	1	31.34	1	20.34
	(a)$\alpha_L = 0.075$ $n_L = 2.50$	0.826	0.072	1.10	34.47	1.05	21.35
	(b) $\alpha_L = 0.035$ $n_L = 3.25$	0.911	0.08	1.06	33.18	1.06	21.36
	(c) $\alpha_L = 0.075$ $n_L = 3.25$	0.89	.079	1.11	34.85	1.08	22.0
Group 2 $\alpha_B < \alpha_L$ $n_B > n_L$ $\Phi_\alpha = -1.14$ $\Phi_n = +0.23$	Homo. Sim. $\alpha_B = 0.035$ $n_B = 3.25$	1	0.387	1	20.39	1	17.99
	(a) $\alpha_L = 0.075$ $n_L = 3.25$	0.893	0.346	1.19	24.45	1.04	18.78
	(b) $\alpha_L = 0.035$ $n_L = 2.5$	0.813	0.315	1.04	21.34	0.923	16.62
	(c) $\alpha_L = 0.075$ $n_L = 2.50$	0.778	0.301	1.18	24.18	0.997	17.95
Group 3 $\alpha_B > \alpha_L$ $n_B < n_L$ $\Phi_\alpha = +0.53$ $\Phi_n = -0.3$	Homo. Sim. $\alpha_B = 0.075$ $n_B = 2.50$	1	0.1187	1	19.97	1	18.63
	(a) $\alpha_L = 0.035$ $n_L = 2.50$	0.603	0.071	1.36	27.21	0.81	15.15
	(b) $\alpha_L = 0.075$ $n_L = 3.25$	0.985	0.117	1.04	20.89	1.04	19.28
	(c)$\alpha_L = 0.035$ $n_L = 3.25$	0.908	0.108	1.29	25.9	0.902	16.81
Group 4 $\alpha_B > \alpha_L$ $n_B > n_L$ $\Phi_\alpha = +0.53$ $\Phi_n = +0.23$	Homo. Sim. $\alpha_B = 0.075$ $n_B = 3.25$	1	0.760	1	12.16	1	15.99
	(a) α_L=0.035 n_L=3.25	0.32	0.244	1.75	21.44	0.66	10.58
	(b) $\alpha_L = 0.075$ $n_L = 2.5$	0.77	0.584	1.11	13.54	0.94	15.05
	(c) $\alpha_L = 0.035$ $n_L = 2.5$	0.22	0.167	1.80	21.96	0.61	9.91

Table 5.4 Results of simulation experiments when both VG parameters are variable

Volumetric proportion of lenses is 20% and aspect ratio ($\frac{\lambda_V}{\lambda_H}$) of lenses is 4.

(degree of contrast is higher)

		Norm. V_{avg}	Actual V_{avg}	Norm. TSI	Actual TSI	Norm. VSI	Actual VSI
Group 1	Homo. Sim. $\alpha_B = 0.025$ $n_B = 3.00$	1.0	0.2345	1.0	29.28	1.0	19.45
$\alpha_B < \alpha_L$ $n_B < n_L$	(a) $\alpha_L = 0.085$ $n_L = 3.00$	0.887	0.208	1.13	33.25	1.08	21.03
$\Phi_\alpha = -2.4$ $\Phi_n = -0.416$	(b) $\alpha_L = 0.025$ $n_L = 4.25$	0.900	0.211	1.08	31.66	1.06	20.59
	(c) $\alpha_L = 0.085$ $n_L = 4.25$	0.914	0.214	1.14	33.40	1.09	21.20
Group 2	Homo. Sim. $\alpha_B = 0.025$ $n_B = 4.25$	1.0	0.934	1.0	19.86	1.0	17.1
$\alpha_B < \alpha_L$ $n_B > n_L$	(a) $\alpha_L = 0.025$ $n_L = 4.25$	0.948	0.885	1.12	22.19	1.049	17.95
$\Phi_\alpha = -2.4$ $\Phi_n = +0.294$	(b) $\alpha_L = 0.025$ $n_L = 3.00$	0.492	0.459	1.10	21.77	0.7631	13.05
	(c) $\alpha_L = 0.085$ $n_L = 3.00$	0.7082	0.6613	1.12	22.26	0.9789	16.74
Group 3	Homo. Sim. $\alpha_B = 0.085$ $n_B = 3.00$	1	0.545	1	12.7	1	16.4
$\alpha_B > \alpha_L$ $n_B < n_L$	(a) $\alpha_L = 0.025$ $n_L = 3.00$	0.138	0.0752	1.919	24.38	0.5301	8.695
$\Phi_\alpha = +0.705$ $\Phi_n = -0.416$	(b) $\alpha_L = 0.085$ $n_L = 4.25$	1.02	0.5559	1.058	13.44	1.02	16.77
	(c) $\alpha_L = 0.025$ $n_L = 4.25$	0.177	0.0967	1.88	23.90	0.5367	8.803
Group 4	Homo. Sim. $\alpha_B = 0.085$ $n_B = 4.25$	1	2.536	1	7.21	1	14.15
$\alpha_B > \alpha_L$ $n_B > n_L$	(a) $\alpha_L = 0.025$ $n_L = 4.25$	0.0445	.1128	2.751	19.83	0.339	4.79
$\Phi_\alpha = +0.705$ $\Phi_n = +0.294$	(b) $\alpha_L = 0.085$ $n_L = 3.00$	0.7664	1.943	1.434	10.34	0.861	12.18
	(c) $\alpha_L = 0.025$ $n_L = 3.00$	0.0423	0.1072	2.81	20.33	0.356	5.041

5.4 Summary

The effects of unsaturated soil properties on moisture movement in heterogeneous soil are summarized in this section. In the following subsections heterogeneous simulation results will be discussed. The effect of heterogeneity on the moisture plume movement would be discussed, when only n is spatially variable parameter. Then the effect of heterogeneity on moisture plume would be discussed when only α is spatially variable parameter. Finally, the effect of heterogeneity would be discussed when both VG parameters are spatially variable.

Lenses with different degree of uniformity in pore size distribution than background soil has caused reduced average velocity. It reduces the average velocity significantly only when the background soil has more uniform pore size distribution. Relative permeability in soil with more uniform pore size distribution is smaller at very dry condition (higher capillary pressure). Therefore, considerable amount of water is confined in lenses when the surrounding soil has more uniform pore size distribution. The average velocity is further reduced if degree of contrast between background and soil properties is increasing. Average velocity is decreasing with increasing volumetric proportion of lenses. Average velocity is also increasing with increasing aspect ratio of lenses. This effect of aspect ratio on average velocity of the moisture plume is more significant when background soil has less uniformity in its pore size distribution. In this case, water has to travel longer distance transversely before finding more permeable soil.

TSI is increased due to different pore size distribution of lenses. TSI is increasing with the increasing degree of contrast. Again, the effect of degree of contrast between background soil and lenses on TSI is more significant when background soil has more uniformity in its pore size distribution. Scattered lenses that hold considerable amount of water has caused this increased TSI.

Whether VSI is increased or decreased due to lenses with different pore size distribution depend on the relative uniformity of pore size distribution of soil or lenses. Increased VSI is observed when background soil has less uniform pore size distribution. Lenses tend to spread water in all directions because of its smaller relative permeability. Reduced VSI is observed when background soil has more uniform pore size distribution. Since water is confined in lenses with surrounding soil with smaller relative permeability, shrinkage occurs in the vertical extent of the moisture plume. VSI is increasing with increasing volumetric proportion of lenses when background soil is less uniform in its pore size distribution. On the other hand, VSI is decreasing with increasing volumetric proportion of lenses. VSI is decreasing with increasing aspect ratio of lenses.

Lenses with different texture than background soil reduce the average velocity of the moisture plume in heterogeneous soil. When coarser lenses are surrounded by finer background soil, water avoids the coarser soil due to its low permeability. When finer lenses are surrounded by coarser soil, water enters into finer lenses much faster and is confined there due to low permeability of the surrounding coarse soil. Vertical movement of the moisture plume is restricted due to these reasons. Average velocity is

decreasing with increasing volumetric proportion and aspect ratio of lenses. Degree of contrast between textural properties of background and lenses does not have any effect on average velocity after some critical heterogeneity index. The effect of aspect ratio on the average velocity is more significant in heterogeneous medium where background soil is finer.

Increased TSI of the moisture plume in heterogeneous medium is observed due to different texture of the background soil and lenses. TSI is increasing with increasing degree of contrast. Again, degree of contrast has no effect on the average velocity of the moisture plume after certain critical heterogeneity index. Average velocity of the moisture plume is increasing with increasing volumetric proportion of lenses. Similarly, average velocity of the moisture plume is increasing with increasing aspect ratio of lenses. Again, the effect of aspect ratio is more significant when background soil is coarser.

VSI could be increased or decreased due to lenses with different pore size distribution depending on the relative textural properties of the background soil or lenses. It has been observed that VSI is increased due to lenses of coarser texture and decreased due to lenses of finer texture. Coarser lenses surrounded by finer soil have a tendency to disperse water in all directions due to its low relative permeability and results in higher vertical spreading. In contrast, water is absorbed much faster in finer lenses surrounded by coarser soil and confined there, because of low permeability of surrounding coarser soil. These effects restrict the vertical spreading of the moisture plume. VSI is

increasing with increasing volumetric proportion of lenses when coarser lenses are surrounded by finer background soil. But VSI is decreasing with increasing volumetric proportion of lenses when finer lenses are surrounded by coarser soil. Larger aspect ratio of lenses results in reduced VSI irrespective of the texture of background soil or lenses.

Heterogeneous simulation results are summarized in the section 5.3.4.3 when both VG parameters are spatially variable. When background soil is finer and less uniform in its pore size distribution, average velocity is reduced and both TSI and VSI are increased due to heterogeneity. Although, the effect of individual VG parameter on average velocity of the moisture plume are not cumulative.

When background soil is finer and more uniform in its pore size distribution, average velocity and VSI of the moisture plume is decreased and TSI is increased. The effect of individual VG parameter on average velocity and TSI of the moisture plume are not cumulative. n is the dominant parameter i.e. pore size distribution is the controlling properties here.

When background soil is coarser and less uniform in it pore size distribution, average velocity and VSI is reduced. The effect of individual VG parameter on TSI of the moisture plume is not cumulative. The dominant parameter in this case is α i.e. texture of background soil or lenses.

When background soil is coarser and more uniform in its pore size distribution, average velocity and VSI of the moisture plume are reduced and TSI is increased. The effects of individual VG parameter on all flow properties are cumulative. The dominant parameter in this case is α i.e. texture of background soil or lenses.

Chapter 6: Effective parameters

6.1 Introduction

This chapter makes an effort to answer the critical question: can the mean movement of the moisture plume in unsaturated heterogeneous medium be reproduced in an equivalent homogeneous medium. If it is not possible then what is the best that can be done in a given situation. In order to do this, first all heterogeneous simulation results are categorized into groups based on the impact of heterogeneity on flow properties. Then each group of heterogeneous simulations is examined to determine whether practical and useful effective parameters can be estimated for these heterogeneous medium using Type curves (Chapter 4), which are produced from homogeneous simulation results.

Section 6.2 discusses results when the porous medium is one-dimensional and the domain is layered. All 1D heterogeneous simulations are categorized into two groups based on the impact of heterogeneity on the mean flow behavior of the moisture plume. Section 6.2.1 discuss Type I impact of heterogeneity. Section 6.2.2 discuss Type II impact of heterogeneity. Feasibility of estimating effective parameters are also discussed in the above two sections.

Similarly, Section 6.3 differentiates all 2D heterogeneous simulations into three groups based on the impact of heterogeneity. Sections 6.3.1 to 6.3.3 analyze results of each type of impact when the heterogeneous medium is 2D and type of heterogeneity is

random block. Section 6.4.1 shows an example of Type I impact of heterogeneity in 2D medium. Section 6.4.2 shows an example of Type II impact of heterogeneity in 2D medium. Section 6.5 presents the summary of Chapter 6.

6.2 Effective parameters for 1D domain with layered heterogeneity

All 1D heterogeneous simulations are divided into two categories based on the trend of change of flow properties due to heterogeneity. When both average velocity and vertical spreading index of a moisture plume are reduced because of heterogeneity, we refer it as Type I impact of heterogeneity. On the other hand, when average velocity is decreased and vertical spreading index is increased because of heterogeneity, we refer it as Type II impact of heterogeneity. In the following two sections, we will examine whether a single set of parameters (effective parameters) can capture the effect of heterogeneity satisfactorily.

6.2.1 Type I impact of heterogeneity on 1D medium

The effect of heterogeneity on flow properties is characterized as Type 1 impact of heterogeneity when both average velocity and vertical spreading index are reduced because of heterogeneity. Figure 5.1, 5.3, 5.5, 5.7 show that both flow properties are reduced because of lenses with different soil properties only when the magnitude of background soil properties are higher than that of lenses ($\Phi_\beta > 0$). In other words, this type of impact of heterogeneity is observed when background soil has more uniformity in its pore size distribution or has a texture of coarser-grained soil. In order to estimate

effective parameters for heterogeneous medium, Type Curves (Figure 4.14, 4.15) for 1D simulations can be used. As we can see from these Type curves, any change of VG parameter values in certain direction lead to change in average velocity in the same direction and vertical spreading in the opposite direction. For example, if VG parameter values are reduced in a homogeneous simulation, average velocity will be decreased while the vertical spreading index will be increased. So, it is evident that no single set of parameters can adequately capture the Type I impact of heterogeneity. Average velocity of the moisture plume in such heterogeneous medium can be simulated by reducing VG parameters in homogeneous medium but in that case vertical spreading index will be overestimated. Again, reduced vertical spreading index of the moisture plume in heterogeneous medium can be reproduced by increasing VG parameters in homogeneous medium but in that case average velocity of the moisture plume will be overestimated. With increased degree of contrast between background soil and lens properties, average velocity of the moisture plume in such a heterogeneous medium is reduced considerably that there are no realistic effective VG parameters that can match even the average velocity only. Such small average velocity is the result of layered heterogeneity. Water is virtually confined into the lenses and background soil with reduced relative permeability acts as a blockade to resist water to migrate further downwards. Therefore, we can safely conclude that the impact of these types of heterogeneity in layered medium cannot be duplicated by an equivalent homogeneous medium by adjusting VG parameters only. One approach to match such a low average velocity could be to reduce the saturated hydraulic conductivity of equivalent homogeneous medium in spite of the fact that both soils have the same saturated conductivity.

6.2.2 Type II impact of heterogeneity in 1D medium

Next, we characterize the results of heterogeneous simulations as Type II impact of heterogeneity when average velocity of the moisture plume in heterogeneous medium is decreased while vertical spreading is increased. This type of effect is observed only when the texture of background soil is finer or uniformity of pore size distribution in background soil is smaller provided the other characteristics of soils represented by VG parameters in background and lenses are same. Figures 5.1, 5.3, 5.5, 5.7 demonstrate such impact of heterogeneity. Theoretically, these types of heterogeneous medium may be replaced by an equivalent homogeneous medium with effective parameters since any change in VG parameters in any direction in homogeneous simulation leads to change average velocity and vertical spreading index of the moisture plume in opposite direction. When background soil has less uniform pore size distribution, average velocities are not reduced significantly because of heterogeneity and remains nearly constant with increasing heterogeneity. In such cases, it is more likely to find a set of appropriate effective parameters. On the other hand, when the texture of background soil is finer, average velocity of the moisture plume is reduced significantly due to heterogeneity and continues to reduce with increasing degree of contrast between background and lens properties. In such cases, it is improbable to match such a small average velocity by adjusting only VG parameters especially when the degree of contrast is very large.

6.3 Effective parameters for 2D domain with block heterogeneity

All 2D heterogeneous simulations, results of which are reported in Chapter 5, are classified into three types based on the impact of heterogeneity. In the following three subsections, each type of impact of heterogeneity would be discussed.

6.3.1 Type I impact of heterogeneity in 2D medium

In the majority of cases increasing heterogeneity (i.e., greater degree of contrast between soils, larger proportion of lens material, higher aspect ratio) results in a slowing of the vertical movement of the moisture plume, increased transverse spreading and decreased vertical spreading. We define this as Type I impact of heterogeneity. As we can see from Type I curves (Figure 4.17, 4.18), matching the reduced average velocity in heterogeneous medium requires reduction of VG parameters in an equivalent homogeneous simulation and this reduction will yield increased transverse and vertical spreading. Therefore, it is apparent that all three flow-properties of heterogeneous simulation of this type cannot be captured by a single set of VG parameters. However, it is more likely to match both average velocity and transverse spreading to some extent by reducing VG parameters in a homogeneous simulation, in that case, vertical spreading would be overestimated. Section 6.4.1 demonstrates a comparative analysis of ineffectiveness of reproducing the reduced vertical spreading in a homogeneous medium by an example. So, if the modeler's interest is in vertical location of center of moisture plume or the extent of spreading in transverse direction, single set of VG parameters may

produce satisfactory results. But if the interest is in the extent of spreading in vertical direction or the transient location of wetting front of the moisture plume, single set of VG parameters in homogeneous simulation will give erroneous results.

It has been found that effective parameters estimated based on average velocity and TSI are significantly different from the estimated effective parameters based on VSI only. So relative permeability function must be different in two directions. This observation is amenable with the findings of other researches. Several authors observed that effective hydraulic conductivity in unsaturated heterogeneous soil is anisotropic and the degree of anisotropy is not constant but depends strongly on saturation (Yeh et al., 1985, Kueper and Frind, 1991, Braun et al., 1998, Ataie-Ashtiani et al., 2001). Yeh et al. (1985) derived an equation (6.1) for anisotropy in unsaturated hydraulic conductivity in a layered medium for stochastic unsaturated flow model. Unsaturated hydraulic conductivity function proposed by Gardner (1958) was used in their work.

$$\frac{\hat{K}_x(h)}{\hat{K}_z(h)} = \exp\left(\frac{\sigma^2_{\ln K_s} + h^2\sigma_a^2}{1 + A\lambda_1(2J_1 - 1)}\right) \qquad (6.1)$$

where $\hat{K}_x(h), \hat{K}_z(h)$ = effective unsaturated hydraulic conductivity in transverse and vertical directions; σ_a^2 = variance of fluctuation of slope of log K (h); A = mean of slope of log K (h); λ_1 = correlation length in transverse direction; J_1= pressure head gradient in transverse direction. They show that the ratio of anisotropy can be strongly dependent on the mean capillary pressure especially when the mean capillary pressure is very high.

Braun (1998) suggested a method to estimate anisotropic ratio for relative permeability for a representative elementary volume (REV) of a heterogeneous medium with periodic heterogeneity for multiphase flow. Ataie-Ashtiani et al. (2001) modified a numerical multiphase flow model to take into account the effect of anisotropy in relative permeability. They found relatively better performance of the model to capture the average effect of heterogeneity in a homogeneous medium. The research work presented in this thesis also imply that without the inclusion of saturation dependent anisotropy in relative permeability in the unsaturated flow model, it is improbable to reproduce the enhanced transverse extent and reduced vertical extent of the moisture plume when the model domain is packed with a homogeneous soil.

6.3.2 Type II impact of heterogeneity

In some heterogeneous simulations, increasing heterogeneity results in a slowing of the vertical movement of the moisture plume and increased transverse and vertical spreading. We define this as Type II impact of heterogeneity. This type of impact is common when coarse-grained lenses are embedded in fine-grained background soil (Figure 5.25, 5.27, 5.29) or when more uniform lenses are embedded in less uniform background soil (Figure 5.11, 5.21,5.23). Again, Group 1 heterogeneous simulations (Table 5.3 & 5.4) where both VG parameters in background soil are smaller, experience the Type II impact of heterogeneity. Since we know from the Type curves that decrease in VG parameters in homogeneous simulations will result in reduced average velocity and increased transverse and vertical spreading of the moisture plume, it is more likely to

capture all three flow properties of the heterogeneous medium of this type by equivalent homogeneous simulations. Effective VG parameters in this type of heterogeneous medium must be smaller than VG parameters used in background soil. Section 6.4.2 demonstrate the effectiveness of a single set parameters to capture the Type II impact of heterogeneity on all flow properties. It is noteworthy that with increasing aspect ratio transverse spreading keeps increasing while vertical spreading decreasing (Figure 5.28 & Figure5.30). As the aspect ratio tends to infinity, i.e. when there is continuous layering of lenses, water is confined to the fine-grained background soil and tends to disperse laterally in the fine soil due to capillarity. Water, in such a situation, can more easily spread laterally and vertical spreading of the moisture plume would be limited. Then the impact of this type of heterogeneity approaches to Type I impact of heterogeneity. In that case it would be difficult to capture the vertical spreading of the moisture plume by a single set of parameters (effective parameters).

6.3.3 Type III impact of heterogeneity

In very few performed heterogeneous simulations, results show that heterogeneity results in slowing down all three flow-properties i.e. average velocity; transverse spreading index and vertical spreading index are reduced because of heterogeneity. We refer this as Type III impact of heterogeneity. This effect is observed only when the degree of contrast and volumetric proportion of lenses are small and when background soil has more uniformity in its pore size distribution and texture of background and lenses are same. Since the trends of change of spreading in both directions are same, we may

reproduce spreading of the moisture plume in heterogeneous plume by an equivalent homogeneous model using a single set of effective parameters. But in that case average velocity will be overestimated. So, again it depends on the goal of modeling. In many cases our interest is in the overall extent of the moisture plume. In those cases, effective parameters may produce satisfactory results. As the heterogeneity increases, Type III impact becomes Type I impact i.e. instead of decreased; increased spreading in transverse direction is observed.

Figure 6.1 shows the three types of impact of heterogeneity on the extent of the moisture plume. Solid-line ellipse represents the extent of the moisture plume in a homogeneous medium. Dotted ellipse represents the extent of the moisture plume in a Heterogeneous medium whose background soil properties are identical to the homogeneous medium.

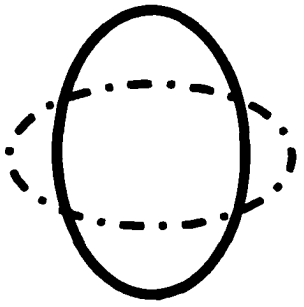

(a) Type I impact

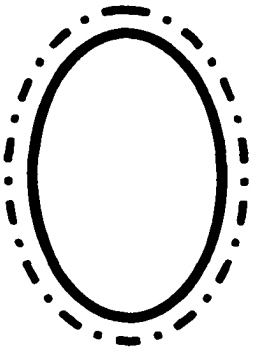

(b) Type II impact

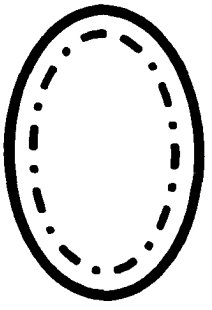

(c) Type III impact

Figure 6.1 Three different types of impact on flow properties due to heterogeneity in soil properties; solid line represents the extent of the moisture plume in a homogeneous soil and the dotted line represents the extent of the moisture plume after lenses are added to that soil.

6.4 Examples

In the following two sections, we will evaluate the effectiveness of effective parameters approximated from Type curves for two different heterogeneous mediums. First example, where Type I impact is observed and the second example where Type II impact is observed.

6.4.1 Finer lenses with less uniform pore size distribution

In this example, fine-grained lenses with less uniform pore size distribution (Φ_n = +0.294 and Φ_α = 0.705) is embedded in coarse-grained background soil with more uniform pore size distribution. This heterogeneous simulation results are taken from Group 4 category in Table 5.4. Type I impact of heterogeneity is acute in this type of configuration because the effect of texture and pore size distribution of lenses on flow properties is cumulative. The best possible effective parameters based on average velocity and transverse spreading index are estimated from the type curves (Figure 4.16 and 4.17) by trial and error methods. Table 6.1 presents four such trials to estimate the best possible effective parameters. It is apparent from Table 6.1 that the best possible value of α_{eff} and n_{eff} to reproduce both average velocity and transverse spreading are 0.085 and 2.40 respectively. A homogeneous simulation is run using this set of parameters. Comparison between the results of heterogeneous and equivalent homogeneous simulation shows (illustrated in Figure 6.2- 6.4) how good the matching is. For comparison purposes an addition plot is made in the same graph where background soil properties are used as effective parameters.

Table 6.1 Effective parameters based on average velocity and TSI.

Trial	α_{eff}	n_{eff} based on average velocity	n_{eff} based on TSI
1	0.025	2.58	4.17
2	0.045	2.56	3.02
3	0.065	2.51	2.62
4	0.085	2.43	2.40

Figure 6.2 illustrates the transient location of the center of mass of the moisture plume in heterogeneous medium with actual soil properties, in equivalent homogeneous medium with estimated effective parameters and in homogeneous medium with background soil properties. Reviewing the plots it is apparent that effective parameters can reproduce the transient evolution of the location of the center of mass to some extent although not quiet satisfactorily. Figure 6.3 presents spreading of the moisture plume in transverse direction as a function of vertical distance traveled by the center of mass in the heterogeneous medium, in the equivalent homogeneous medium and in the homogeneous medium with background soil properties. The Figure shows that there is a good agreement between heterogeneous and equivalent homogeneous simulation results.

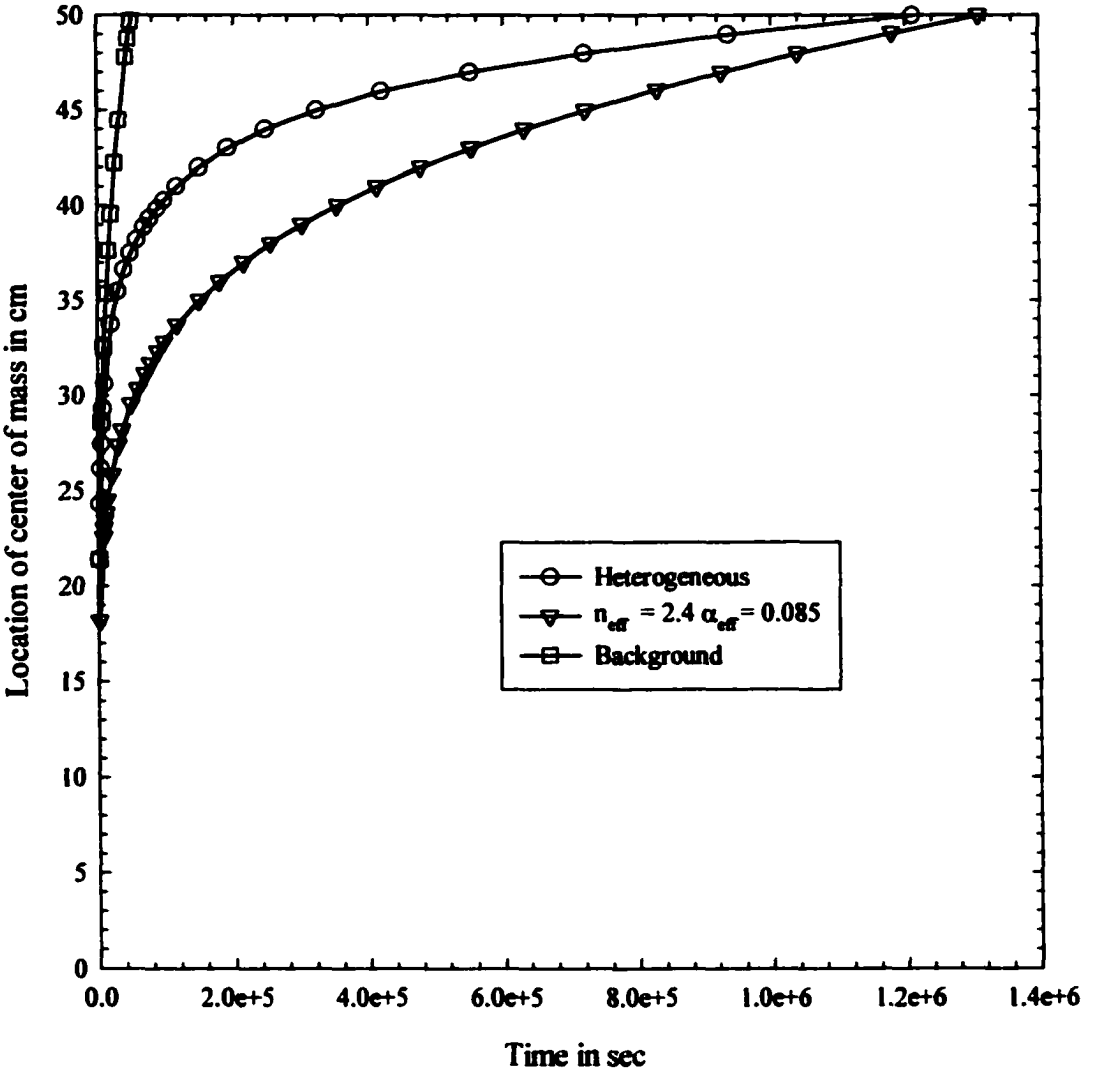

Figure 6.2 Comparison between transient location of center of mass of the the moisture plume in a heterogeneous medium and in a homogeneous medium (using effective parameters estimated based on average velocity and TSI); Lenses characteristics: Finer texture & less uniform pore size distribution.

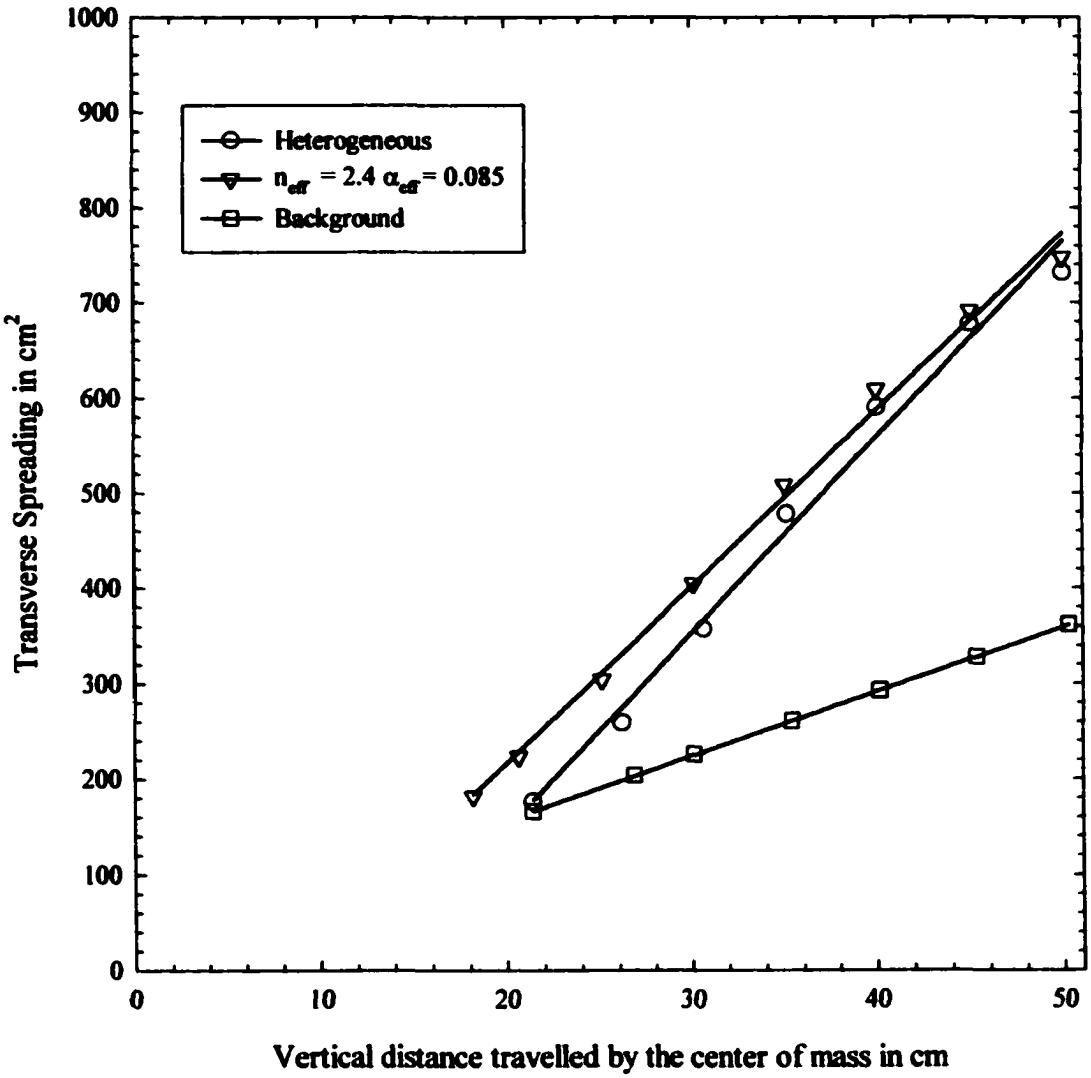

Figure 6.3 Comparison between transverse spreading in a heterogeneous medium and in a homogeneous medium (using effective parameters estimated based on average velocity and TSI); leneses characteristics: finer texture & less uniform pore size distribution.

Figure 6.4 shows spreading of the moisture plume in vertical direction as a function of vertical distance traveled by the center of mass of the moisture plume in the heterogeneous medium, in the equivalent homogeneous medium and in the homogeneous medium with background soil properties. It is evident from these plots that there is a significant difference between the heterogeneous and equivalent homogeneous simulation results. Effective parameters consistently overestimate vertical spreading of the moisture plume. This example suggests that it is unlikely to capture the Type I impact of heterogeneity on the average movement of the moisture plume by a single set of parameters.

6.4.2 Coarser lenses with more uniform pore size distribution

In this section, we will examine an example where fine-grained soil with less uniform pore size distribution (Φ_n = -2.4 and Φ_α = -0.416) contains coarse-grained lenses with more uniform pore size distribution. This heterogeneous simulation results are taken from Group 1 category in Table 4. Type II impact of heterogeneity is common in this arrangement of heterogeneous medium i.e. average velocity is reduced and both transverse and vertical spreading are increased due to heterogeneity. Type II impact is more robustly realized in such arrangement of background and lens soil because of the cumulative effect of texture and pore size distribution of lenses. Since we know from the type curves (Figure 4.16, 4.17, 4.18), any change of VG parameters in homogeneous simulations results a change in average velocity in one direction and transverse and vertical spreading in opposite direction, it is probable that there is a single set of effective

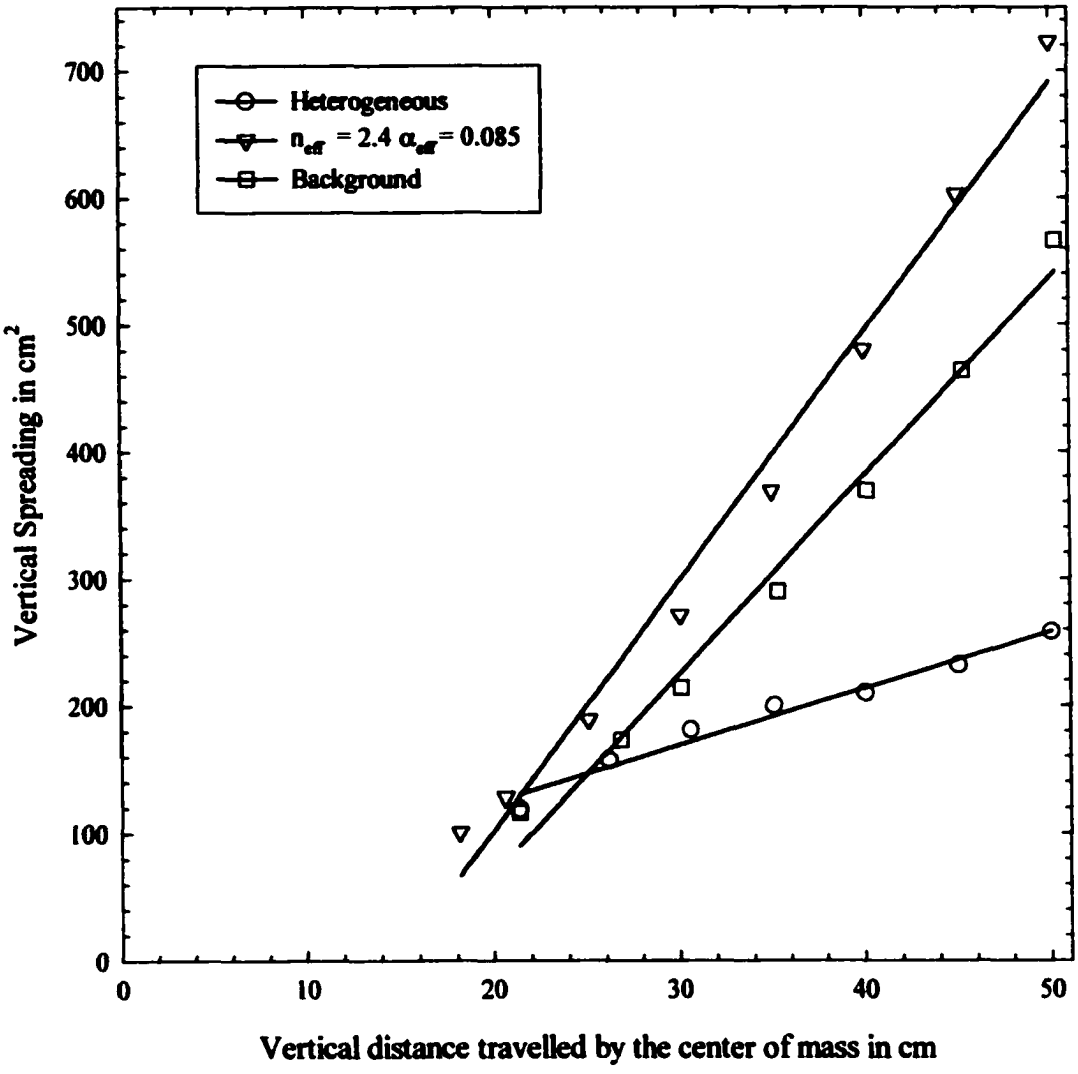

Figure 6.4 Comparison between vertical spreading in a heterogeneous medium and in a homogeneous medium (using effective parameters estimated based on average velocity and TSI); characteristics of lenses: finer texture & less uniform pore size distribution.

parameters, which can capture all three, flow properties for this type of heterogeneous medium. Type curves guide us to estimate effective parameters for this heterogeneous medium based on all flow properties. Table 6.2 presents few trials to estimate the best possible effective parameters based on all flow properties in the selected heterogeneous medium. It is apparent from Table 6.2 that the best possible value of α_{eff} and n_{eff} to reproduce average velocity, transverse spreading and vertical spreading are 0.015 and 3.04 respectively. Equivalent homogeneous simulation results are obtained using these effective parameters. Comparison between the results of heterogeneous and equivalent homogeneous simulation shows (illustrated in Figure 6.5 - 6.7) how good the matching is. For comparison purposes an addition plot is made in the same graph where background soil properties are used as effective parameters.

Table 6.2 Effective parameters based on average velocity, TSI and VSI

Trial	α_{eff}	n_{eff} based on average velocity	n_{eff} based on TSI	n_{eff} based on VSI
1	0.015	3.04	3.03	2.91
2	0.025	2.94	2.54	2.39
3	0.045	2.83	2.22	2.1
4	0.065	2.72	2.11	2.01

Figure 6.5 shows the transient evolution of the location of the center of mass of the moisture plume in three different mediums. The first plot is for heterogeneous medium with actual soil properties. Second plot is for the equivalent homogeneous medium with

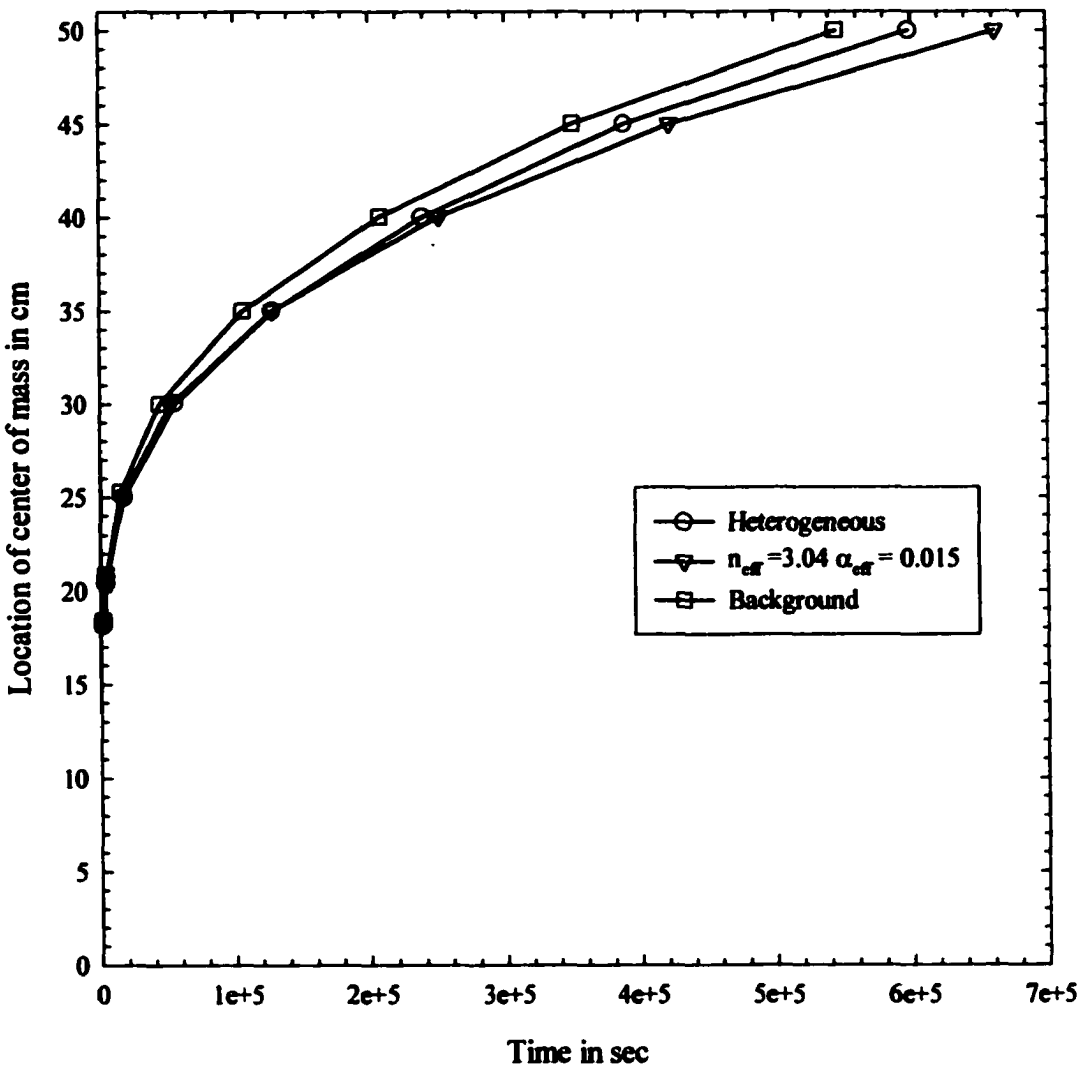

Figure 6.5 Comparison between transient location of center of mass of the moisture plume in a heterogeneous medium and in a homogeneous medium (using effective parameters estimated based on average velocity and TSI); lenses charcteristics: coarser texture & more uniform pore size distribution

estimated effective soil properties. The third plot is for a homogeneous medium with background soil properties. Reviewing all these plots it is apparent that effective parameters can reproduce the transient evolution of the vertical location of the center of mass of the moisture plume. Figure 6.6 presents spreading of the moisture plume in transverse direction as a function of vertical distance traveled by the center of mass in the heterogeneous medium, in the equivalent homogeneous medium and in the homogeneous medium with background soil properties. It is evident that transverse spreading of the moisture plume in heterogeneous medium can be adequately reproduced by effective parameters in equivalent homogeneous medium. Figure 6.7 shows vertical spreading of the moisture plume as a function of the vertical distance traveled by the center of the moisture plume in the heterogeneous medium, in the equivalent homogeneous medium and in the homogeneous medium with background soil properties. It is apparent that effective parameters in equivalent homogeneous medium can predict the vertical spreading sufficiently. In comparison to Type I impact of heterogeneity, Type II impact of heterogeneity on the mean movement of the moisture plume can be better captured by effective parameters.

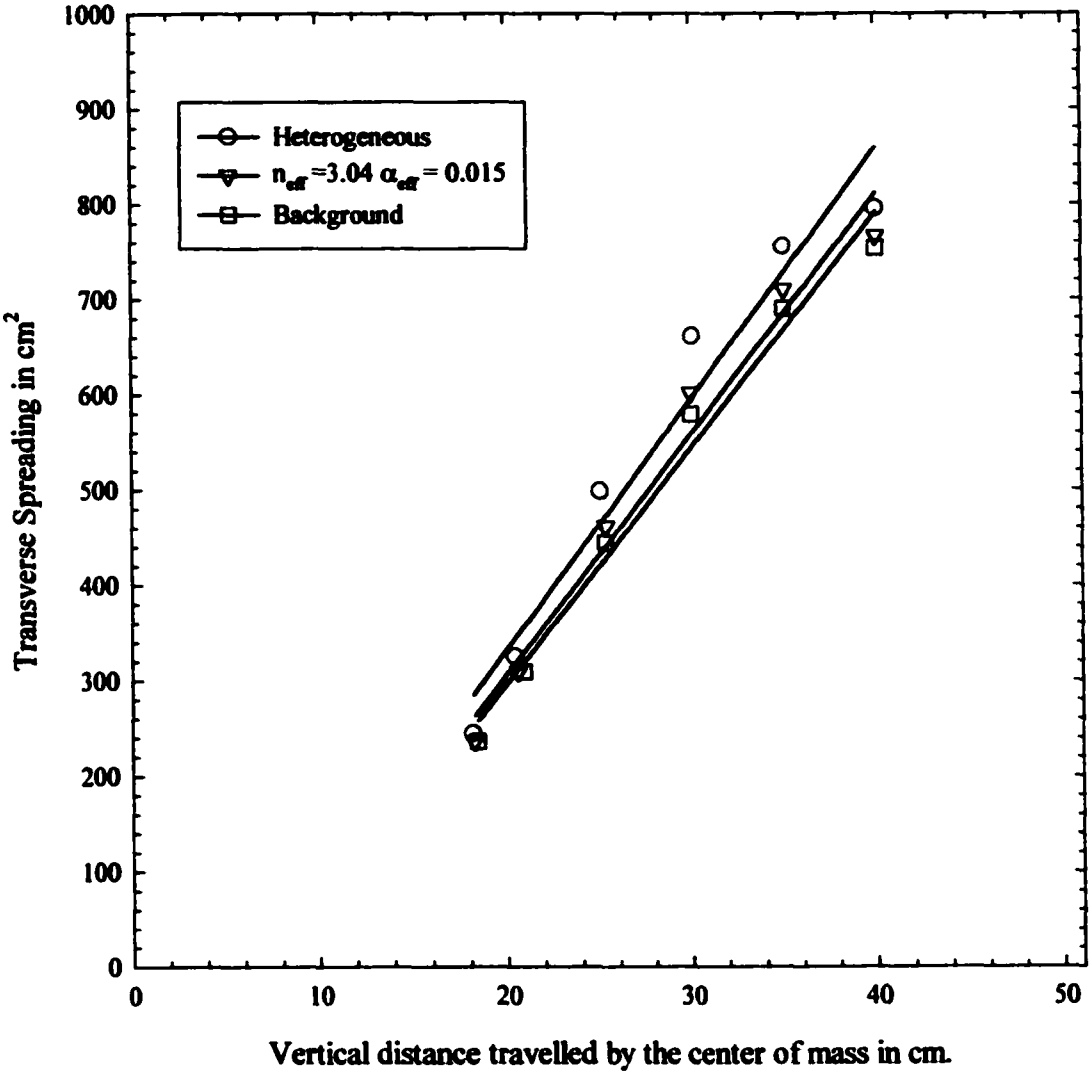

Figure 6.6 Comparison between transverse spreading in a heterogeneous medium and in a homogeneous medium (using effective parameters estimated based on average velocity and TSI); lenses characteristics: coarser textue & more uniform pore size distribution

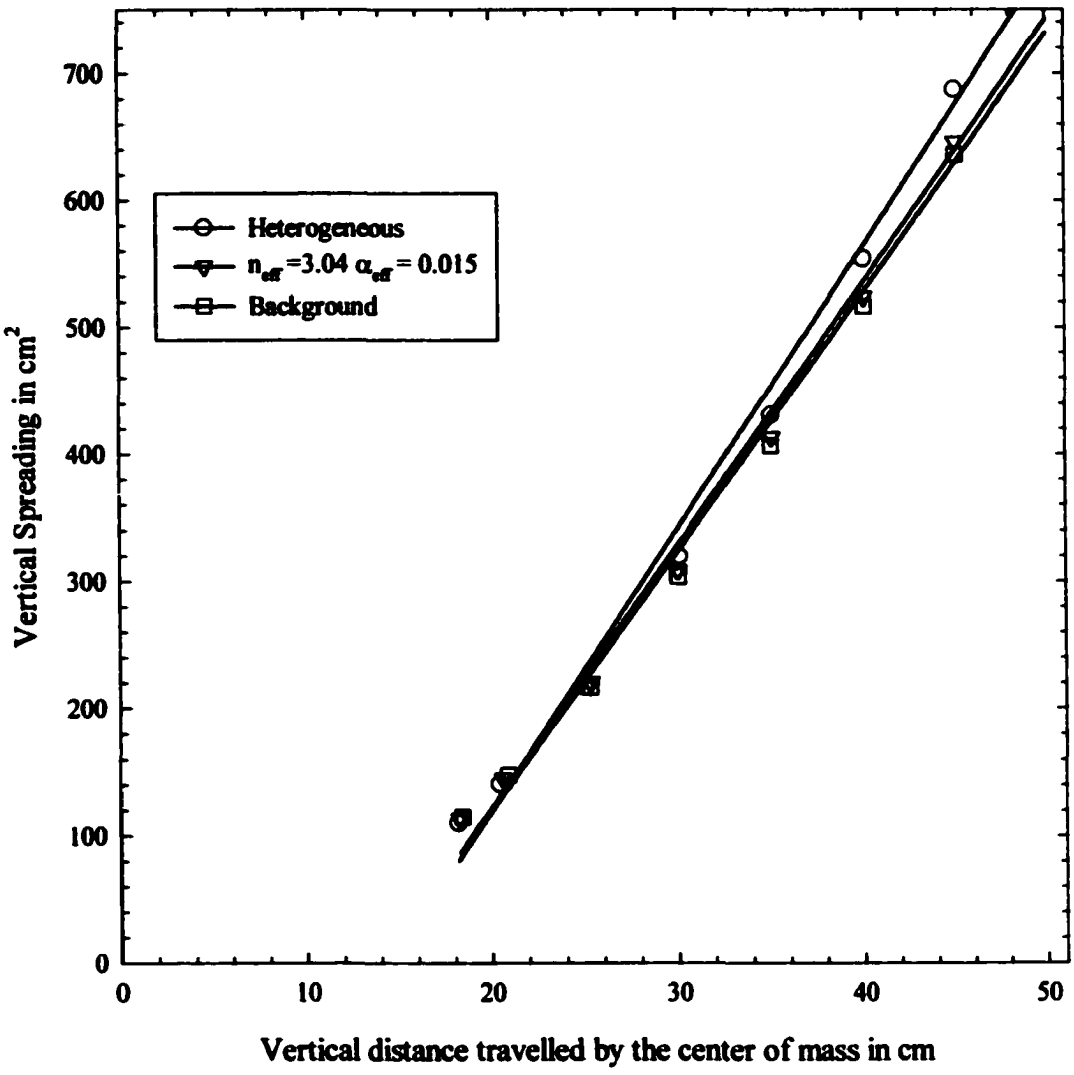

Figure 6.7 Comparison between vertical spreading in a heterogeneous medium and in a homogeneous medium (using effective parameters estimated based on average velocity and TSI); characteristics of lenses: coarser texture & more uniform pore size distribution.

6.5 Summary

Chapter 6 demonstrates the type of impact of heterogeneity for both 1D and 2D heterogeneous medium. Three different type of impact have been observed in flow properties because of heterogeneity depending on the configuration of background and lenses. When the transverse extent of the moisture plume is elongated and the vertical extent of the moisture plume is shrunk in a heterogeneous medium, this type of impact due to heterogeneity is called Type I impact. When both transverse and vertical extents of the moisture plume are stretched out in a heterogeneous medium, this type of effect is called as Type II impact of heterogeneity. When both transverse and vertical extents of the moisture plume are shrunk in a heterogeneous medium, this type of effect is called as Type III impact of heterogeneity. For Type I impact of heterogeneity single set of parameters can be estimated based on average velocity and TSI, in that case the VSI would be significantly overestimated if this single set of parameters would be used in a homogeneous simulation. It is more likely to capture the Type II impact of heterogeneity in a homogeneous medium by a single set of parameters. For Type III impact of heterogeneity, a single set of parameters can be estimated based on TSI and VSI, in that case average velocity would be overestimated if this single set of parameters would be used in a homogeneous medium. Therefore, it can be concluded that single set of effective parameters cannot capture the effect of heterogeneity adequately.

Chapter 7: Summary and conclusion

7.1 Summary

Heterogeneities in soil properties have significant influence on the average velocity and spreading behavior of the moisture plume in unsaturated soil. The migration of wetting front of moisture plume is controlled by the capillary pressure continuity requirements at the interface between different porous media, which lead to moisture content discontinuities and thus significant variations in relative permeability across the interface. Experimental results (Butts, 1996) show that the presence of heterogeneities can drastically change the pattern of migration and the type of flow that develops. These results suggest that effects of heterogeneity should not be ignored. In particular, for numerical simulations, one approach would be to include a detailed description of the observed variations of different soil properties. In practice, the costs of obtaining the necessary field and laboratory data would be unrealistic. Furthermore, this approach seems excessive, as the goals of such a modeling study are often risk evaluation of groundwater quality rather than a detailed description of the local flow or contaminant concentrations. It is often appropriate to replace the heterogeneous medium with an equivalent homogeneous medium by a set of effective parameters. The question is how to estimate effective parameters, which will integrate the effect of these local heterogeneities and how it relates to heterogeneity (degree of contrast, aspect ratio of correlation length and volumetric proportion of each material) of the medium. The work described in this dissertation has demonstrated a method of estimating effective

parameters and its feasibility to replace a heterogeneous medium with an equivalent homogeneous medium for the case of unsaturated flow.

For practical purposes the detailed moisture distribution is not of our interest. We are interested in more overall measures and assessments of time rate of change of moisture content distribution, which is frequently referred as moisture plume in this thesis. Spatial moments of moisture content are the tools, which are used to estimate the global location and extent of the moisture plume as described in Chapter 3.

Results of the homogeneous simulations are presented in chapter 4. Infiltration and redistribution experiments are performed for a range of VG parameters since our focus is only on these two parameters (α, n). During infiltration in 1D simulations, effects of two types of boundary conditions have been evaluated. In case of constant head boundary condition, whether the average velocity of the moisture plume increase or decrease with increasing n depends on the ratio α^{-1}/BCh. In case of constant flux boundary condition, the average velocity is insensitive to VG parameters. In addition, the vertical spreading of the moisture plume is insensitive to VG parameters for both constant head and constant flux boundary conditions. Therefore, it is difficult to establish any relationship between VG parameters and flow properties during infiltration. During redistribution, all three flow-properties (average velocity, TSI, VSI) were estimated for each simulation. These results provide a relationship between flow properties and VG parameters. It has been found that average velocity is increasing with increasing value of VG parameters. On the other hand, TSI and VSI are decreasing with increasing value of

VG parameters. The graphic representations of these relationships are named as type curves, based on which effective parameters can be estimated (Figure 4.14, 4.15 for 1D simulations and Figure 4.16, 4.17, 4.18 for 2D simulations).

Results of the heterogeneous simulations are presented in chapter 5. A wide variety of heterogeneous mediums are selected systematically to establish a relationship between flow properties and heterogeneity (degree of contrast, aspect ratio of correlation length and volumetric proportion of each material) of the medium. These relationships would help us to estimate the most appropriate effective parameters for any heterogeneous medium. The general observations are: (a) average velocity of the moisture plume is decreasing with increasing degree of contrast, increasing aspect ratio and increasing volumetric proportion; (b) TSI of the moisture plume is increasing with increasing degree of contrast, increasing aspect ratio and increasing volumetric proportion of lenses; (c) VSI of the moisture plume is decreasing with increasing degree of contrast, increasing aspect ratio and increasing volumetric proportion of lenses when Φ is positive and VSI is increasing with heterogeneity when Φ is negative; (d) heterogeneity in general slows down the vertical movement of moisture plume and enhance the transverse spreading consequently reduce the vertical spreading only when Φ is positive.

Chapter 6 demonstrates the type of impact of heterogeneity for both 1D and 2D heterogeneous medium. Three different type of impact have been observed in flow properties because of heterogeneity depending on the configuration of background and

lenses. Results of 1D heterogeneous simulations are not satisfactorily reproduced by a single set of effective parameters in homogeneous medium. In 2D cases, most of the time simulated results using single set of parameters did not satisfactorily reproduce all flow properties. In few cases, specially when $\Phi < 0$, it is more likely to capture the effect of heterogeneity by a single set of parameters. In general, single set of parameters can be estimated based on any two flow-properties, in that case the third properties would be overestimated or underestimated if those effective parameters would be used in a homogeneous simulation.

7.2 Conclusion

In this work, we made an attempt to define and derive effective parameters for the case of infiltration and redistribution by using unsaturated flow model. It has been found that it is not possible to define effective parameters for realistic infiltration simulations. For constant flux boundary condition, upper part of the soil domain becomes saturated quickly when the ratio of flux and saturated hydraulic conductivity is greater than one and thus VG parameters has no effect on flow properties. When the boundary flux is smaller than saturated hydraulic conductivity, flow is so slow (because of initial high tension) that no relationship between VG parameters and flow properties were found.
For constant head boundary condition, the amount of infiltrating water into the soil column depends on the magnitude of boundary condition and also on the VG parameters. Therefore, it is difficult to establish a consistent relationship between VG parameters and flow properties.

During redistribution, a consistent relationship between VG parameters and flow properties can be developed for both 1D and 2D flow. With the aid of these relationships, it has been found that it is not possible to capture the effect of heterogeneity on all three-flow properties of the moisture plume. Nonetheless, in Type I impact of heterogeneity, average velocity and transverse spreading of the moisture plume can be reproduced by a single set of parameters. In such case vertical spreading of the moisture plume would be significantly overestimated if selected single set of parameters were used as an effective parameters in a homogeneous simulation. In type II impact of heterogeneity, average velocity and transverse spreading of the moisture plume can be reproduced by a single set of parameters. In that case vertical spreading of the moisture plume would be slightly underestimated if those parameters were used as an effective parameters in a homogeneous simulation. It should be noted here that when aspect ratio of lenses are large, Type II impact approaches to Type I impact of heterogeneity. In Type III impact of heterogeneity, transverse spreading and vertical spreading of the moisture plume can be reproduced by a single set of parameters. In that case average velocity of the moisture plume would be slightly overestimated if those parameters were used as an effective parameters in a homogeneous simulation.

7.3 Future research

The research reported in this dissertation demonstrates the inadequacy of capturing the effect of heterogeneity on the mean movement of the moisture plume by a single set of parameters using unsaturated flow model. Since most cases, Type I impact of heterogeneity is observed and the effect of heterogeneity is more significant than Type II and Type III impact of heterogeneity, future research should concentrate on Type I impact of heterogeneity. One possibility to reproduce Type I impact of heterogeneity i.e. reduced average velocity, increased transverse spreading and reduced vertical spreading of the moisture plume in a homogeneous medium, is to modify the unsaturated flow model. It could be more possible to capture the effect of heterogeneity on all flow properties adequately if hysteresis of θ-h-k_r relationship and anisotropy in relative permeability are introduced in the unsaturated flow model. It is discussed in the next paragraphs why this approach may work based on the results that we have found.

It has been observed from moisture profile (Figure 5.6 & 5.8) of heterogeneous soil that wetting front of moisture plume encounters difficulty entering the coarser soil. As a result moisture content at the wetting front of the moisture plume is expected to be relatively small. However, in the drying front of the moisture plume, water tends to stay in finer soil. This characteristic of water retention results in relatively large soil moisture content at the drying front of the plume. These features of the moisture plume suggest that there might be two effective moisture retention curves, one for drying cycle and another for wetting cycle. Since the unsaturated flow model used in this research does

not account for hysteresis that occurs due to pore scale variation of soil properties, the hysteresis effect observed in large scale may be due to heterogeneity. The result is consistent with the stochastic results of Mantoglou (1987(b)), as they showed that soil property variability on a scale larger than the pore scale, produces a large-scale hysteresis.

Next question is how we estimate these effective drying and wetting moisture retention functions (or the parameters that define these functions) for a given heterogeneous medium. The Type curves, which we have already developed, can guide us to estimate these parameters. Generally, VG parameters that correspond to drying curves are smaller than that corresponds to wetting curve. The single set of parameters, which can reproduce both reduced average velocity and increased transverse spreading, can be assigned for drying curve. Similarly the single set of parameters that can match the reduced vertical spreading can be assigned for wetting curve. Since there is more than one set of parameters that can match the same vertical spreading, we will have a number of different wetting curves. Hysteretic moisture retention functions can be integrated in the unsaturated flow model. When pressure head at any node is higher than the pressure head at previous time step ($\partial h / \partial t > 0$), the computer code will use the drying curve. Similarly, if pressure head at any node is smaller than the pressure head at previous time step ($\partial h / \partial t < 0$), the computer code will use the wetting curve. A new set of type curve can be developed by plotting the output variables (V_{avg}, TSI and VSI) against input variables (n_d, n_w/n_d for different α_d, α_d/α_w where n_d = drying n, n_w = wetting n, α_d = drying α and α_w = wetting α). It is expected that this new set of Type curves

would be helpful to estimate effective parameters that can capture adequately the effect of heterogeneity on the mean movement of the moisture plume.

The effect of heterogeneity on the mean movement of the moisture plume can also be explained by the anisotropic nature of the moisture retention function. It has been found that two different sets of VG parameters are required to reproduce increased transverse and reduced vertical spreading. It implies that moisture retention function has directional dependence. Therefore, relative permeability is anisotropic. Since relative permeability in soil depends on the moisture content or the capillary pressure head, this anisotropy in relative permeability is also dependent on moisture content or capillary pressure head. Although this finding contradicts the common assumption that α and n are scalar quantity, other researchers have already suggested similar observation, which is anisotropy in relative permeability function due heterogeneity in large scale (Yeh, 1985, Mantoglou, 1987(c), Ataie-Ashtiani, 2001).

It is anticipated that if the unsaturated flow model can be modified to handle this saturation dependent anisotropy in relative permeability, it could capture sufficiently the effect of heterogeneity on the mean movement of the moisture plume. The single set of parameters, which can reproduce both reduced average velocity and increased transverse spreading, can be assigned transverse direction. The single set of parameters that can match the reduced vertical spreading can be assigned for vertical direction. Since there is more than one set of parameters that can match the same vertical spreading, we will have a number of different curves for vertical direction. The modified

unsaturated flow model will use moisture retention functions for transverse direction to calculate transverse unsaturated conductivity between two nodes when $z_i = z_{i+1}$ or else it will use moisture retention functions for longitudinal direction to calculate vertical unsaturated conductivity. Now after integrating the aniosotropic curves in the modified unsaturated flow model, a new set of type curve can be developed by plotting the output variables (V_{avg}, TSI and VSI) against input variables (n_T, n_T/n_L for different α_T, α_T/α_L where n_T = transverse n, n_L, = Vertical/Longitudinal n, α_T = transverse α and α_L = Vertical/Longitudinal α). It is expected that this new set of Type curves would guide us to estimate effective parameters that can capture adequately the effect of heterogeneity on the mean movement of the moisture plume.

Comparison between the results obtained by the modified unsaturated flow models would be helpful to select the better model for capturing the effect of heterogeneity on the mean movement of the moisture plume.

Chapter 8: Appendices

8.1 Appendix A: Subroutine for spatial moment calculation

```
      subroutine centroid

      implicit integer*4(i-n)
      implicit real*8 (a-h,o-z)


      include 'dimen.par'
      include 'units.par'
      include 'flags.inc'
      include 'space.inc'
      include 'time.inc'
      include 'press.inc'
      include 'conc.inc'
      include 'param2.inc'
      include 'imat.inc'

      INTEGER incc(125000,8)
      DIMENSION xloc(125000), yloc(125000),zloc(125000)

      open(777,file='mom.out')

       if (ipr.eq.0) then
          do j=1,nny
           do i=1,nnx
             do k=1,nnz
               inode = k+nnz*(i-1+nnx*(j-1))
               xloc(inode)=x(i)
               yloc(inode)=y(j)
               zloc(inode)=z(i,j,k)
             end do
           end do
         end do

        totmass=0.0
c031797
         do je=1,ney
         do ie=1,nex
          do ke=1,nez
           iel = ke + nez * ( ie-1 + nex * (je-1) )
```

```
          dx=x(ie+1)-x(ie)
          dy=y(je+1)-y(je)
          dz=z(ie,je,ke+1)-z(ie,je,ke)
          sumpr=0.0
          sumth=0.0
          do jj=1,2
           do ii=1,2
            do kk=1,2
          inode =ke+kk-1+(nez+1)*((ie+ii-1)-1+(nex+1)
     +   *((je+jj-1)-1))
            sumpr=sumpr+pr(inode)/8
            sumth=sumth+fncth(pr(inode),imatl(iel))/8
            end do
         end do
        end do
c061297
          csumth(iel)=sumth-oldth(iel)
c           csumth(iel)=sumth
c           csumth(iel)=sumth-oldth(10)

          totmass=(totmass + csumth(iel)*1*dx*dy*dz)
            end do
          end do
        end do



        totint=0
        totint2=0
        totint3=0
        totint4=0
        totint5=0
        totint6=0


       do jj=1,ney
        do ii=1,nex
         do kk=1,nez
c*****   calculate cbare for each element
       cbare=0
       ie=kk+nez*(ii-1+nex*(jj-1))
       ij=kk+nnz*(ii-1+nnx*(jj-1))
       incc(ie,1)=ij
       incc(ie,2)=ij+nnz
       incc(ie,3)=incc(ie,2)+1
       incc(ie,4)=ij+1
```

```
      incc(ie,5)=ij+nnx*nnz
      incc(ie,6)=incc(ie,5)+nnz
      incc(ie,7)=incc(ie,6)+1
      incc(ie,8)=incc(ie,5)+1
c****integral (assume constant porosity);

      ie=kk+nez*(ii-1+nex*(jj-1))

       delx=xloc(incc(ie,2))-xloc(incc(ie,1))
       dely=yloc(incc(ie,5))-yloc(incc(ie,1))
       ztop=zloc(incc(ie,1))
       zbot=zloc(incc(ie,4))
       delz=zbot-ztop

       xr=xloc(incc(ie,2))
       xl=xloc(incc(ie,1))
       yb=yloc(incc(ie,5))
       yf=yloc(incc(ie,1))

    totint=totint+(delx*dely*csumth(ie)*den*abs(ztop**2-zbot**2)/2)
    totint2=totint2+(delx*dely*delz*csumth(ie)*den
   + *abs((ztop+zbot)/2)**2)
    totint3=totint3+(delz*dely*csumth(ie)*den*abs(xr**2-xl**2)/2)
    totint4=totint4+(delx*dely*delz*csumth(ie)*den
   + *abs((xr+xl)/2)**2)

    totint5=totint5+(delz*delx*csumth(ie)*den*abs(yb**2-yf**2)/2)
    totint6=totint6+(delx*dely*delz*csumth(ie)*den
   + *abs((yb+yf)/2)**2)

        enddo
       enddo
      enddo

c*****  location of center of mass:
      zbar=totint/totmass
      zvar=(totint2/totmass)-zbar**2
      xbar=totint3/totmass
      xvar=(totint4/totmass)-xbar**2
      ybar=totint5/totmass
      yvar=(totint6/totmass)-ybar**2
      write(777,509)t,totmass,xbar,ybar,zbar,xvar,yvar,zvar
 509    format(1x,E12.6,2X,E10.4,5F10.4,2x,F10.3)
      endif
      return
      end
```

8.2 Appendix B: References

Aris, R., On the dispersion of a solute in a fluid flowing through a tube, Proc. R. Soc. London, Ser. A, 235, 67-78, 1956.

Ataie-Ashtiani B. Hassanizadeh, Oostrom M., Celia M.A., White M.D., Effective parameters for two phase flow in a porous medium with periodic heterogeneities, Journal of contaminant hydrology vol. 49, 87-109, 2001.

Bennett G.D., C. Zheng, Applied contaminant transport modeling, Van Nostrand Reinhold publishing inc., 1995.

Bouloutas, T., Improved numerical methods for modeling flow and transport process in partially saturated porous media, PhD thesis, Dept. of Civil Engineering, Massachusetts Institute of Technnology, 1989.

Braun, C., Hassanizadeh, S.M., Helmig, R., Two-phase flow in stratified porous media: effective parameters and constitutive relationships. Proceedings of the international conference computational methods in water resources, Crete, Greece, 15-19, pp. 43-50, June, 1998.

Brooks, R. H. and Corey A. T., Hydraulic properties of porous media, Hydrlogy papers 3, Colorado State University, Fort Collins, pp. 27, 1964.

Butts, M.B., Jensen, K.H., Effective parameters for multiphase flow in layered soils, Journal of Hydrology, 183, 101-116, 1996.

Carsel R. F., Parrish R. S., Developing joint probability distributions of soil water retention characteristics. Water Resour. Res., 24(5), 755-769, 1988.

Celia, M. A., Bouloutus E. T. and Zarba R. L., A general mass-conservative numerical solution for the unsaturated flow equation, 26(7), 1483-1496, 1990.

Celia, M. A., Description of a three-dimensional groundwater flow and contaminant transport simulator, Princeton University, 1992.

Dagan, G., Bresler, E., Models of groundwater flow in statistically homogeneous porous formations, Water Resour. Res., 15(1), 47-63, 1979.

Dagan, G., Analysis of flow through heterogeneous random aquifers, 2, Unsteady flow in confined formations, Water Resour. Res., 18(5), 1571- 1585, 1982b.

Dagan, G., Bresler, E., Unsaturated flow in spatially variable fields 1. Derivation of models of infiltration and redistribution, Water Resour. Res., 19(2), 413-420, 1983.

Ferrand L.A., Celia M.A., The effect of heterogeneity on the drainage capillary pressure~saturation relation, Water Resour. Res., 28(3), 859-870, 1992.

Freeze, R. A., and Cherry, J.A., Groundwater, Prentice Hall, Englewood Cliffs, NJ, 1979.

Freyberg, D. L., A natural gradient experiment on solute transport in a sand aquifer 2. Spatial moments and the advection and dispersion of nonreactive tracers, Water Resour. Res., 22(13), 2031-2046, 1986.

Gardner , W. R., Some steady state solutions of the unsaturated moisture flow equation with application to evaporation from a water table, Soil Sci., 85(4), 228-232, 1958.

Ghosh, R. K., Estimation of soil moisture characteristics from mechanical properties of soils, Soil Sci., 130, 60-83, 1980.

Gupta, S.C. and Larson, W. E., Estimating soil water retention characteristics from particle size distribution, organic matter percent, and bulk density, Water Resour. Res., 15, 1633-1635, 1979.

Gutjahr, A.L., Gelhar, L.W., Bakr, A.A. and McMillan, J.R., Stochastic analysis of spatial variability in subsurface flows, 2: Evaluation and application. Water Resour. Res., 14(5), 953-959, 1978.

Hills, R. G.; Porro, I.; Hudson, D.B; Wierenga, P. J. Modeling one-dimensional infiltration into very dry soils 1. Model development and evaluation, Water Resour. Res., 25(6), 1259-1269, 1989.

Kueper, B. H., Frind, E. O., Two phase flow in heterogeneous porous media: 1 Model development, Water Resour. Res., 27(6), 1049-1057, 1991.

Mantoglou, A., Gelhar, L. W., Stochastic modeling of large-scale transient unsaturated flow systems, Water Resour. Res., 23(1), 37-46, 1987.

Mantoglou, A., Gelhar, L. W., Capillary tension head variance, mean soil moisture content, and effective specific soil moisture capacity of transient unsaturated flow in stratified soils, Water Resour. Res., 23(1), 47-56, 1987.

Mantoglou, A., Gelhar, L. W., Effective hydraulic conductivities of transient unsaturated flow in stratified soils, Water Resour. Res., 23(1), 57-67, 1987.

Mattax, C.C. and Dalton R.L., Reservoir simulation SPE, Monograph volume 13, Richardson,TX (1990).

Maulem, Y., A new model for predicting the hydraulic conductivity of unsaturated porous media, Water Resour. Res., 12(3), 513-522, 1976.

Mishra, S., Parker, J. C., Effects of parameter uncertainty on predictions of unsaturated flow, Journal of Hydrology, 108,19-33, 1989.

Mohanty, B. P., Bowman, R. S., Hendrickx, J.M.H. and Van Genuchten,M.T., New-piecewise-continuous hydraulic functions for modeling preferential flow in an intermitent-flood-irrigated field, Water Resour. Res., 33(9), 2049-2063, 1997.

Nielsen, D. R., Van Genuchten, M. Th., Biggar, J. W., Water flow and solute transport processes in the unsaturated zone, Water Resour. Res., 22(9), 89S-108S, 1986.

Polman, D. J., Mclaughlin, D., Luis, S., Gelhar, L. W., Ababou, R., Stochastic modeling of large scale flow in heterogeneous unsaturated soils, Water Resour. Res., 27(7), 1447-1458, 1991.

Rahman, M.R., Computational investigation of effective hydraulic properties for the unsaturated zone, MS thesis, CCNY,1994.

Rajaram,H., Ferrand L.A., Celia M.A., Prediction of relative permeabilities for unconsolidated soils using pore-scale network models, Water Resour. Res., 33(1), 43-52, 1997.

Rawls, W. J., Brakensiek, D., L. and Miller N., Green-Ampt infiltration parameters from soils data, Journal of Hydraulic Engineering, ASCE, Vol. 109, No 1, pp. 62-70, 1983

Russo, D., Upscaling of hydraulic conductivity in partially saturated heterogeneous porous formation, Water Resour. Res., 28(2), 397-409, 1992.

Schroth, M. H., Ahearn, S. J., Selker, J.S. and Istok, J.D., Charcterization of Miller-similar sands for laboratory subsurface hydrologic studies. Soil Sci. soc. Am. J., 60, 1331-1339, 1996.

Stevens, J.H. 'Analysis and modeling of infiltration and solute transport experiments in unsaturated sand and gravel, Cape Cod, Massachusetts'
MSc thesis, Princeton University, NJ., 1994.

Vogel, T.; Van Genuchren, M. Th.; Cislerova, M., Effect of the shape of the soil hydraulic functions near saturation on variably-saturated flow predictions, Advances in Water Resources, 24, 133-144, 2001.

Van Genuchten, M. Th., A closed-form equation for predicting the hydraulic conductivity of unsaturated soils, Soil science soc. Am. J., vol. 44, pp.892-898, 1980.

Warrick, A. W., Numerical approximation of darcian flow through unsaturated soil, Water Resour. Res., 27(6), 1215-1222, 1991.

Wildenschild, D and Jaensen, K. H., Laboratory investigation of effective flow behavior in unsaturated heterogeneous sands, Water Resour. Res., 35(1), 17-27, 1999.

Yeh, J. T. C., Gelhar L. W., and Gutjahr A.L., Stochastic analysis of unsaturated flow in heterogeneous soils, 1, Statitically Isotropic Media, Water Resour. Res., 21(4), 447-456, 1985.

Yeh, J. T. C., Gelhar L. W., and Gutjahr A.L., Stochastic analysis of unsaturated flow in heterogeneous soils, 2, Statitically Anisotropic Media with variable α, Water Resour. Res., 21(4), 457-464, 1985.

Yeh, J. T. C., Gelhar L. W., and Gutjahr A.L., Stochastic analysis of unsaturated flow in heterogeneous soils, 3, Observations and Applications, Water Resour. Res., 21(4), 465-472, 1985.